Mendelova univerzita v Brně
Agronomická fakulta

DISERTAČNÍ PRÁCE

Brno 2021 Caleb Mensah, MSc.

Mendelova univerzita v Brně
Agronomická fakulta
Ústav agrosystémů a bioklimatologie

Analysis of eddy covariance data measured in terrestrial ecosystem

„Analýza eddy kovariančních dat měřených v terestrickém ekosystému“

Disertační práce

Vedoucí práce:
prof. RNDr. Ing. Michal Vladimír Marek, DrSc.

Vypracoval:
Caleb Mensah, MSc

Brno 2021

Čestné prohlášení

Prohlašuji, že jsem práci: Analysis of eddy covariance data measured in terrestrial ecosystem („Analýza eddy kovariančních dat měřených v terestrickém ekosystému“) vypracoval/a samostatně a veškeré použité prameny a informace uvádím v seznamu použité literatury. Souhlasím, aby moje práce byla zveřejněna v souladu s § 47b zákona č. 111/1998 Sb., o vysokých školách a o změně a doplnění dalších zákonů (zákon o vysokých školách), ve znění pozdějších předpisů, a v souladu s platnou Směrnicí o zveřejňování závěrečných prací. Prohlašuji, že tištěná podoba závěrečné práce a elektronická podoba závěrečné práce zveřejněná v aplikaci Závěrečné práce v Univerzitním informačním systému je identická.

Jsem si vědom/a, že se na moji práci vztahuje zákon č. 121/2000 Sb., autorský zákon, a že Mendelova univerzita v Brně má právo na uzavření licenční smlouvy a užití této práce jako školního díla podle § 60 odst. 1 autorského zákona.

Dále se zavazuji, že před sepsáním licenční smlouvy o využití díla jinou osobou (subjektem) si vyžádám písemné stanovisko univerzity, že předmětná licenční smlouva není v rozporu s oprávněnými zájmy univerzity, a zavazuji se uhradit případný příspěvek na úhradu nákladů spojených se vznikem díla, a to až do jejich skutečné výše.

V Brně dne:……..

……
podpis

DEDICATION

To my late son, Joseph Boateng Mensah, who I lost in 2021. You will forever remain in my heart of hearts. Also to prof. RNDr. Ing. Michal Vladimír Marek, DrSc., who I consider as a life Mentor.

ACKNOWLEDGEMENTS

I would like to express my profound gratitude to my supervisor prof. RNDr. Ing. Michal Vladimír Marek, DrSc. to my supervisor specialist Mgr. Ladislav Šigut, Ph.D. and consultant Dr. Georg Jocher for their inspiration, technical advice, and for providing me with the suitable condition to work on this very interesting research studies. Special thanks also goes out to Mgr. Marian Pavelka and Dr. Manuel Acosta, who shared with me their valuable experience and the knowledge in terrestrail ecosystem carbon dynamics and other micrometeorological and ecophysiological measurements techniques and who provided me many fruitful discussions and recommendations. Sincere thanks to all the staff at the Department of Matter and Energy Fluxes and CzechGlobe as a whole including Mgr. Jana Halfarová, for their assistance and guidance in understanding and applying the principle of eddy covariance in forest carbon flux analyses. I would also like to extend my heartfelt gratitude to all from the Department of Agrosystems and Bioclimatology, other colleagues from MENDELU and my family who all contributed directly and indirectly to the success of my research studies.

Finally, thanks to all of my reviewers for the useful and constructive comments. The Ph.D. thesis was supported by the Ministry of Education, Youth and Sports of the Czech Republic (CR) within the CzeCOS program, grant number LM2018123. The publications are further an output of the Global Research Institute CAS (CzechGlobe).

CONTENTS

LIST OF TABLES

LIST OF FIGURES

ABSTRACT

Increase in the concentration of greenhouse gases and aerosols, mainly caused by anthropogenic activities, alters the earth radiation budget that has led to the increase of the earth's mean surface temperature by 1.2 °C since the preindustrial era. Carbon dioxide (CO_2) is the main suspect of causing global warming because combustion of fossil fuel injects CO_2 into the atmosphere. Thus, vegetation- atmosphere exchange of CO_2 is being studied intensively to determine the source and sink potentials of different ecosystems. Many methods have been used to successfully carry out such research works but the Eddy Covariance method is one of the most efficient recent techniques commonly used. The method depends on direct and fast measurements of CO_2 concentration and vertical wind component within the constant flux layer of the atmospheric boundary layer. These measurements are carried out over several hundreds of sites all over the world on a long-term basis to characterize ecosystem exchanges of trace gases, water and energy and to validate process-based models. This thesis aims to provide a novel insight into the analysis and comparison of eddy covariance data measured at different forest ecosystems within the Czech Carbon Observatory system (CzeCOS) over several years. Central European beech (at Štítná) and spruce species (at Bílý Kříž and Rájec), growing under contrasting climatic conditions, were studied. To demonstrate how actual gross primary productivity (GPP) courses compare to potential GPP (GPP_{pot}) courses expected under near-optimal environmental conditions, we computed normalized GPP (GPP_{norm}) with values between 0 and 1 as the ratio of the estimated daily sum of GPP to GPP_{pot}. Furthermore, the presented results also show the impacts of a central European summer drought in 2015 on GPP at the two Norway spruce forest sites that represented two contrasting climatic conditions – cold and humid climate at Bílý Kříž (CZ-BK1) vs. moderately warm and dry climate at Rájec (CZ-RAJ).

Keywords:
eddy covariance, European beech, Norway spruce, regression modeling, climate change, drought, soil moisture, machine learning

ABSTRAKT

Zvyšování koncentrace skleníkových plynů a aerosolů, způsobené především antropogenní činností, mění radiační bilanci Země, což vedlo ke zvýšení průměrné povrchové teploty Země o 1.2 °C v porovnání s obdobím před průmyslovou revolucí. Proto je intenzivně studována výměna CO_2 mezi vegetací a atmosférou, abychom určili potenciál výdeje a příjmu CO_2 různých ekosystémů. Hodnocení těchto aspektů bylo prováděno řadou různých metod, ale jednou z nejefektivnějších a šířeji používaných se v nedávné době stala eddy kovarianční metoda. Metoda je založena na přímém a rychlém měření koncentrace CO_2 a vertikální složky větru ve vrstvě konstantního toku hraniční vrstvy atmosféry. Tato dlouhodobá měření se provádí na stovkách ekosystémových stanic napříč celým světem a umožnují charakterizovat ekosystémovou výměnu stopových plynů, vody a energie a validovat procesní modely. Tato disertační práce má za cíl poskytnout nové poznatky z analýzy a porovnání víceleté řady eddy kovariančních dat měřených v různých lesních ekosystémech v rámci České observační sítě uhlíku (CzeCOS). Bukový (ve Štítné) a dva smrkové porosty (na Bílém Kříži a v Rájci) jako typické dřeviny střední Evropy byly studovány na zmíněných lokalitách s kontrastním klimatem. Aby bylo možno porovnat chod hrubé primární produkce (GPP) s chodem potenciální GPP (GPP_{pot}) očekávaném za téměř optimálních podmínek prostředí, vypočítali jsme normalizovanou GPP (GPPnorm) s hodnotami mezi 0 a 1 odpovídající poměru stanovené denní sumy GPP a GPPpot. Prezentované výsledky dále ukazují dopady letního sucha ve střední Evropě v roce 2015 na GPP dvou porostů smrku ztepilého které reprezentují kontrastní klimatické podmínky – chladné a vlhké na Bílém Kříži (CZ-BK1) oproti mírně teplým a sušším podmínkám v Rájci (CZ-RAJ).

Klíčová slova:
eddy kovariance, buk lesní, smrk ztepilý, hrubá primární produkce, regresní modelování, klimatická změna, sucho, půdní vlhkost, strojové učení

LIST OF ABBREVIATIONS USED IN THE TEXT

IPCC	Intergovernmental Panel on Climate Change
GHGs	Greenhouse Gas Emissions
CO_2	Carbon dioxide
ppm	parts per million
UNFCCC	United Nations Framework Convention on Climate Change
EC	Eddy Covariance
VPD	Vapour Pressure Deficit (hPa)
FLUXNET	Global Flux tower network
ABL	Atmospheric Boundary layer
M	horizontal mean wind velocity (m s^{-1})
U*	friction velocity (m s^{-1})
Ƙ	von Kármán's constant (0.41; dimensionless)
z	measurement height from a reference plane (m)
Z_0	roughness length (m)
h_c	average forest canopy height (m)
d	zero-plane displacement height (m)
Ri	Richardson number
ϕ_i	mean velocity that depends on the Richardson's number
u	longitudinal wind speed component (m s^{-1})
v	cross-wind wind speed component (m s^{-1})
w	vertical wind speed component (m s^{-1})
TKE	turbulent kinetic energy
θ	Eddy entities
q	Specific humidity (dimensionless)
CH_4	Methane
N_2O	Nitrous oxide
O_3	Ozone
NO_2	Nitrous dioxide

NO	Nitric Oxide
SO_2	Sulfur dioxide
Tair	Air temperature (°C)
H	Sensible heat (W m^{-2})
LE	Latent heat (W m^{-2})
F_{CO2}	CO_2 flux (μmol m^{-2} s^{-1})
λ	latent heat of vaporization (J kg^{-1})
d_{CO2}	molar density of CO_2 (μmol m^{-3})
UT	friction velocity threshold (m s^{-1})
T_o	Reference temperature
θ	Potential temperature (K)
P_0	Reference pressure (≈ 100 kPa)
GPP	Gross primary production [g (C) ha^{-1} growing $season^{-1}$]
NPP	Net primary productivity [g (C) ha^{-1} growing $season^{-1}$]
R_a	Autotrophic respiration
R_h	Heterotrophic respiration
NEE	Net Ecosystem CO_2 exchange (μmol m^{-2} s^{-1})
NEP	Net Ecosystem production [g (C) ha^{-1} growing $season^{-1}$]
R_p	Photorespiration
R_m	Maintenance respiration
R_s	Growth respiration
R_{eco}	Ecosystem respiration (μmol m^{-2} s^{-1}; g (C) ha^{-1} growing $season^{-1}$)
PAR	Photosynthetically active radiation (μmol m^2 s^{-1}; MJ m^{-2} day^{-1})
ET	Evapotranspiration
WUE	Water use efficiency
CUP	Carbon Uptake period
CzeCOS	Czech Carbon Observation System
GPP_{pot}	potential gross primary production
ICOS	Integrated Carbon Observation System
RH	Relative air humidity (%)

CNI	clearness index (dimensionless)
DI	Diffuse index
SVWC	Soil volumetric water content (m^3 m^{-3})
RMSE	Root mean square error
QC	Quality Control
AQC	Automated Quality Control
τ	Momentum flux (kg m^{-1} s^{-2})
MQC	Manual Quality Control
Ts	Soil temperature
P	Precipitation (mm)
DOY	Day of year
GPP_{norm}	Normalized gross primary productivity
SMLR	Stepwise multi-linear regression
RF	Random forest
SPEI	Standardized Precipitation-Evapotranspiration Index
LRC	Light- response curve
α	Apparent quantum yield [mol (CO_2) mol^{-1} (phot.)]
GPP_{max}	Asymptotic maximum assimilation rate at the light saturation point (µmol m^2 s^{-1})
CZ-BKF	Wet/ humid Norway spruce forest ecosystem at Bílý Kříž
CZ-RAJ	Dry Norway spruce forest ecosystem at Rájec
CZ-Stn	Beech forest ecosystem at Štítná
NY	Years with normal conditions
DY	Drought-affected year

1 INTRODUCTION

The recent rapid changes in the global climate have gradually led to rising air temperatures (approximately 1.0 °C above pre-industrial levels), changing precipitation patterns, increasing the occurrence and severity of climatic stress conditions that significantly impact the distribution and survival of plant and animal species (IPCC, 2013). The effects of these environmental changes mainly occur concurrently with other anthropogenic (human-induced) disturbances such as pollution (greenhouse gas emissions), increased deforestation, and land degradation due to urban expansion, increased agricultural activities, and the exploitation of natural resources (Stocker et al., 2014). These natural and anthropogenic stress conditions threaten the viability and resilience of individual plant and animal species. Consequently, this affects the natural ecosystem functioning and lead to extinction in many plant and animal species (Aitken et al., 2008; Jezkova & Wiens, 2016). With global warming, the distribution of terrestrial ecosystems is currently changing since plants and animals follow the shifting climate (Lenoir et al., 2010). Both the rate and intensity of global warming pose severe threats to many natural ecosystems by altering their physiology and seasonal activities. For instance, in Europe, phenological changes in plants, such as flowering and leaf senescence are sensitive to the rise in global temperatures (Parmesan & Yohe, 2003; Cleland et al., 2007). Also, research has shown that the leaf-out of temperate trees has increased by 8-15 days since the 1950s (Fu et al., 2019). Likewise, though many species and ecosystems may migrate to mountainous slopes from lower elevations, the intense warming effect will also shrink these mountainous or upper latitude zones which are mainly characterized by cold conditions (Chen et al., 2011). Thus, climate change will further alter the composition (type of species) and function (fluxes of energy and matter) of the natural ecosystem. Subsequently, this may lead to the local extinction of many plant and animal's species which are unable to adapt to the changing climate (Lenoir et al., 2010). Also, other plants may change their physiological processes to endure the harsh climatic conditions.

Although climate extremes have negatively impacted many natural ecosystems, others have proved to be resilient by either withstanding or recovering from these events. However, the frequent occurrences and severity of these climatic stress conditions will further increase their vulnerability and pose much danger to these natural ecosystems. Additionally, increase in human-induced activities continue to exacerbate the impacts of climate change, and as such

there are many uncertainties as to how climate change will affect the complex interactions and responses among species within many ecosystems and biodiversity across the globe (Vitasse et al., 2021). Therefore, there is the need for more studies that seek to improve our understanding of the impacts of climate change and how these terrestrial ecosystems may respond to these abnormal changes. Also, advances in these studies will help identify some opportunities that could help to better manage and prevent decline of some natural ecosystems. Such efforts should be aimed at lessening the detrimental effects of climate change on species and ecosystems by focusing on ways to maintain habitats and the overall ecosystem structure.

Therefore, the efficient management of these natural ecosystems could provide nature-based solutions that could help reduce greenhouse gas (GHGs) emissions and support human society in adapting to climate change. For example, the release of carbon dioxide (CO_2) into the atmosphere has mostly contributed to global warming the most compared to other GHGs emitted by anthropogenic activities (Haustein et al., 2017). Its current concentration is at its highest level of 412 parts per million (ppm) since the last 800,000 years, further representing a 47% increase in the concentration of atmospheric CO_2 since the beginning of the Industrial Age. These levels of CO_2 keep rising mainly due to the intensive use of fossil fuels (electricity and heat production, industry, transportation, etc.), land-use change, and cement production (Friedlingstein et al., 2019). When fossil fuels like coal and crude oil are burnt, they release much of the carbon stored in plants through photosynthesis over a million years back into the atmosphere over a few years. Thus, the introduction of national and regional policies that promote sustainable agroforestry practices, restore forest ecosystems, and use of certain alternative energy sources such as renewable energy technologies (wind, solar, hydro, wave, tidal, and bioenergy) will minimize GHG emissions and reduce global warming (Shukla et al., 2019). Hence, countries under the United Nations Framework Convention on Climate Change (UNFCCC) have been urged through the Nationally Determined Contributions (NDCs) of the Paris Agreement in 2015 to adopt such national policies and strategies that minimize GHG emissions (Keller et al., 2018).

Generally, both the terrestrial biosphere and the marine environments play a significant role in absorbing about half of the CO_2 that is emitted by fossil-fuel combustion. The plant biomass removes about 30% of anthropogenic CO_2 emissions (2-3 billion tonnes of carbon per year) from the atmosphere (Le Quèrè et al., 2018). To better understand the global carbon budget (emission and absorption of CO_2), there is the need to understand and improve upon the scientific techniques that measure and quantify the flux of CO_2, water vapour, and energy

between the terrestrial ecosystems and the atmosphere (Aubinet et al., 2012; Baldocchi, 2014). Over the past three decades, the eddy covariance (EC) technique has also provided the direct means to estimate the fluxes of GHGs between different terrestrial ecosystems (forest, agricultural fields, wetlands, urban areas, etc.) and the atmosphere, with their dynamic response to extreme meteorological/ climatic conditions (Baldocchi, 2008). Though the terrestrial ecosystems continue to play a vital role in atmospheric carbon sequestration (conversion of atmospheric CO_2 into carbohydrates), recent changes in land use and land cover coupled with the occurrence of harsh extreme climatic events (i.e. rising global temperatures and long summer drought, variability in rainfall amount and distribution) have severely threatened the sequestration capacity of carbon within these ecosystems (Grace, 2004; Ma et al., 2016).

Subsequently, further changes in the climate will affect the physiological responses of plants. An increase in atmospheric CO_2 is expected to increase the plant's water use efficiency and enhance photosynthetic capacity while ensuring increased growth (Schime et al., 2015). In contrast, extreme temperature and variability in precipitation patterns might harm plants beyond their physiological limits, further causing a decrease in water availability and changes to soil conditions, making it difficult for plants to thrive (Parmesan & Yohe, 2003). Additionally, at the ecosystem scale, increasing temperatures will increase the vapour pressure deficit (VPD) and decrease the water use efficiency and the photosynthetic capacity of the ecosystem. It is thus difficult to predict which effect will prevail in the future and whether terrestrial vegetation will continue to serve as a carbon sink or even become a source. These efforts are further complicated by non-linearity and feedbacks (positive and negative) observed in biosphere-atmosphere exchange by its connection with human activities (Canadell et al., 2007; Monson and Baldocchi., 2014).

Vegetation- atmosphere exchange of CO_2 is being studied intensively to determine the source and sink potentials of different ecosystems (Siebicke et al., 2012). Turbulent flux measurements of CO_2 are obtained by the eddy covariance (EC) technique and are collected in a global flux tower network FLUXNET (Baldocchi et al., 2001; Aubinet et al., 2012). The EC method provides an accurate statistical approach to measure the emission and consumption rates of gases, such as CO_2, by computing the turbulent fluxes. The method depends on direct and fast (20 Hz) measurements of the actual gas transport by air vortices (eddies) along the vertical axis within the constant flux layer of the atmospheric boundary layer. These measurements are carried out over several hundreds of sites all over the world on a long-term basis to characterize

ecosystem exchanges of trace gases, water, and energy and to validate process-based models (Pastorello et al., 2020).

2 REVIEW OF LITERATURE

2.1 FOREST ECOSYSTEM-ATMOSPHERE INTERACTION

2.1.1 Turbulent Flow dynamics above the forest canopy

Terrestrial ecosystem-atmospheric interactions mainly occur within the troposphere (lowermost and most dynamic layer of the atmosphere with an average depth of 11 km; Stull, 1988; Levi et al., 2020). These complex and dynamic interactions are crucial for transporting atmospheric quantities such as moisture, heat, momentum, and pollutants, both vertically and horizontally through the atmospheric boundary layer (thin layer of the troposphere that is in direct contact with the earth's surface; ABL). Since the forest ecosystems cover approximately 30% of the terrestrial land cover, many studies have specifically been conducted to understand the exchange of matter and energy between the atmosphere and the underlying forest ecosystems (Aubinet et al., 2012; Baldoocchi et al., 2001; Law et al., 2001; Belcher et al., 2012; McGloin et al., 2018; McGloin et al., 2019; Jocher et al., 2020). The thickness of the ABL above the ground surface can span from tens of meters to several kilometres and changes over time and space often with significant diurnal cycle. This layer is characterized by turbulence (chaotic air motions approximated by eddies of different sizes and speeds), separated from the rest of the troposphere above (the free atmosphere) by capping inversion. The mean wind and turbulence are the main air motions that allow transport of matter and energy within the ABL. The mean wind dominates the horizontal transport; turbulence dominates the vertical transport. Airflow within the surface layer (the lowest layer of the ABL) interacts directly with the earth's surface and is modified by surface forcing on different timescales (usually about an hour or less). In the presence of a forest canopy, the roughness sublayer (that reaches about 2-3 heights of the forest canopy) refers to the part of the surface layer that is affected by the roughness elements such as leaves, branches or individual trees (Garratt, 1994; Monson and Baldocchi, 2014). The roughness of the forest surface increases turbulence in the airflow above the canopy (which causes a drag on airflow near the surface and reduces wind speed) and enhances sensible heat and moisture exchange between the forest and the surrounding air (Rotenberg and Yakir, 2010). Moreover, convection could be caused due to the increase in moisture content of the air above the forest canopy. This leads to cloud formation and an enhancement in rainfall (Mitxelena, 2020). Trees also move in the direction of the wind, which further slows down the wind speed and causes turbulence to increase (Su et al., 1998). Forests modify the weather and

climate through the exchanges of sensible and latent heat, moisture, momentum, and CO_2 with the atmosphere. Micrometeorological measurements are carried out on tall towers mostly reaching above the roughness sublayer into the inertial sublayer (the layer in which fluxes of matter and energy are assumed not to change with height) to obtain information on fluxes of matter and energy from a forest ecosystem.

Moreover, diurnal thermal variations also generate turbulence within the mixed layer (about 1.5 km) above the ground (Manson and Baldocchi, 2014; Fig. 2.1). This turbulent flow of air within this mixed layer is caused by wind shear (variation of wind velocity with height), and buoyancy associated with canopy or surface heating aids in the uniform mixing of heat, momentum, moisture, and pollutants both vertically and horizontally. However, the presence of a statically stable layer of air at the top of the mixed layer (referred to as the entrainment zone) inhibits the vertical extent of turbulence (Seibert et al., 2000). After sunset, the turbulence that existed within the mixed layer decays, and the upper part of this layer is now referred to as the residual layer, where concentrations of gases remain unchanged. During the nighttime, due to the radiative cooling from near the surface of the earth, the lower part of the previously mixed layer is marked by a statically stable boundary layer with very weak turbulence and no mixing. The weak turbulence suppresses vertical transport coupled with pressure gradient forces that drive horizontal winds. After sunrise, the mixed layer is restored and expands depending on the thermal conditions within the day. Thus, the atmospheric condition (stability and instability) affects the quality and spatial representativeness of the eddy data (Vesala et al., 2008; Mauder et al., 2013).

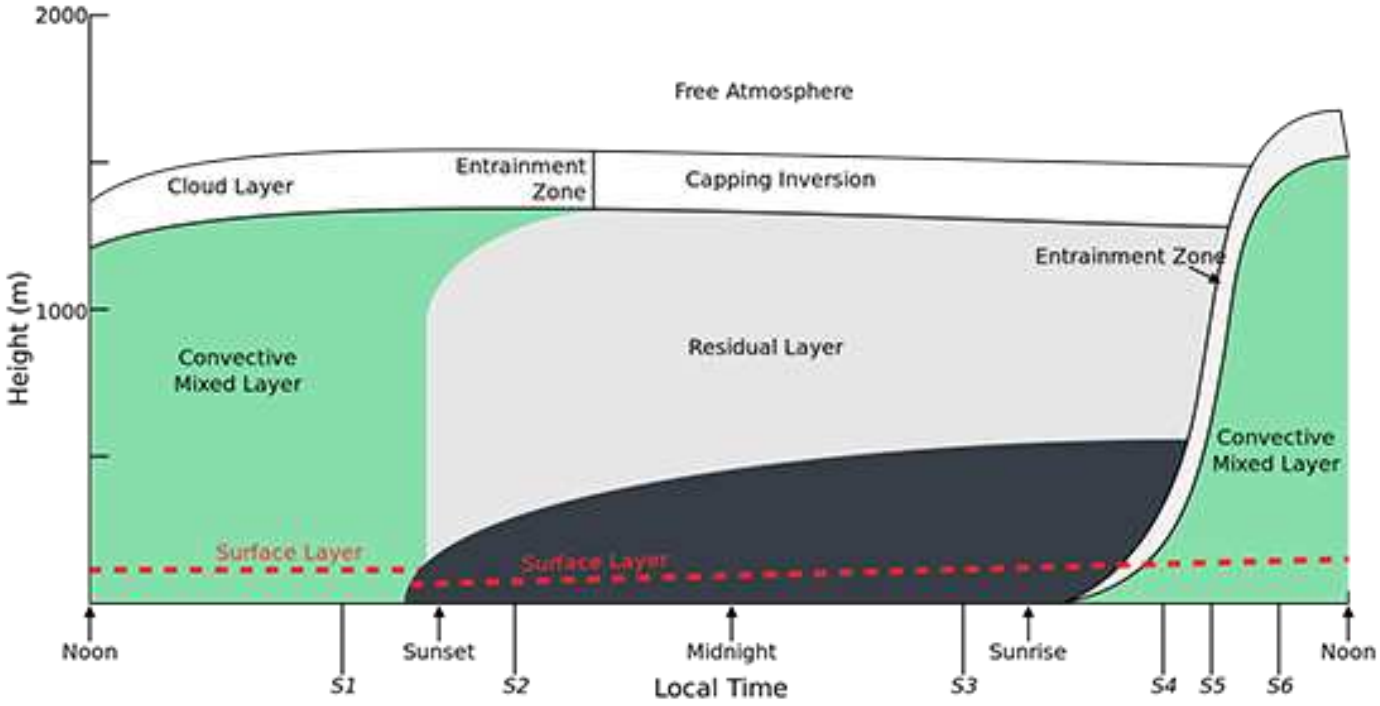

Fig. 2.1: Diurnal evolution of the atmospheric boundary layer (ABL). The black area is the stable (nocturnal) boundary layer. S1 = late afternoon, S2 = just after sunset, S3 = just before sunrise, S4 = just after sunrise, S5 = mid-morning, and S6 = late morning are used as time markers. Source: Stull, R. (1988).

Near the forest canopy, shear stress increases and airflow loses momentum to obstacles such as trees in the opposite direction of motion (due to frictional force). Hence, it is only near the surface that the mechanical turbulence can significantly contribute to air mixing (Raynor, 1971; Jiao-jun et al., 2004; Zhu et al., 2006; Monson and Baldocchi, 2014). For conditions within the surface layer that are considered as statically neutral, airflow in a forest stand (Fig. 2.3) follow a classic logarithmic law which can be expressed empirically by equation 1, using the so called Monin-Obukhov similarity theory (Monin and Obukhov, 1954):

$$M = U^* \frac{1}{K} ln\left(\frac{z-d}{Z_o-d}\right) + \phi_i \qquad (1)$$

where M is the horizontal mean wind velocity in m s^{-1} at height z, U* is the friction velocity in m s^{-1}, K is the von Kármán's constant (0.40, dimensionless); z is the measurement height from a reference plane in meters; Z_0 is the roughness length in meters; h_c is the average forest canopy height; d is the displacement distance ($0 \leq d \leq h_c$); and ϕ_i is the mean velocity that depends on

the Richardson's number (Ri, dimensionless). Under statically neutral conditions, U* can be interpreted as the tangential velocity of eddies (Foken, 2008). The term (z - d) provides scaling that allows inter-site comparisons and eliminates singularities during daytime and nighttime transitions.

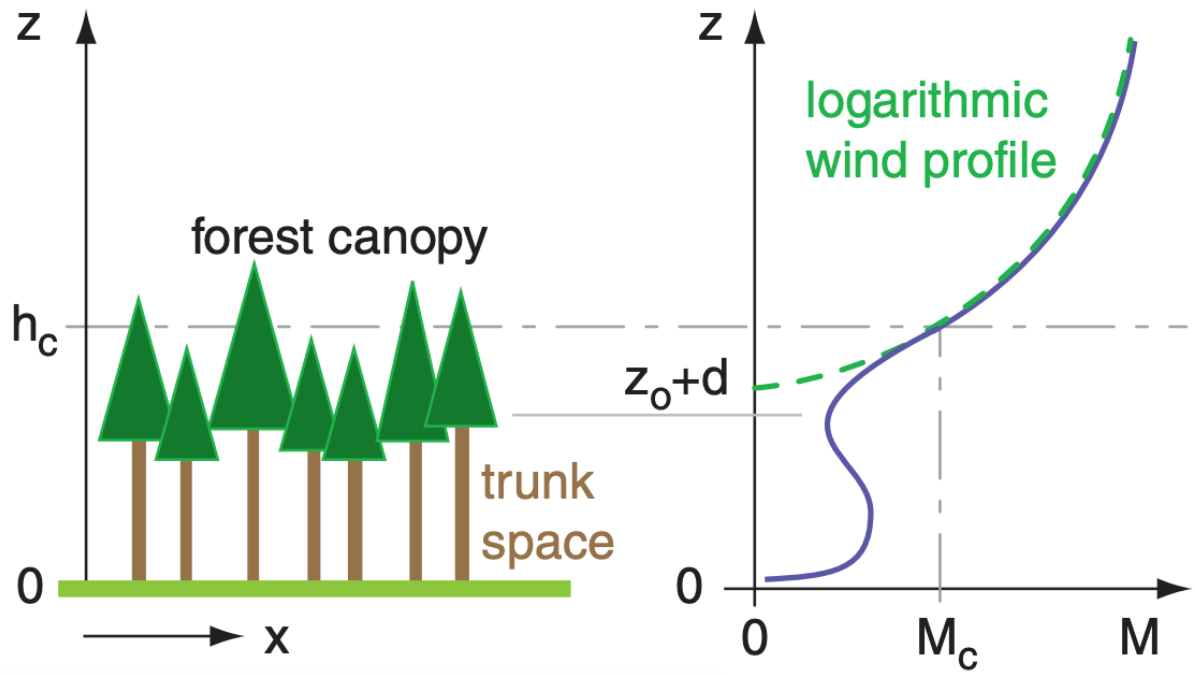

Fig. 2.3: Canopy airflow for forest canopies with an open trunk space (without many leaves, branches, or smaller underbrushes). Left: Sketch of the forest canopy. Right: Solid blue line represents the Wind profile, and the dashed green line also shows the logarithmic profile extrapolated to zero wind M. M_c is the average wind speed at the average forest canopy height, h_c; Z_0 is the roughness length in meters; d is the displacement distance ($0 \leq d \leq h_c$). Source: https://geo.libretexts.org/ (accessed on 7th March 2021)

Within the topmost part (2/3) of the forest canopy, an exponential formula describes the average wind speed M profile (Zhu et al., 2000):

$$M = M_c \,.\, exp\left[a.\ \left(\frac{z}{h_c} - 1\right)\right] \qquad \text{for } 0.5h_c \leq z \leq h_c \qquad (2)$$

where M is the horizontal mean wind velocity in m s^{-1} at height z, M_c is the average wind speed at the average forest canopy height, h_c; z is the measurement height from a reference plane in meters; $\alpha \approx 1.0 - 1.1$ for conifer trees.

Although the typical patterns of airflow above the forest canopy has been observed to have widely been characterized by the logarithmic wind profile, other studies by Baldocchi and Meyers (1988), Turnipseed et al. (2003), Yi et al. (2005), Queck and Bernhofer (2010), and Sypka and Starzak (2013) have observed an S-shaped wind profile with an exponential Reynolds‘ stress profile. This S-shaped wind profile is mainly due to a secondary wind maximum that has been observed within the trunk space of the forest and a secondary minimum wind speed in the region of large foliage density.

Also, the airflow or wind speed (air with velocity and direction) could be characterized as three superimposing components within the Cartesian coordinate system: 1) parallel or longitudinal component (u) along the x- coordinate; 2) perpendicular or crosswind component (v) along y- coordinate, and; 3) vertical or oblique component (w) along the z- coordinate. The contribution of each of these wind components to the wind speed varies with time and also exhibits regular and chaotic patterns. Air motions could be classified into three categories: the mean wind, waves and turbulence (Fig. 2.2). The horizontal transport of both matter and energy is influenced by mean wind, whereas the vertical transport is dominated by turbulence (Stull et al., 1988). The mean wind is also characterized by regional pressure gradients and local orographic effects that are associated with the local weather conditions. The waves often exhibit periods of several hours, and as such, their effects are often neglected in the application of the eddy method. Turbulence which is of significant interest in micrometeorology is observed as the random deviations from the mean wind (Monson and Baldocchi, 2014). Thus, scientists quantify the surface-atmosphere exchanges above the forest canopy through the eddy covariance method by measuring the variations in the vertical wind speed and the atmospheric scalar quantity of interest from towers extending above the forest.

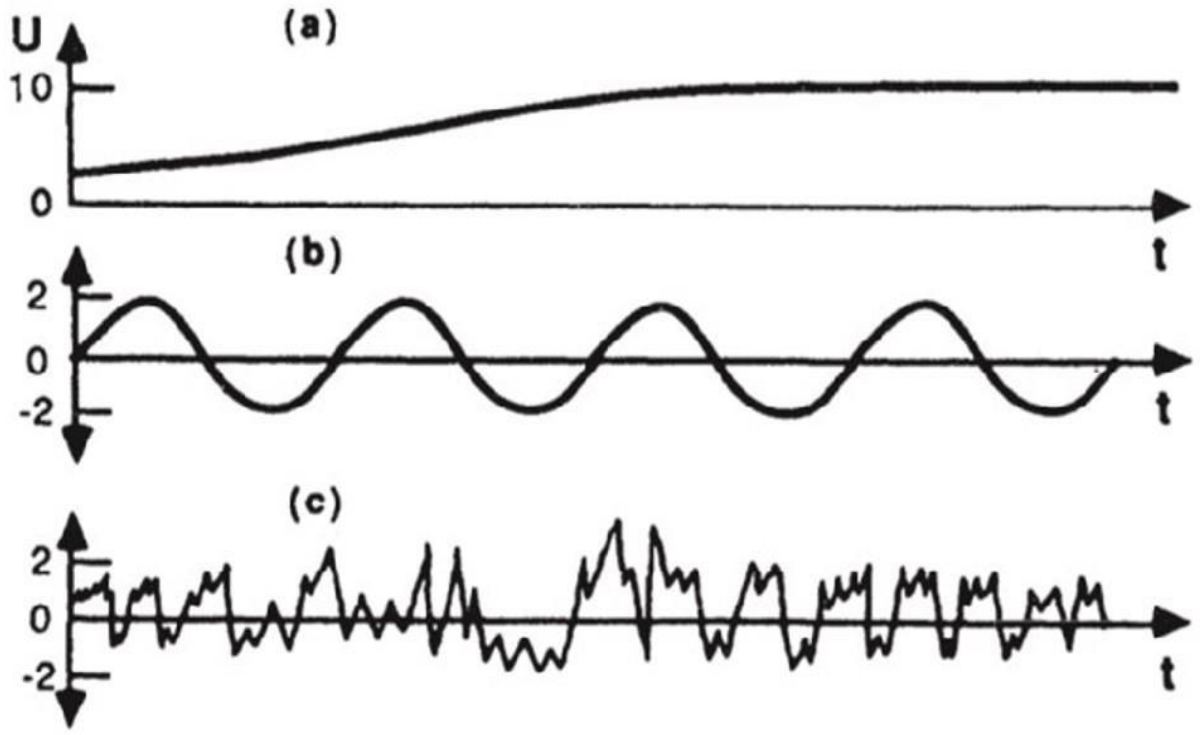

Fig. 2.2: The idealization of (a) mean wind, (b) waves, and (c) turbulence. In reality waves or turbulence are often superimposed on a mean wind, where U is the component of wind in the x- coordinate (after Stull, 1988). Source: Haggagy, 2003.

Generally, the turbulent air motions are usually described as vertically oriented vortices, eddies, that are advected along with the mean wind. Although the eddies carry vital information on the fluxes above the active surface, it is impossible to measure those required properties of eddies at a given time across the relevant spatial domain. Therefore, Taylor's frozen turbulence hypothesis offers the solution for this challenge (Taylor, 1938). This hypothesis states that under conditions when the properties of eddies are assumed not to change significantly over time, their properties are sampled while they pass along the sensor. Through this way, the signal is first obtained from the leading edge and later from the trailing edge of the hypothetical eddy. The time delay between these registered signals is given by the eddy sizes (in diameter) and the mean wind speed. This approach is valid in cases when the eddies develop over longer timescales than the required time to pass the sensor.

The real turbulence comprises a mixture of eddies with different sizes (on the scales from millimetres to kilometres) and varying timescales (from seconds to days). The eddies with larger sizes tend to increase with height above surface and break apart into smaller ones while

energy is transferred towards lower scales in inertial cascade. The turbulent kinetic energy (TKE) being one of the most important variables in micrometeorology (a measure of turbulence intensity), is produced by fluid shear, friction or buoyancy and transferred through the energy cascade, which is later dissipated to heat by molecular viscosity. Large eddies with low cyclic frequencies are characterized by majority of the TKE while the eddies of other intermediate sizes neither create nor consume this energy. The Kolmogorov microscale also refers to the length scale associated with the most efficient energy dissipation and can be approximated to about 1 millimetre (Kolmogorov, 1941). Thus, only the eddies with smaller sizes convert kinetic energy to internal due to their inability to overcome the viscous forces. Similarly, the main contribution to the momentum, heat, and moisture transport comes from the larger eddies and decreases with size. Turbulence is significantly (10^5 fold) more effective in the transport of scalar entities than molecular diffusion (Foken, 2008) and produces the flow per unit surface area per unit of time called flux density, commonly termed as flux. The direction of the net flux mostly opposes the density gradients of transported entities since the exchange between the atmosphere and active surface follows the thermodynamic laws. Therefore, the net flux in biogeochemical systems is mainly determined by the magnitude of sources and sinks that describes the general property of different processes that creates (e.g. respiration, transpiration, inertia) or consumes (e.g. photosynthesis, condensation, viscosity) matter and energy. Generally, a negative flux sign is used to describe situations when the turbulent flux direction is towards the surface from the atmosphere.

The Reynolds' decomposition introduced in 1895 by Osborne Reynolds is a mathematical concept that allows us to estimate turbulent fluxes (Reynolds, 1895). In assuming that turbulence is statistically not changing with time, the Reynolds decomposition is applied to split the instantaneous values of the wind vector element (w) and the eddy entities (θ, and specific moisture, q) into mean and fluctuating parts (Kaimal and Finnigan, 1994) as shown below;

$$\begin{aligned} w &= \overline{w} + w' \\ \theta &= \overline{\theta} + \theta' \\ q &= \overline{q} + q' \end{aligned} \tag{3}$$

2.2 APPLICATION OF EDDY COVARIANCE IN FOREST CARBON MONITORING

2.2.1 The Eddy Covariance System

The EC system comprises a fast response ultrasonic anemometer, and infrared gas analyser placed on a meteorological mast within an inertial sublayer. These instruments allow for the measurement of the wind components (u, v, and w), air temperature, and fluxes of water vapour and CO_2 at a required frequency of 10 Hz or more (Aubinet et al., 2012). Half-hourly flux data are obtained from the post-processing of high-frequency signals. Currently, recent improvements in the scalar concentration measurements have also enabled the measurements of less abundant greenhouse gases such as CH_4, N_2O, other volatile compounds (e.g., isoprene, monoterpenes), and gaseous pollutants (O_3, NO_2, NO, SO_2).

2.2.2 Theoretical Considerations of the Eddy Covariance Method

Over the last two recent decades, the eddy covariance technique has emerged as the most direct and non - destructive approach to measure and study the matter and energy exchange between the atmosphere and the terrestrial ecosystems over multiple years (Stull, 1988; Foken et al. 2012). Turbulence, as observed above, the canopy leads to the transfer of atmospheric entities such as momentum, heat, and water vapour across a plane normal to the vertical wind component per unit mass and unit time (Stull, 2000). Hence, implying a correlation between the wind vector and the atmospheric entity. The theoretical basis of the Eddy flux estimation was described in chapter 2.1.1 by introducing the Taylor's frozen turbulence and a mathematical concept of Reynold's decomposition. The solutions of Reynolds' decomposition for scalar entities (absolute air temperature- Tair, water vapour and CO_2) allows us to compute the vertical fluxes of sensible heat (H), latent heat (LE) and CO_2 (F_{CO2}) as;

$$H = \overline{\rho}\, c_p\, \overline{w' Tair'}\ , \tag{4}$$

$$LE \equiv \lambda E = \lambda \overline{\rho}\, \overline{w'\, q'}, \tag{5}$$

$$F_{CO2} = \overline{w'\, d'_{CO2}}\ , \tag{6}$$

Where H and LE are W m^{-2} and F_{CO2} in μmol m^{-2} s^{-1} with additional constants and variables are included to account for the correct units. An overbar represents the mean over averaging period, a prime represents the deviation from the mean, with λ as the latent heat of vaporization (J kg^{-1}), q is the specific humidity (dimensionless) and d_{CO2} is molar density of CO_2 (μmol m^{-3}).

Practically, the acquired raw signals need to be corrected, converted to suitable units, and controlled as to its quality by means of a processing software. There is also the need to correct for errors caused by challenges with the set-up (as a result to factors such as instrument tilt and separation) and physical principles (such as instrument heating). Each of the half – hourly flux measurement is assigned a quality code based on the operation of the instrument, intensity of turbulence, and the steady state conditions as required by the method. According to Aubinet et al. (2012) all data not meeting the quality requirements are rejected and gap – filled. Analysis of the flux footprint is also very important. The fraction of the upwind surface carrying effective sources and sinks that contribute to the measurement point is referred to as the flux measurement's footprint. This defines the measurement's spatial context (Schuepp et al., 1990). The distance from the flux tower up to the farthest point of the footprint (the fetch) should not exceed the ecosystem of interest. Consequently, if this conditions are not met, flux data from areas extending beyond the ecosystem of interest need to flagged and removed from further analysis. Equations 13 – 15 impose certain assumptions as air density fluctuations, advection (horizontal and vertical mean flow divergence), horizontal turbulent flux divergence and horizontal variation of the vertical flux are negligible. This approximation is mainly valid under well – mixed conditions over flat, homogenous terrain.

In order for the EC fluxes to represent the underlying physiological processes (biotic fluxes such as ecosystem sensible heat flux, evapotranspiration, and the net carbon uptake), a storage flux indicating time-dependent storage of matter or energy within the control volume needs to be accounted for (Aubinet et al., 2012). This storage term mainly becomes significant during night - time periods and shortly after convective mixing in the morning period. Thus, for an accurate representation of the sink or source nature of the active zone, the storage flux component must be well accounted for during the overall flux computation. Moreover, since the maximum potential for storage of matter and energy are realized below the measurement level within the forest ecosystem, its derivation requires sampling of Tair, relative humidity, and CO_2 fluxes in the vertical profile for the respective fluxes.

Studies by Goulden et al. (1996) and Massman and Lee (2002) have shown that under stable atmospheric conditions, the eddy method underestimates CO_2 fluxes. In practice, all sites are

affected and the simple addition of the storage term does not solve this limitation due to the presumed decoupling and advection effect (Aubinet et al., 2012). The underestimation of the night – time CO_2 flux represents selective systematic error (Moncrieff et al., 1996) and could lead to considerable overestimation of annual NEP if not corrected (Falge et al., 2002; Goulden 2006). Therefore, the accepted treatment for such error is the u^* filtering (Barr et al., 2013; Papale et al., 2006; Reichstein et al., 2005). Since is considered as a measure of the intensity of turbulence, the CO_2 flux response to u^* during the night – time can be used to identify the u^* threshold (UT) below which such underestimated fluxes are derived due to low convective mixing. This leads to the exclusion and gap – filling of CO_2 fluxes that are measured at u^* values below UT.

2.2.3 The complexity of vertical exchange above tall canopies

The measurement of atmospheric fluxes over complex ecosystems such as forests have been complicated due to the height of the roughness element that interferes with the physical interaction between the canopy and the atmosphere (Barr et al., 2007; Wilson et al., 2002; Belcher, 2005; Dupont and Patton, 2012). As a result of these interactions, turbulence above these tall vegetation is strongly affected by tree phenology, leaves, and branches that influence atmospheric airflow within and above the canopy. This section discusses the effect of such complications on matter and energy flux measurements.

2.2.3.1 Canopy Waves and Flow Decoupling

The canopy flow within and above the forest cover is significant in the atmosphere-forest ecosystem interaction. Under convective atmospheric conditions, the airflow within the open canopy is coupled by turbulent exchange to airflow above. However, during the transition to strongly stable atmospheric conditions, both airflows (within and above the canopy) decouple, and vertically coherent waves are observed to form within the forest canopy, even if the flow above remains fully turbulent. Due to the formation of these within-canopy waves, large random errors could be introduced into the measurement of the change in storage and advection terms in the mass balance equation. Therefore, it is needed to better understand the

dynamics that lead to such decoupled flow and the impact of within-canopy canopy flows on ecosystem-scale estimates of the exchange of scalars (Finnigan, 2004; Katul et al., 2013; Thomas et al., 2006; Thomas et al., 2013).

According to Brunet and Irvine (2000), the active turbulence near the top of a canopy has similar flow characteristics of a plane mixing layer due to the missing rigid boundary at the crown interface. These atmospheric flows are affected by diabatic stability and during stably stratified airflows, turbulence is suppressed when the local Richardson number, R_i exceeds a critical value of $Ri_c = ¼$ (Miles 1964; van Gorsel et al., 2008). The Ri is mathematically defined as (Richardson, 1920);

$$\mathrm{Ri} = \left[\frac{\left(\frac{g}{T_0}\right)\left(\frac{\delta\theta}{\delta z}\right)}{\left(\frac{\delta U}{\delta z}\right)^2}\right] \tag{7}$$

where g represents the acceleration of gravity, with T_o as the reference temperature, θ is the potential temperature (the temperature that an unsaturated dry air parcel may assume if brought adiabatically or reversibly to a reference pressure, $P_0 \approx 100$ kPa from its initial state), z is the height, and U is the mean wind speed.

Moreover, for values of $Ri_c > ¼$, the turbulent flow of air loses kinetic energy as fluid parcels get displaced in the stable density gradient at a faster rate than it can gain energy from the mean shear. Thus, confirming turbulence suppression in real atmospheric flows under stability, though Ri may not precisely be ¼. Other studies carried out by Lee et al. (1997), and Katul et al., 2013 in several sites have shown that large fluctuations in both temperature and wind vector could occur within canopies even if $Ri > Ri_c$. There is strong evidence of the significant impact of wind shear at the inflection of the wind profile on flow instabilities (Kelvin-Helmholtz waves), especially at the top of the canopy (Katul et al., 2013). Therefore, under stable conditions, waves retain their initial form when turbulence is weak, as Lee et al. (1997) demonstrated. For instance, considering the structure of nocturnal inversion that occurs on clear nights (atmospheric stably stratified conditions), the airflow above the canopy is decoupled from the within - canopy flow. As a result, turbulence gets suppressed, leading to the so-called night - time CO_2 flux underestimation, as explained by Aubinet et al. (2012), Thomas et al. (2007), and Jocher et al. (2017). Additionally, according to studies by Fitzjarrald and Moore (1990) and Jocher et al. (2017), sub canopy EC measurements are promising approach for filtering periods affected by decoupling. Also, the presence of organized structures above forest ecosystems with sloped forest floor like in the young Norway spruce forest at Bílý

Kříž (downhill flows on the lee side of the mountain crest) have been observed (Alekseychik et al., 2013; Potužníkova et al., 2015; Schilperoort et al., 2020). Vertical exchange of heat, water vapour, and CO_2 can be significantly affected by decoupling, density flows, and advective transport mechanisms.

To minimize the effect of decoupling in flux measurements, Papale et al. (2006), Barr et al. (2013), and Alekseychik et al. (2013) used the so-called "u_* filtering" method at the quality control stage to flag and remove all flux data with low friction velocities (u*). Hence, ensuring the analyses of eddy covariance data with sufficient turbulence. Based on the sensitivity of CO_2 flux to u* over different timescales, u* threshold derived from the u* filtering method could vary for various forest sites. However, in the study by Barr et al. (2013), a stable u* threshold was derived for 28 out of 38 tested sites, though they were higher in other studies where u* threshold varied with time. Another limitation in the u* filtering method as highlighted by Jocher et al. (2020), is the inability of this approach to consider the significant impact of buoyancy forcing. To avoid such limitation, Bosveld et al. (1999) proposed the inclusion of a term into the u* filtering method that examines an aerodynamic Richardson number based on the u* above the canopy and the difference in temperature within the forest canopy and the ambient temperature. Even so, very accurate information on the profile of air temperature and radiometric surface temperatures above the canopy is needed to derive the decoupling threshold, and these are generally not available (Schilperoort et al., 2020).

Moreover, another method that analyses deviations in the vertical wind speed (σ_w) within and above the forest canopy has been proposed by Thomas et al. (2013) to address the challenges with u* filtering. In a recent study at the spruce forest stand with complex terrain in Bílý Kříž, Jocher et al. (2020) applied Telegraphic approximation (TA) to determine the relationship between the "above - and below - canopy" air flow. High values of TA between the two air masses indicated coupling, while low values showed decoupling (Cava et al., 2004). Such filtering approach employing below – canopy EC measurements has the potential to improve and minimize the effect of decoupling, thus improving the accuracy of measurements (Thomas et al., 2013; Jocher et al., 2018).

2.3 FOREST ECOSYSTEM CARBON DYNAMICS

Forest ecosystem comprises the living organisms of the forest, and extends from the lowest soil layers affected by the roots and biotic processes to the surrounding air over the forest canopies (Waring and Running, 2010). Since most living organisms depend on plants for life, a good knowledge about the practical factors that affect the productivity of plants or the forest through photosynthesis is of great significance (Prentice et al., 2001; Nemani et al., 2003). These forest ecosystems also serve as open systems that directly exchange matter and energy with other systems (atmosphere, and aquatic ecosystem). The carbon cycle begins with the forest ecosystems when plants sequester CO_2 from the atmosphere through photosynthesis into reduced sugars. Mostly about half of the total amount of CO_2 fixed into the forest stand (termed as the gross primary production- GPP) are later used by plants in autotrophic respiration (R_a) to produce and maintain living cells. This process releases the stored CO_2 back into the atmosphere. The net primary productivity (NPP) refers to the carbon products that remain after the balance between GPP and carbon released by R_a (i.e. GPP – R_a) stored in leaves, branches, stems, roots and other plant reproductive organs. Both the GPP and the NPP are generally measured at the ecosystem scale and over more extended periods. Plants usually shed their leaves and roots, and their dead organic matters form detritus that release CO_2 back into the atmosphere through heterotrophic respiration (R_h). Thus, the net ecosystem production (NEP) also refers to the net amount of CO_2 that is fixed by photosynthesis and lost by both autotrophic and heterotrophic respiration (as shown below):

$$\text{NEP} = \text{GPP} - R_a - R_h \tag{8}$$

Through the NEP, an ecosystem may be considered a carbon sink or source (typically drought spell or prolonged cloudy conditions) in relation to the atmosphere. Therefore, the estimation of the forest GPP (total amount of CO_2 fixed into the forest stand) from the net ecosystem CO_2 exchange (NEE; Fig. 2.3) is useful in providing detailed information on the ecosystem's photosynthetic capacity (in sequestering carbon) and how these environmental factors could control forest productivity at specific periods (Beer et al., 2010; Marek et al., 2011; Lal et al., 2018; Murthy et al., 2019). Thus, over the last few decades, ecologists have continuously sought to gain a broader understanding on the significant impact of such environmental factors (such as radiation, temperature and water) and other biological factors on these exchange of matter and energy between the forest ecosystem and the atmosphere. NEE

measured during the day – time include GPP, photorespiration (R_p), maintenance respiration (R_m), and growth respiration (R_s) of autotrophic plants with R_h:

$$\text{Day – time NEE} = \text{GPP} - R_p - R_m - R_s - R_h \quad (9)$$

However, at night – time hours, the photosynthetic terms such as GPP and R_p are absent:

$$\text{Night – time NEE} = -R_{eco} = -R_m - R_s - R_h \quad (10)$$

where R_{eco} is the total ecosystem respiration without the R_p and is mainly controlled by temperature.

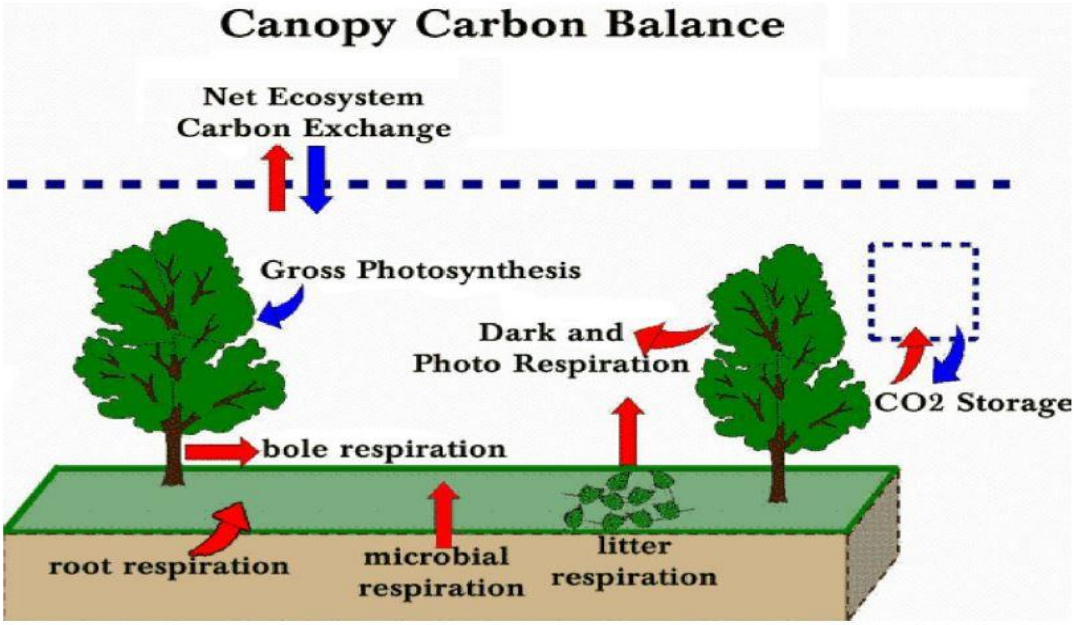

Figure 2.3: Net Ecosystem CO_2 Exchange (NEE) within a Forest Ecosystem.
Source: https://slideplayer.com/slide/2407916/ (accessed on 7th March 2021)

2.3.1 Environmental drivers of forest carbon fluxes

The rate at which plants photosynthesize mainly depends on the amount of the sun's visible radiation that is absorbed by the plant canopy, i.e., the interception of photosynthetically active radiation (PAR, MJ m^{-2} day^{-1}, from 400 to 700 nm) due to its low albedo (reflectivity of the surface = 0.08). Thus, the amount of PAR is a key biophysical factor in controlling basic biological processes like photosynthesis and assimilate production (Fleisher et al., 2010; Tian

et al., 2016). However, the amount of light energy (from the sun) that can be absorbed or intercepted by trees and forest stands primarily depends on the forest ecosystem's crown and canopy characteristics (Binkley et al., 2013). The Beer's Law for absorption of sunlight explains the logarithmic trend of light absorption through the crown of a forest stand, as the existing layer of leaves successively absorbs the incident light (Binkley et al., 2013). There are also other studies that have been conducted to investigate further the effect of such variations in the intensity and quality of light absorption on forest GPP, forest dynamics, and competition between individual tree species (Duursma and Mäkelä, 2007; Balandier et al., 2009; Urban et al., 2007; Tian et al., 2010; Urban et al., 2012). For instance, Urban et al. (2007) showed how the spruce forest canopy CO_2 absorption in Bílý Kříž of the Czech Republic varied directly with a change in the balance of direct and the diffuse components of the incoming solar radiation. Within such a dense forest canopy structure, diffuse radiation was more efficiently utilized for canopy photosynthesis than direct radiation. This phenomenon explains the less efficient use of radiation by the forest stand at high irradiance (during clear sunny conditions) due to the saturation rates at which photosynthesis occurs (Roderick et al., 2001).

Additionally, other environmental factors that could significantly affect forest growth and health are air temperature, humidity, and soil moisture. Generally, plants obtain water by absorbing water by the roots and distributing it to all parts of the plant via the xylem. On the other hand, water is lost into the atmosphere via transpiration through the plant stomata (i.e., small pores that appears on the surface of leaves through which gas exchange occurs between plants and the atmosphere) which also controls the uptake of CO_2 for photosynthesis. As such, through photosynthesis, carbon is assimilated and allocated to plant tissues. Hence, any change in the balance between photosynthesis and respiration/ decomposition will alter the carbon sequestration potential of the forest ecosystem. If the cost of photosynthesis (loss of water vapour) becomes too high, the stomata close to avoid water stress (Gu et al., 2002b). Subsequently, during clear sky conditions with high temperatures and low relative humidity, the stomata close due to increased evaporative demand, and photosynthesis can be significantly reduced (Muraoka et al., 2000). At the forest ecosystem scale, the water use efficiency (WUE, ratio of photosynthetic carbon assimilation over transpiration) is widely recognized as an important variable between the carbon and water cycle and is usually described as the ratio of GPP over evapotranspiration (ET) derived from EC measurements (Law et al., 2001; Hu et al., 2008; Niu et al., 2011). It has also been described in other literature as the ratio of instantaneous photosynthesis to stomata conduction (Beer et al., 2010; McCarthy et al., 2011; Sun et al.,

2016). It is a well – known fact that during meteorological and edaphic drought events, high vapour pressure deficit (VPD; which is defined as the difference between the saturation and actual vapour pressure) within the forest ecosystem typically causes a decline in the plant's stomatal conductance, which minimizes the loss of water from the plant and also prevent water tension within the xylem at the cost of reduced photosynthesis (Zhu et al., 2011). As a consequence of its direct effect on plant physiology, high VPD values leads to an increased rate in loss of water vapour from moist soils and in turn causes drying and heating of terrestrial surfaces, which contributes to the frequent occurrences and severity in drought events and plant stress (Dai, 2013). Thus, the impact of increasing VPD on the WUE of plants remain a major determinant of plant water relations and continues to become an important point of study for different forest ecosystems with contrasting climatic conditions and water availability over the upcoming decades due to the global temperature – driven rise (Way et al., 2013; Grossiord et al., 2020).

2.2.2 Seasonal variations of Net Ecosystem CO_2 exchange (NEE) within temperate forest ecosystem

The changes in the photosynthetic capacity of plants comprise both diurnal and seasonal cycles. The variations in light availability, which is associated with the earth's rotation, mainly drives the diurnal photosynthetic cycle. However, the seasonal photosynthetic cycle is more complex as it is controlled by internal biological processes and also driven by the periodic variations in a set of interdependent environmental factors such as photoperiodic signals, radiation, temperature, nutrient and moisture availability (Parmesan and Yohe, 2003). For instance, the phenology of woody plants within the temperate latitudes alternate between periods of rest (dormancy) to shoot growth and flowering mainly due to both photoperiodic signals (relative length of days/nights) and the annual course of temperature (heating or cooling) (Schwartz, 2003; Cleland et al., 2007; Leith, 2013). Also, the effect of phenology on NEP in both the boreal and temperate forest ecosystems has well been documented, and this is evidenced by its control on the seasonal onset and ending of the carbon uptake period (CUP; Black et al., 2000; White and Nemani, 2003; Barr et al., 2004; Churkina et al., 2005; Baldocchi et al., 2008). Thus, the timing of leaf-out and dormancy (senescence) plays an important role in determining the length of the growing season and subsequently the carbon sequestration

capacity of forest ecosystems (Tang et al., 2005; Richardson et al., 2006; Xie et al., 2016). These seasonal variations of the CUP within the forest ecosystems affect the global carbon cycle and, therefore the need to better understand the physiological responses of different plant species to the changes in environmental conditions across different forest sites. The continuous-time series of EC fluxes provide detailed analysis on these key phenological factors that regulate the seasonal cycles of canopy conductance and the photosynthetic capacity of specific forest ecosystems (Gu et al., 2002b; Barr et al., 2007). These EC analyses also have the potential to explain the main processes that control the spring startup and autumn break in photosynthesis, which indicates factors and threshold values that are similar across different forest sites and years (Baldocchi et al., 2008).

The temperate forests are mainly dominated by deciduous and coniferous evergreen tree species that are physiologically dormant during the cold winter conditions. For the deciduous tree species, the plants drop their leaves in autumn, thereby causing high seasonal changes in the light availability to the understory. During the leaf senescence, the chlorophyll is deteriorated by plant hormonal signals to the leaves. As such, the nutrients from the leaves are translocated to the stem and trunk tissues before the leaves fall off (Huctchison & Matt, 1977; Hoch et al., 2003; Dreiss and Volin, 2013). Buds get formed and become dormant until the following spring period when a rise in temperature triggers leaf growth. The timing of the bud break and expansion of the leaf area differs for canopy tree species, with the development of the forest canopy starting over a month or more (Hoch et al., 2003). Once the leaf–out period starts and the growing season begins, about 1% - 5% of sunlight gets to the forest floor, and the openness of the forest canopy due to the leaf senescence creates an opportunity for maximum light penetration to the understory vegetation (Gill et al., 1998; Dreiss and Volin, 2013). However, with the onset of the warm season, herbaceous plants, shrubs and small trees start their growth before the forest canopy. Also, since there is maximum incident solar radiation flux mostly in the spring months, light is efficiently transmitted through the forest, and most understory plants easily reach photosynthetic capacity before leaf – out (Augspurger, 2008; Richardson & O'Keefe, 2009). Other shade-tolerant species within the forest ecosystem continue to grow after the forest canopy closure (Kudo et al., 2008).

Additionally, the seasonal cycles of the carbon fluxes within the temperate deciduous forests are unique since foliage must first be produced before the occurrence of photosynthesis. As a result of this, the growing season is shortened, and R_{eco} becomes the dominant carbon flux during the first 4–5 months of the year (Richardson et al., 2007). Therefore, the CUP, which is

potentially a useful indicator of annual carbon sequestration, is mainly controlled by the length of the main growing season and this has much predictive power on the spatial variation of annual NEE (Baldocchi et al., 2001; Barr et al., 2007). For instance, the length of CUP can explain about 80% of the spatial variance in the annual NEE of deciduous forests across the temperate region. Although photosynthesis begins later in a deciduous forest compared to an evergreen coniferous forest, the photosynthetic carbon gain rates of deciduous forests are much higher (sometimes twice the rate as in the coniferous evergreen forest stands) (Gaumont-Guay et al., 2008). Also, due to the shortening of the growing seasons, the temperate deciduous forests are potentially susceptible to the change in climate and other related extreme weather events (Vose et al.,2012).

In contrast to the temperate deciduous tree species, the evergreen conifers either have flat, triangular-shaped or thick needle-like leaves that increase their leaf area for photosynthesis and also make them well-adapted against desiccation (Sprugel et al., 1989; Brodribb et al., 2010). The rate of an area or massed–based leaf photosynthesis in the needle-leaved evergreen tree species is lower than in deciduous tree species except when reduced over the leaf's life (Bushing & Fujimori, 2005). The evergreen forests are well known to retain their leaves for a more extended period, whereas the temperate deciduous trees only keep their leaves for one growing season. Due to the evergreen nature of the canopy of these temperate forests, the understory vegetation generally experiences low light availability (Brantley & Young, 2009). As a result of this effect, the understory plants within these evergreen temperate forests are well adapted to respond quickly by maximizing their light capture as well as their photosynthetic capacity under such low light conditions (sun flecks, and brief unpredictable periods of high sunlight). The shaded plants within these forests allocate more growth to leaves and are displayed as larger and thinner leaves that have a more horizontal area to easily capture light (Boardman, 1977; Bushing & Fujimori, 2005). Physiologically, shady leaves saturate at low light levels and have lower light compensation points that enable them to maintain positive rates of photosynthesis at such low light conditions.

Plant phenology remains as one of the most visible biological indicators of ongoing climate change. Despite the significant effect of photoperiod on the phenology of some European tree species (Vitasse and Basler, 2013; Way and Montgomery, 2015), Tair has a rather dominant effect in determining the seasonal onset and senescence (Vitasse et al., 2009; Shen et al., 2014). Thus, given the effect of temperature on the seasonal changes of NEP within the temperate forest ecosystems, global warming is the most immediate threat to the structure

and function of these temperate forest ecosystems. Long-term observational ecological records have shown that due to regional and global change in temperatures, there have been observed shift in phenological events such as earlier leaf-out and flowering in spring and the overall delayed leaf senescence in fall especially for deciduous forest canopies (Sparks et al., 2000; Chuine and Beaubien, 2001; Linderholm, 2006; Tape et al., 2006). The warm spring periods coupled with the late cessation of the growing season (Groisman et al., 1994; Fu et al., 2020) has caused the leaves to grow earlier, sometimes by up to a month, thereby increasing the growing season's length and the CUP of these temperate forests (Beaubien and Freeland, 2000; Ahas et al., 2002; Lu et al., 2006; Schwartz et al., 2006; Sherry et al., 2007). Results from several studies (Menzel and Fabian, 1999; Jackson et al., 2001; Cao et al., 2004) have shown that the lengthening of the growing season by ~ 5 – 10 days may cause a 30% increase in the annual NPP of these temperate forest ecosystems. However, such a significant increase in the NPP can only be possible if the GPP responds well to higher temperatures than R_{eco}.

Furthermore, studies by Barr et al. (2004) and Piao et al. (2008) have shown that the lengthening of the growing season by a number of days due to the earlier onset of the spring phenology will enhance the net carbon uptake than a lengthening of the growing season by the same number of days in autumn. Though not all forests may respond similarly, these studies based their findings on the more significant radiative inputs with longer days, adequate moisture availability from snowmelt, and relatively lower evaporative demand in spring than in autumn. The increase in the carbon sequestration capacity of these forest ecosystems due to the lengthening of the growing season will help mitigate climate change by increasing the terrestrial carbon sink.

Moreover, due to global warming, more frequent and intense heat waves (IPCC, 2014) coupled with low precipitation amounts that mainly occur during the growing season period may further advance or delay leaf senescence (Breshears et al., 2006; Allen et al., 2010). Consequently, the impact of these hot drought periods on forest productivity will be severe, especially over forest sites characterized by drier climatic conditions with limited availability of moisture (Ciais et al., 2005; Allen et al., 2010; Orth et al., 2016; Mensah et al., 2021a). Additionally, the decrease in GPP with such hot drought conditions during the growing season will result in a lower net carbon uptake (NEE) within the temperate forest ecosystems and turn these forests into carbon source ecosystems (Ciais et al., 2005; Richardson et al., 2006; Xu et al., 2011). However, the GPP response to drought may vary from site to site depending on the type of species, the local climate and other additional factors (Teuling et al., 2010; Wolf et al.,

2013). For instance, the 2003 European heatwave and drought was considered as the most severe drought stress event on the continent over the last century and resulted in an estimated loss of about 30% in GPP and a net carbon release of 0.5 P gC yr^{-1} mostly within eastern and western European (14 forest sites) forest ecosystems (Cias et al., 2005; Granier et al., 2007). According to Cias et al. (2005), although microbial and plant respiration were expected to be enhanced under warmer temperatures, a significant reduction in both the GPP (in response to stomatal closure) and R_{eco} (due to diminished substrates and drought) was generally observed over all the 14 investigated forest sites. Subsequently, similar impacts of severe drought conditions across Europe during the growing season were also observed for 2015 and 2018 (Trnka et al., 2020). However, unlike for the 2003 summer drought impacting central France, the Mediterranean region and parts of eastern Europe, the 2015 and 2018 summer droughts affected mainly central Europe, Southern Scandinavia and an area surrounding the Baltic sea, that were less likely adapted to extreme dry climatic conditions (Buras et al., 2020). This further resulted in forest dieback and an increased frequency of forest fires (Orth et al., 2016; Buras et al., 2020). In Europe, the frequent occurrence of extreme drought events (such as that in 2003, 2015 and 2018) may hinder the effects of the expected warming and lengthening of the growing season and affect the long-term health and productivity of forest ecosystems which will reduce their carbon sequestration capacity. Thus, given the wide-ranging impacts of drought under both short and long-term periods across different forest ecosystems, there is the need for more studies to understand the physiological responses of different tree species to drought and to predict the future impacts connected with climate change (Horton et al., 2015; Sippel et al., 2017; Zscheischler and Seneviratne, 2017; Pfleiderer and Coumou, 2018).

In forest ecosystems that are repeatedly affected by drought stress conditions, the survival of the tree species depends on species‘ resistance, avoidance, or tolerance to environmental stress conditions (acclimation potential) during its life cycle (Beikircher and Mayr, 2009; Taiz and Zeiger, 2010). The acclimation potential of specific tree species is mainly driven by either structural or functional adjustments or by a combination of both to the changing environmental conditions. High phenotypic plasticity, which refers to the ability of a specific genotype to exhibit different phenotypes in response to unique environmental factors (Sultan, 2000), may therefore be necessary to allow individual species to acclimatize well to the changing climatic conditions. Some other long-lived woody plant species may instead adapt well (experience genetic changes over several generations and through natural selection) than acclimatize (Debat and David, 2001). Also, through acclimation, trees sustain a more negative water potential

without suffering hydraulic failure during repeated drought events. For example, some forest ecosystems within a moderately dry climate adapt to severe and frequently occurring drought episodes by adjusting the species diversity, the leaf area index and thickness, and undergoing some physiological acclimation mechanisms. Despite these adaptation processes to withstand drought within these types of forest ecosystems, the primary productivity measured is usually very low as compared to other forest sites with humid climates (Reichstein et al., 2003; Reichstein et al., 2005; Bréda et al., 2006).

3 AIMS

The thesis will focus on the analysis and comparison of eddy covariance data measured at different forest ecosystems within the CzeCOS sites for several years. The comparison of matter and energy fluxes across different sites will help to better understand the response of forest ecosystem gross primary production (GPP) under contrasting climatic conditions and forest types. The fluxes of GPP and net ecosystem productivity (NEP) provide integrated information about ecosystem evapotranspiration and the balance between photosynthesis and respiration. The measured variables representativeness of the physiological processes can be however reduced under certain conditions. The identification of such site specific micrometeorological features within different forest types would increase the reliability of measured eddy covariance data. The seasonal courses of GPP provide in-depth details on the forest response to changes in environmental factors. However, these systematic changes in estimated GPP differ from site to site during the growing season, depending on the species type, local climate and additional factors. Such contrasting GPP responses of specific species (representing physiological responses of individual species to warming and other climatic conditions) under comparable environmental conditions across different forest sites are poorly understood. Hence, the need to investigate near-optimal environmental conditions for different plant species, under which GPP could reach maximal theoretically attainable values (potential GPP, GPP_{pot}). Moreover, analyses using the mean daily estimated GPP during the growing season will also ensure the exclusion of suboptimal environmental conditions on forest GPP.

The specific objectives include:

- to determine the main environmental variables that influences the ratio between actual and optimal GPP across beech and spruce forest ecosystems within the CzeCOS sites and the potential role of acclimation to local climate using two sets of regression models.
- to assess the different effects of a severe drought stress event during the growing season of 2015 on GPP at two spruce forest ecosystems with contrasting climatic conditions- cold and humid climate at Bílý Kříž vs. moderately warm and dry climate at Rájec within the CzeCOS sites.
- to determine the effect of critical site-specific environmental variables (such as the VPD and soil volumetric water content) on the drought stress response at two spruce forest stands with contrasting microclimatic conditions.

4 MATERIALS AND METHODS

The material and methods section of this study gives a well detailed information about the eddy related measurements and other approaches in estimating certain micrometeorological terms of the doctoral thesis.

4.1 CzeCOS ecosystem stations

For this study, EC measurements from the growing season of 2012-2016 at three different forest ecosystem stations that represent different climatic conditions within the Czech Republic (Central Europe), and which belong to CzeCOS (the Czech Carbon Observation System; http://www.czecos.cz/, website accessed on 7 March 2021) and the FLUXNET Network (Flux Tower Network; https://fluxnet.fluxdata.org/, website accessed on 7 March 2021) are used. The EC data were collected from the wet spruce forest site at Bílý Kříž with a FLUXNET site ID of CZ-BK1, a dry spruce forest site at Rájec with a FLUXNET site ID of CZ-RAJ and European beech forest site at Štítná with FLUXNET site ID of CZ-Stn. CZ-BK1 is a candidate for ICOS (Integrated Carbon Observation System; https://www.icos-cp.eu/, accessed on 6 March 2021) network. All the forest stands are even-aged monocultures whereas the forest stands in both CZ-BK1 and CZ-RAJ are dominated by Norway spruce with CZ-Stn representing an European beech monoculture. Characteristics of the sites used in this research are presented in Table 4.1.

Table 4.1: Characteristics of the investigated Sites (as in Mensah et al., 2021b).

Site Name	CZ-BK1	CZ-RAJ	CZ-Stn
Location	Moravian-Silesian Beskydy Mountains	Drahanska Highland	White Carpathian Mountains
Coordinates	49°30'08"N 18°32'13"E	49°26'37"N 16°41'48"E	49°02'09"N 17°58'12"E
Elevation (m a.s.l.)	875	625	540
Topography	Mountain ridge (13° slope with SSW exposure)	Hilly (5° slope with NEE exposure)	Mountainous (10° slope with WSW exposure)
Ecosystem type	Coniferous evergreen forest	Coniferous evergreen forest	Deciduous broadleaf forest
Prevailing species	Norway spruce (*Picea abies* (L.) Karst.)	Norway spruce (*Picea abies* (L.) Karst.)	European beech (*Fagus sylvatica* L.)
Canopy height (m) Stand age (years)	16 (mean, as of 2015) 35 (as of 2016)	33 (mean, as of 2015) 113 (as of 2016)	31 (mean, as of 2015) 115 (as of 2016)
Mean seasonal air temperature (May – September, °C)	14*	16*	17*
Total seasonal precipitation (May – September, mm)	2730*	1635*	1719*
Seasonal sum of reference evapotranspiration (May – September, mm)	2036*	2325*	2166*
Soil type	Haplic and Entic Podzol	Modal Cambisol oligotrophic	Eutric Cambisol
References	Jocher et al., (2020)	McGloin et al., 2019	Krupkova et al., 2019

*2012 – 2016 study period

4.2 Micrometeorological Measurements

Standardized measurements of the following parameters were made at each site: air temperature (Tair) and relative humidity with the EMS33 temperature and humidity sensors (Embedded Moisture Sensor, Vancouver, BC, Canada); the hourly precipitation (P) was determined by using a Precipitation Gauge 386C (Met One Instruments, Grants Pass, OR, USA); the incoming photosynthetic active radiation (PAR) were also made using LI-190R Quantum Sensor (LI-COR, NE, USA) at both Bílý Kříž and Štítná and with an EMS12 sensor (EMS, CZ) at Rájec; soil moisture profiles were measured by using the CS616 (Campbell Scientific, North Logan, UT, USA) sensors at the spruce forests in . Overall description of the instrumentation at the studied forest stands, including soil temperature measurements (Ts), is given in Table 4.2. The vapour pressure deficit (VPD; hPa) at each forest stand was computed from Tair (ºC) and relative air humidity (RH; %) according to Monteith and Unsworth (2013). The daily sum of PAR values (MJ m^{-2} day^{-1}) were also derived following Thimijan & Heins (1983).

The effect of both diffuse and direct radiation on the daily mean GPP values were also analysed by grouping the dataset into sunny and cloudy days based on the clearness index (CNI). The CNI refers to the ratio of solar irradiation transmitted through the atmosphere onto the earth's surface relative to extra-terrestrial irradiation. The sunny days are classified as days with CNI > 0.7, with cloudy days characterized as CNI < 0.4, and all CNI values of 0.4 - 0.7 were grouped as partly cloudy days (Sanchez et al., 2012).

Table 4.2: Description of ancillary microclimatic measurements (as in Mensah et al., 2021b).

Site Name	CZ-BK1	CZ-RAJ	CZ-Stn
Air Temperature and Humidity Profile			
Instrument	EMS 33 temperature and humidity sensor	EMS 33 temperature and humidity sensor	EMS 33 temperature and humidity sensor
Height (m)	2.0, 7.6, 12.6, 13.5, 14.3, 14.8, 15.4, 16.5, 18.7	2.0, 11.0, 23.0, 29.0, 35.0, 42.0	2.0, 12.0, 22.0, 28.0, 33.0, 38.0, 44.0
Net Radiation			
Instrument	CNR1 Net radiometer (Kipp & Zonen)	CNR1 net radiometer (Kipp & Zonen)	CNR1 net radiometer (Kipp & Zonen)
Measurement Height (m)	Sensor initially placed at 20 m, then changed to 22 m in August, 2013	42 m	42 m
Soil Temperature (Ts)			
Instrument	Pt 1000	NA	Pt 1000
Measurement Depth (m)	0, 0.05, 0.10, 0.20, 0.30, 0.50	NA	0, 0.05, 0.10, 0.20, 0.30, 0.50

***** EMS - Environmental Measuring System

4.3 Soil water content simulations

The soil volumetric water content (SVWC) was not directly measured through-out the entire day within the period of analyses, and as such, a simulated daily SVWC values were used instead. These simulated daily SVWC values were performed by the soil water balance model, R-4ET (which is an R software package for Empirical Estimate of Ecosystem EvapoTranspiration, Fischer et al., 2018). The soil water balance model was calibrated by using the Bayesian statistics implemented in the R package BayesianTools (Hartig et al., 2019) with

Differential-Evolution Markov chain Monte Carlo sampler. In the Bayesian calibration, the model input parameters were iteratively updated to provide a probability distribution of the calibrated parameters which represents the uncertainty in the measured data and the model structure. A repetition of the simulations was done 4.8×10^6 times, with the first 1.8×10^6 runs based on prior distribution, while the remaining 3.0×10^6 constrained by a posterior distribution that results from the first set of runs. A number of these iterations were treated as burin-in and set to 0, with the thinning parameter that determines the interval of recording was set to 1. These high number of iterations were necessary to attain a good input parameter convergence with the narrow distribution. To inspect convergence, the Gelman diagnostics was applied with a criterion for potential scale reduction factor being less than 1.2 for all the parameters (Gelman and Rubin, 1992; Brooks and Gelman, 1998). Finally, a selection of parameters from their probability distributions was also conducted using a maximum *posteriori* probability estimate, i.e., value indicating the mode of posterior distribution.

The input variables of the main model included meteorological data and leaf area index (see Fischer et al., 2018, for more details). Also, the soil was stratified into 12 layers and was observed to increase in thickness with increasing depth down to 3 m. These soil layers were selected in such a way that the soil layers (used for optimization) all matched the depths of the sensors with an extra ±2.5 cm considering the volume measured by the sensors. At all the sites, the SVWC measurements were carried out within the main root zone area. At the wet spruce forest site in Bílý Kříž, the CS616 (Campbell Scientific, Inc., Logan, UT, USA) sensors were placed at soil depths of 0.05, 0.1, 0.22, 0.34, and 0.42 m. At the dry spruce forest site Rájec, the same type of sensors was also placed at specific soil depths at 0.05, 0.1, 0.2, 0.5, and 0.8 m. Also, at the beech forest stand in Štítná, the ThetaProbe (ML2x 355, Delta-T, UK) sensors were placed at soil depths of 0.05, 0.1, 0.3, 0.6, and 0.9 m. The soil parameters that include the SVWC at saturation, field capacity, wilting point, and the saturated hydraulic conductivity were optimized at all the 12 depths (Fischer et al., 2018). There were additional single parameters relevant for SVWC simulations that were optimized and this included the rooting depth with a Beta parameter that describes the root profile shape (Jackson et al., 1996), surface resistance and the degree of isohydricity (Oren et al., 1999), the water interception capacity of the leaf and bark areas, and curve number indicating a runoff parameter (Fischer et al., 2018). In addition, a uniform distribution of priors was used with the lower and upper limits set to be within ±50 % of the values that was based on the field measurements of the wilting point, the field capacity, and the saturated water content and ±100 % of the remaining parameters that were estimated

from literature or from previous anecdotal analysis. Furthermore, in providing the model with a sufficient spin up time to stabilize and ensure a reliable and robust parametrization, the simulation process was initiated at the start of the year 2010 with the initial conditions of SVWC being set to the field capacity that was estimated from the soil texture (2010 was one of the wettest years at all the forest stands based on a computed standardized precipitation-evapotranspiration index over the region). The overall simulation was performed from 2010-2019 where the observed data for Bayesian calibration were spanning from 2016-2019. Also, these simulated SVWC values averaged over all the depths yielded low root mean square error (RMSE) values at all the forest stands, suggesting realistic SVWC estimates. At the wet spruce forest stand, the simulated SVWC values averaged over all depths yielded a root mean square error (RMSE) of 0.037 m^3 m^{-3}, with a RMSE of 0.017 m^3 m^{-3} at the dry spruce forest stand and 0.032 m^3 m^{-3} at the beech forest site, suggesting realistic SVWC estimates.

4.4 Eddy Covariance Measurements

Unified Eddy systems for flux measurements were installed at all the investigated forest ecosystems. These systems were mounted on meteorological towers at respective height above the forest canopy within the inertial sublayer (detailed description in Table 4.3). The EC system at each of the forest ecosystems consisted of an ultrasonic anemometer (Gill, Instruments, Lymington, UK) measuring at 20 Hz frequency, and a fast-response infrared gas analyser (LI-COR, Lincoln, NE, USA). The processing of EC data (wind components, sonic temperature, CO_2, and water vapour mixing ratios) was performed by using an open-source software known as the EddyPro (Li-COR, USA).

Table 4.3: Description of the eddy covariance systems at the investigated sites (Mensah et al., 2021b).

Site Name	CZ-BK1	CZ-RAJ	CZ-Stn
Ultrasonic Anemometer			
Instrument	Gill HS−50 (Gill Instruments, UK)	Gill R3−100 (Gill Instruments, UK), and later changed to Gill HS-50 on 5th June 2015	Gill R3−100 (Gill Instruments, UK)
Gas Analyzer			
Instrument	LI−7200	Initially LI−7000 (IRG-0226) closed-path gas analyzer, but later changed to LI-7200 on 5th June 2015	LI−7000 closed-path gas analyzer
Measurement Height for the Eddy covariance Set-up (m)	Sensor initially placed at 20.5 m, but was later changed to 25 m on 7th June 2016	41 m	44 m

4.5 Data processing and Analysis

4.5.1 Post-processing of eddy covariance data

The EddyPro was used to calculate fluxes of half-hourly averages of CO_2 and water vapour fluxes from the high frequency (20 Hz) raw data. During this process, the most recent methods for flux corrections, conversions, and thorough quality control scheme (Aubinet et al., 2012;

Foken et al., 2012) were applied. The process involved despiking of raw data and statistical screening, basic quality checking of the turbulent fluxes (integral turbulence characteristics tests and flux stationarity), coordinate rotation by using the planar fit method (Wilczak et al., 2001), detecting and compensating for time lags of signals from the ultrasonic anemometer and the infrared gas analyzer, spectral correction (Moncrieff et al., 2000; Ibrom et al., 2007 and Horst & Lenschow, 2009), footprint estimation and calculating corrected half-hourly final fluxes.

4.5.2 Quality control (QC) of measured fluxes

QC was performed on the corrected half-hourly fluxes output of the EddyPro following Mauder et al. (2013). The automated QC (AQC) scheme comprised checking for problems with instrumentation and data sampling, plausibility limits of the variables used, missing raw data within the half-hour (maximum of 10% is allowed), high-frequency spike percentage within the half-hour (maximum of 1% is allowed), combined steady-state test and test of integral turbulence characteristics (Foken and Wichura, 1996), a large spectral correction factor (an indicator of large flux uncertainty), a large mean vertical wind velocity after planar fit rotation (an indicator of vertical advection), test for the interdependency of CO_2 and water vapour fluxes flags, due to corrections/ conversions (Mauder et al., 2013). A quality flag criterion was set for each flux, and their interdependency due to conversions and corrections was taken into account. Also, a low-frequency despiking method based on the median of absolute deviations from the median (Sachs, 2013) was applied to Papale et al. (2006) to ensure that outliers would not affect the gap-filling results. A directional footprint filter (5° resolution) ensured that most of the flux contributions came from the desired areas. This AQC workflow for all fluxes (τ , CO_2 and water vapour) was applied by using the R software package eddyczechr. The eddyczechr package supports EddyPro output statistics and contains functions for flux aggregation with extended plotting functions for data visualization. The eddyczechr package incorporates the QC flag naming conventions that simplify QC documentation and QC flag aggregation and analyzes the individual sources of flux quality reduction.

Moreover, flux measurements over periods with insufficiently developed turbulence, i.e., low friction velocity (u*), were detected and filtered out. This filtering procedure ensured the exclusion of CO_2 fluxes that were not necessarily indicative of the ecosystem-scale biotic flux due to the insufficient mixing across the forest canopy (Papale et al., 2006; Reichstein et al., 2005; McGloin et al., 2018). The flag system follows the classification of flux data within

the CarboEurope-IP (Mauder and Foken, 2004). Flux data with excellent quality and suitable for fundamental research and development of parametrization are flagged as 0, whereas other flux data with good quality and ideal for general analysis and annual budgets are flagged as 1. However, flux data flagged as 0 refer to those with bad quality and need to be excluded and gap-filled.

On the other hand, a manual QC (MQC) scheme combines steady-state test and test of integral turbulence characteristics (Foken & Wichura, 1996), instrument diagnostics evaluation, plausibility limits (based experience), and visual inspection of data based on the comparison with different meteorological variables and adjacent half-hours.

4.5.3 Gap-filling and flux partitioning

In estimating annual budgets, there was the need to create a continuous flux time series by gap-filling all the missing or excluded data through the application of an R software (R Core Team, 2018) package 'REddyProc' (Wutzler et al., 2018) using marginal distribution sampling (Reichstein et al., 2005). CO_2 flux (which is subsequently considered to be equal to NEE) was partitioned into GPP and ecosystem respiration (R_{eco}). The flux partitioning approach by Lasslop et al. (2010) using daytime data was used in estimating half-hourly GPP values (μmol m^{-2} s^{-1}). These half-hourly GPP values were aggregated to derive daily and monthly sums of GPP values.

4.5.4 Footprint calculation

Two footprint functions applied in EddyPro were used to estimate the footprint fetch of the study sites. Under stable conditions, the Kormann-Meixner analytical model (Kormann and Meixner, 2001) was applied, whereas, under other atmospheric conditions, the Kljun stochastic Langragian model (Kljun et al., 2004) was used to calculate the footprint fetch. Under unstable and neutral conditions, the Kormann-Meixner becomes computationally demanding. The mean 70% fetch (distance from the tower at which cumulative contribution to turbulent fluxes is 70%) was applied in the filtering of the directional footprint.

4.5.5 Estimation of potential and normalized GPP

Potential GPP (GPP_{pot}) is defined here as the estimate of daily GPP sum that can be obtained under near-optimal environmental conditions (PAR, CNI, SVWC, VPD, Tair, Ts, and P) at the given site on a particular day of the year (DOY; Gu et al., 2009). The GPP_{pot} formed the boundary line of a scatter plot of GPP against the DOY values (especially for May-September) pooled over multiple years of data. In estimating the GPP_{pot}, the following set of procedures were applied until there were no outliers as described in Gu et al. (2009):

- Derive the 95th percentile values from the daily sum of GPP pooled over 2012-2016 for each DOY value over a 7-day window (iteratively applied).
- All outliers are detected and removed using the percentile method (i.e., all observations that were found outside the interval formed by the 1 and 99 percentiles were considered as outliers).

Moreover, to better compare the changes in GPP response across all the investigated forest stands, daily normalized GPP (GPP_{norm}) values were derived at each forest ecosystem as the ratio of the estimated daily GPP per the GPP_{pot}. Therefore, GPP_{norm} values ~ 1 indicate days with maximum assimilation rates under the near-optimal environmental conditions. GPP_{norm} values ~ 0 also showed days with extreme adverse effects on forest productivity. In addition, a smoothing spline curve was applied to depict the main trends in seasonal courses of GPP_{norm} during the growing seasons of 2012 - 2016.

A Pearson's correlation coefficient matrix was plotted to determine the statistical relationship between GPP_{norm} and the environmental variables based on a covariance method.

4.5.6 Multi-linear and tree-based regression model analyses

In assessing the response of GPP_{norm} to the environmental factors (PAR, CNI, SVWC, VPD, Tair, Ts, and P) at each site, two methods were tested; (i) a stepwise multi-linear regression (SMLR) and (ii) random forest algorithm (RF). P was excluded from the analyses as this does not represent a direct measure of soil moisture and as such SVWC was used for the

regression analysis. The SMLR selection with interaction terms was used by applying the stepwise regression method (using both the forward and backward direction) in determining the significant terms in the model and eliminate the nuisance (i.e., non-significant terms) variables with 95% probability. In addition, quadratic terms were included in the model to test for non-linearity of the environmental variables with GPP_{norm}. All the statistical analyses were performed using the R software package 'stepAIC' (Version 7.3-54, R Core Team, 2018).

The RF model was also trained and applied to predict GPP_{norm} at each of the forest ecosystems and benchmarked with the SMLR model's performance. The R software package 'randomForest' (with Version 4.6-14, Liaw and Wiener, 2015) was used with the following parameters: the number of trees of the model (ntrees) = 300, with the number of variables in each mode (representing the nodesize) = 5, and the number of variables used in each tree (indicating the mtry) = one third of the total number of samples, as in Liaw and Wiener, (2002) for RF regression. As part of the RF byproduct, the built-in variable importance measures or ranks the environmental variables (the features) according to their relevance (computed from permuting the Out-Of-Bag samples based on the mean decrease in accuracy) in predicting GPP_{norm} at each of the forest ecosystems has been provided (Breiman, 2013). The higher the value of importance of the variable in the model, the higher the value of the mean decrease in accuracy.

4.5.7 Accuracy Test of regression models

The predictive performance of GPP_{norm} at each of the forest ecosystems by both the SMLR model and RF techniques was evaluated. The model prediction accuracy indicators showing the Pearson correlation, the percentage of the variance explained (R^2) with regards to the estimated and predicted GPP_{norm}, and the root mean square error (RMSE) values were derived and compared.

4.5.8 Drought Stress determination

According to Mishra & Singh (2010), drought refers to low available soil moisture and high atmospheric VPD. Thus, to quantify and define dry periods within the context of this study for 2014-2016, the Standardized Precipitation-Evapotranspiration Index (SPEI) was used. The SPEI considers both precipitation and potential evapotranspiration for determining drought over the main growing season. Additionally, the SPEI was calculated for various lags (1, 3, 6, 12, and 24 months) from monthly records. The period of 1981 - 2010 was used as the main baseline years for the SPEI computation. Moreover, the computation of SPEI was performed according to Beguería et al. (2014) and Vicente-Serrano et al. (2010) by using the R package SPEI (Beguería and Vicente-Serrano, 2017). The SPEI indicates an anomaly in the climatological water balance, that is explained as the difference between the reference evapotranspiration and precipitation amount. In deriving the SPEI, the input data were mainly obtained from monthly averages of climate reanalyses ERA5 that is available at 0.25° spatial resolution. The reference evapotranspiration was derived from the air temperature at 2 m, with air dew point temperature in 2 m, and the wind speed in 2 m that is converted from the original 10 m height using the logarithmic profile law, and shortwave incoming radiation following the methodology by Allen et al. (1998). Using the SPEI values, Table 4.5 shows the categorization of dryness/wetness severity at each of the investigated forest site, according to the SPEI classification as used by Yu et al. (2014) in Table 4.4. The positive values represent moisture and the negative values indicates drought.

Table 4.4: The Standardised Precipitation- Evapotranspiration Index (SPEI) categories based on the classification of SPEI values by Yu et al., 2014.

Drought/ Wet Severity	SPEI Value
Extremely Wet	≥ 2.00
Severely Wet	1.50 – 1.99
Moderately Wet	1.00 – 1.49
Near Normal	-0.99 – (-0.99)
Moderate Drought	-1.00 – (-1.49)
Severe Drought	-1.50 – (-1.99)
Extreme Drought	≤ -2.00

Table 4.5: Categorization of dryness/wetness using Standardised Precipitation-Evapotranspiration Index (SPEI) indices for the wet spruce (CZ-BK1) and the dry spruce (CZ-RAJ) forest stations in years (2014 – 2016).

YEARS	CZ-BK1		CZ-RAJ	
	SPEI VALUE	CLASS	SPEI VALUE	CLASS
2014	0.94	Near Normal	0.56	Near Normal
2015	-1.75	Severe Drought	-1.55	Severe Drought
2016	-0.20	Near Normal	-0.87	Near Normal

4.5.9 Light Response Curve Fitting

Using the logistic sigmoid approach by Moffat et al. (2010) as below, the light- response curves (LRC) for the daytime GPP were fitted at half-hourly time resolution:

$$GPP = 2 \times GPP_{max} \left[0.5 - \frac{1}{1+\exp\left(\frac{-2\alpha\, PAR}{GPP_{max}}\right)}\right] \quad (3)$$

where PAR represents the photosynthetically active radiation, with α representing the apparent quantum yield in mol (CO_2) mol^{-1} (phot.) which provides details on the effectivity on the rate of photosynthesis at low light conditions, with the GPP_{max} indicating the asymptotic maximum assimilation rate at the light saturation point in μmol m^2 s^{-1}.

The LRC fitting was performed separately for half-hourly GPP values from 2014 – 2016. However, to eliminate night-time measurements within the two spruce forests, a PAR threshold of 10 μmol m^2 s^{-1} representing light compensation irradiance of 10 μmol m^2 s^{-1} (the light compensation point of NEE) was set to filter out flux data with PAR values below that threshold.

Also, since GPP is affected by changes in VPD and soil moisture (Lasslop et al., 2010 and Migliavacca et al., 2011), the impact of VPD and SVWC on LRC residuals (GPP values without the strongest PAR dependence) were further analysed for both spruce forest stands over the period under study (2014-2016). Subsequently, a piecewise regression was applied to analyse the effect of VPD and SVWC on the LRC residuals in determining site-specific environmental stress thresholds at which the forest GPP declined in both the normal and drought-affected years.

4.5.10 Piecewise regression analyses for the assessment of drought effect

Since both changes in VPD and SVWC are not accounted for by the LRC model used, a piecewise regression of residuals against these environmental variables was analysed. Through this analyses, the specific response of each of the studied spruce forest ecosystem with contrasting climates to severe drought conditions was determined over the growing season during the normal and drought-affected years. The piecewise regression analysis (using the R package in 'segmented' (Muggeo, 2003) and the Davies test (Davies, 2002)) was used to detect the breakpoints in the regression and test for the significant differences in the slope of the residual plot from the LRC model to high VPD and low SVWC conditions.

5 RESULTS

In this chapter, results on the climatic conditions across the forest ecosystems are compared to determine the dryness or wetness of the forest ecosystem. Through this analyses, the main environmental variables also affecting the ratio between estimated gross primary productivity (GPP) and potential GPP (GPP_{pot}) across all the forest ecosystems are compared. Secondly, the impact of severe drought conditions on GPP of drought-sensitive spruce species growing at sites with contrasting climatic conditions are analysed. All these analyses are made using data from May to September from 2012 – 2016 across the wet and dry spruce forest sites in Bílý Kříž and Rájec respectively and at the beech forest ecosystem in Štítná.

5.1 METEOROLOGICAL CONDITIONS AT THE EXPERIMENTAL STATIONS

5.1.1 Variations in meteorological conditions at the spruce and beech forest sites

During the main growing season period of 2012 – 2016, the seasonal sum of precipitation at the spruce forest site in Bílý Kříž was found to be approximately 40% higher than the seasonal sum of precipitation at the dry spruce forest site and 37% higher than in the beech forest site in Štítná (Table 4.1 and Figure 5.1). Additionally, both July and August were mainly characterized by hot and dry conditions across all forest sites, especially at the dry spruce forest site in Rájec with high mean monthly Tair values (which was 10% higher than at the wet spruce forest site and 6% lower than at the beech forest ecosystem in Štítná) and low mean monthly SVWC values (14% lower than at the wet spruce forest stand and 52% lower at the beech forest site in Štítná, Fig. 5.2). Though the highest Tair values were consistently observed at the beech forest site in Štítná, there was sufficient supply of soil moisture during the study period. Between June – September, there were observed statistically significant differences ($p < 0.01$) in the mean monthly VPD and SVWC values at the wet spruce forest site (with low mean monthly VPD values) in comparison with that at the dry spruce and beech forest sites. Thus, these results show a moderately dry climate at the dry spruce forest site in Rájec as compared to the humid climate within the wet spruce forest site in Bílý Kříž. The results further

indicate the contrasting soil water availability at both spruce forest sites with different climatic conditions.

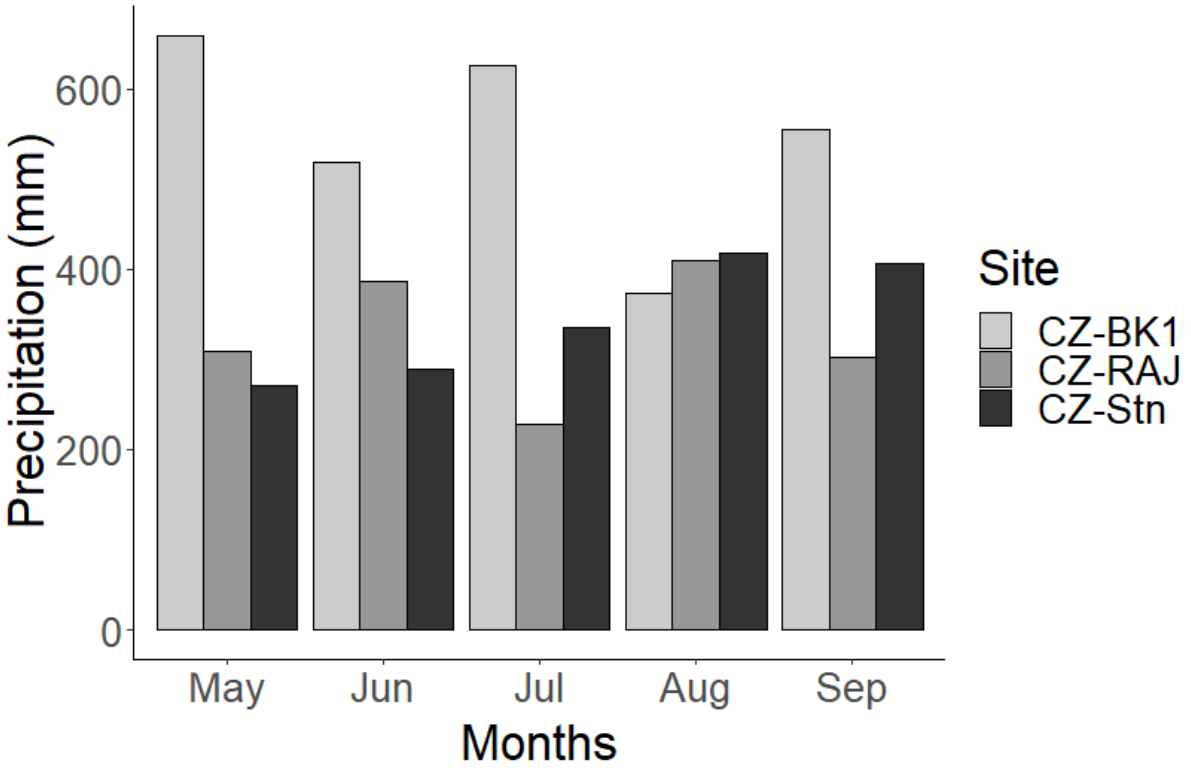

Fig. 5.1: Monthly sums of precipitation for May-September from 2012-2016 at the spruce forest sites in Bílý Kříž (CZ-BK1) and Rájec (CZ-RAJ), and the beech forest in Štítná (CZ-Stn).

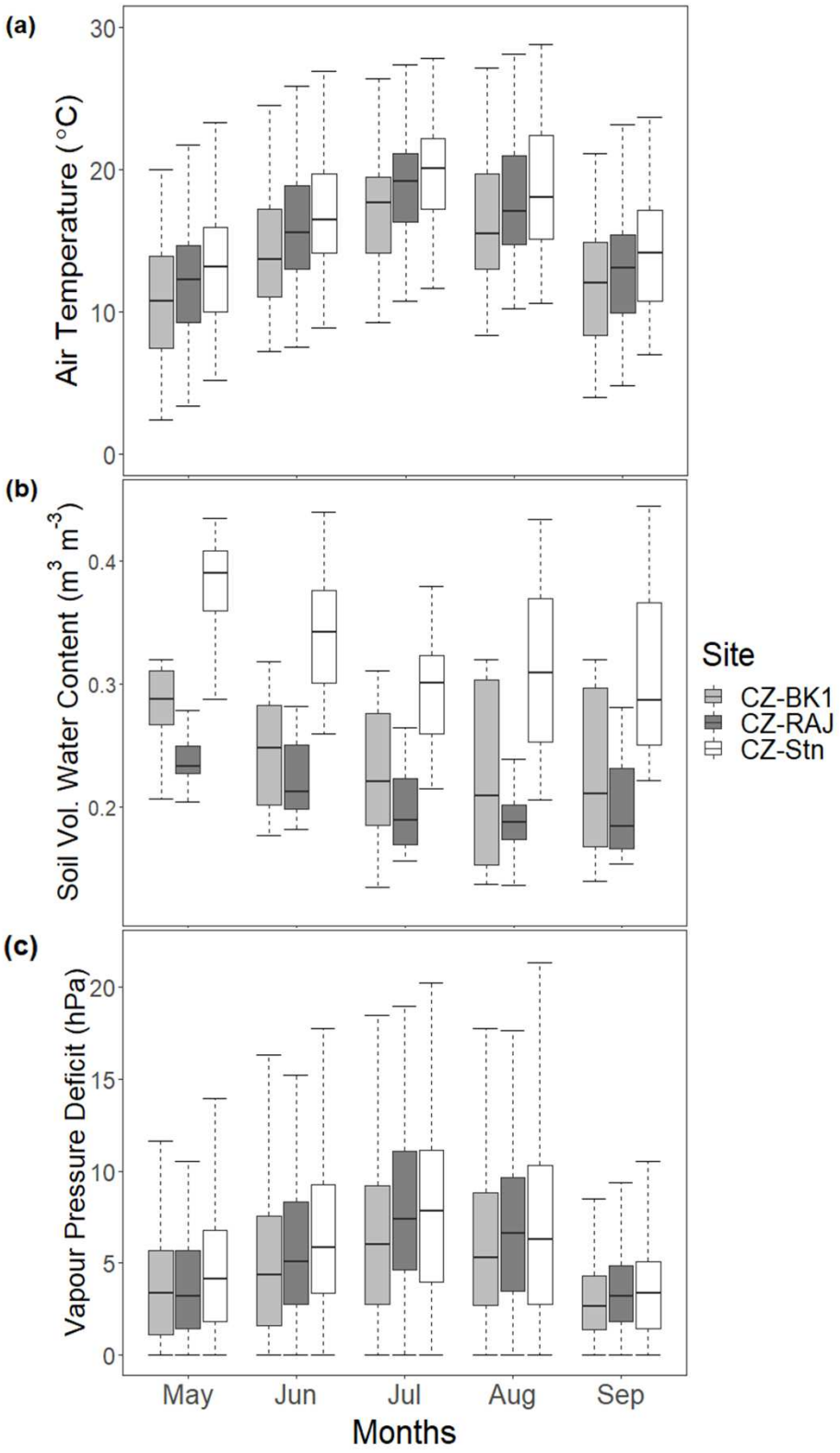

Fig. 5.2: Monthly averages of (a) air temperature, (b) the soil volumetric water content (SVWC), and (c) vapour pressure deficit for May - September of 2012 - 2016 in the spruce forest sites in Bílý Kříž (CZ-BK1) and Rájec (CZ-RAJ), and the beech forest in Štítná (CZ-Stn).

The mean value is shown as the thick horizontal line in the box plot whereas the box represents the upper and lower quartiles. The vertical dotted lines also represent the minimum and maximum values with the error bars (whiskers) portraying the standard deviation.

To understand the effect of a typical drought stress condition as was observed in 2015 on forest GPP within a drought-sensitive species such as the Norway spruce grown at different sites with different climatic conditions, climatic conditions in 2015 was studied and compared with that of two adjacent years (2014 & 2016). The year 2015 was selected as the year with severe drought conditions, while 2014 and 2016 were also characterized as years with normal conditions, based on the SPEI analyses in Table 4.5.

A closer look at the climatic conditions during the growing season of 2015 shows significantly high mean VPD values with low mean SVWC values ($p < 0.01$; Table 5.2) especially in the months of July – August as compared to that of the two adjacent years across both sites. The observed statistically significant differences of the mean VPD and SVWC values ($p < 0.05$; Mann-Whitney-Wilcoxon ranksum test) between the drought stress year of 2015 and the adjacent normal years showed the difference in meteorological conditions during the main growing season of the years under study. Thus, the high mean VPD and low SVWC values of 2015 were good indicators of drought (dryness stress) during the growing season, whereas the mean Tair values were comparable for both 2015 and 2016. Additionally, VPD values during the drought-affected year (DY) of 2015 were mostly observed to be higher at the dry spruce forest with lower mean SVWC values as compared to that of the wet spruce forest. This also depicts the moderately dry climate as observed in the dry spruce forest site in Rájec.

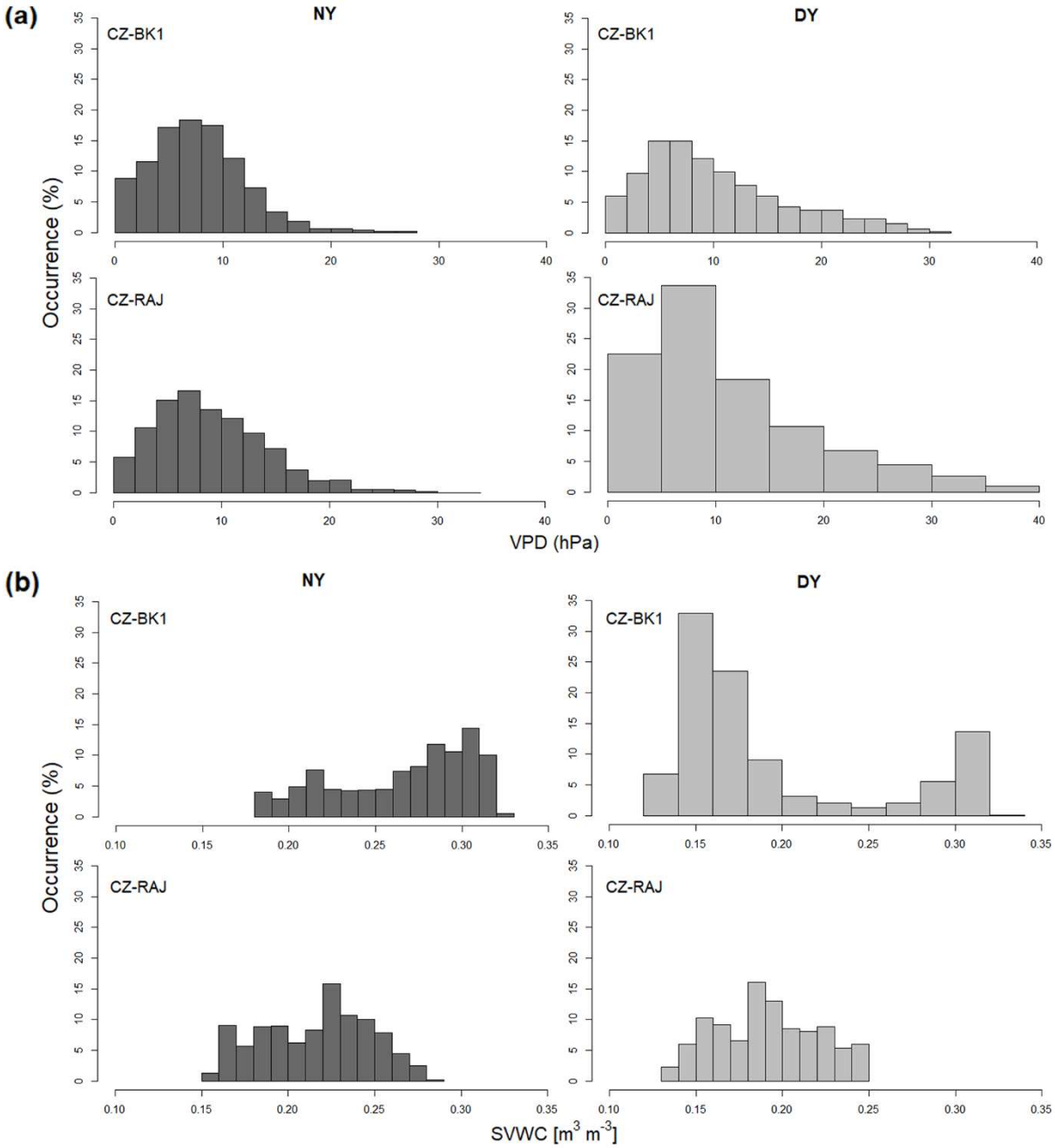

Fig 5.3: Histogram showing the frequency in occurrence of; (a) the vapour pressure deficit (VPD) and (b) the soil volumetric water content (SVWC) during the main growing seasons from 2014 - 2016 at the spruce forest stands in Bílý Kříž (CZ-BK1) and Rájec (CZ-RAJ). The dark colour represents the years with normal conditions (NY) while the grey colour represents the drought-affected- year (DY).

Table 5.2: Mean values of vapour pressure deficit (VPD), air temperature (Tair) and the soil volumetric water content (SVWC) during May- September from 2014-2016 for the spruce forest stands in Bílý Kříž (CZ-BK1) and Rájec (CZ-RAJ).

YEARS	CZ-BK1			CZ-RAJ		
	VPD (hPa)	Tair (°C)	SVWC (m^3 m^{-3})	VPD (hPa)	Tair (°C)	SVWC (m^3 m^{-3})
2014	7.6	13.4	0.28	8.7	14.9	0.21
2015	10.2	14.6	0.19	11.2	15.8	0.19
2016	7.7	14.4	0.25	9.3	16.0	0.22

5.2 Environmental effects on potential gross primary productivity (GPP_{pot}) in spruce and beech forests using a set of regression methods

The annual changes in the mean daily sums of estimated GPP values across all the forest ecosystems under study are shown in Fig. 5.4. The area under the red curve indicates the seasonal changes of GPP_{pot} that shows how much carbon could potentially be assimilated over the years under certain near-optimal environmental conditions at each of the forest sites. Additionally, the changes in estimated GPP during the growing season that shows the phenological responses to warming and other climatic conditions have well been captured in Figure 5.4. Across all the three forest ecosystems, the maximum GPP_{pot} value of approximately 15.81 gC m^{-2} day^{-1} was realized at the wet spruce forest ecosystem and obtained on DOY values ranging from 197 – 203. These were days within the month of July that were characterized by lower mean Tair and high SVWC values as compared to other sites (Fig. 5.2). The results also show that high maximum GPP_{pot} values of approximately 12.97 gC m^{-2} day^{-1} and 14.48 gC m^{-2} day^{-1} were recorded in the month of June at the dry spruce (with DOY values from 170 – 177) and beech (with DOY values of 165-166; 178) forest stands in Rájec and Štítná respectively.

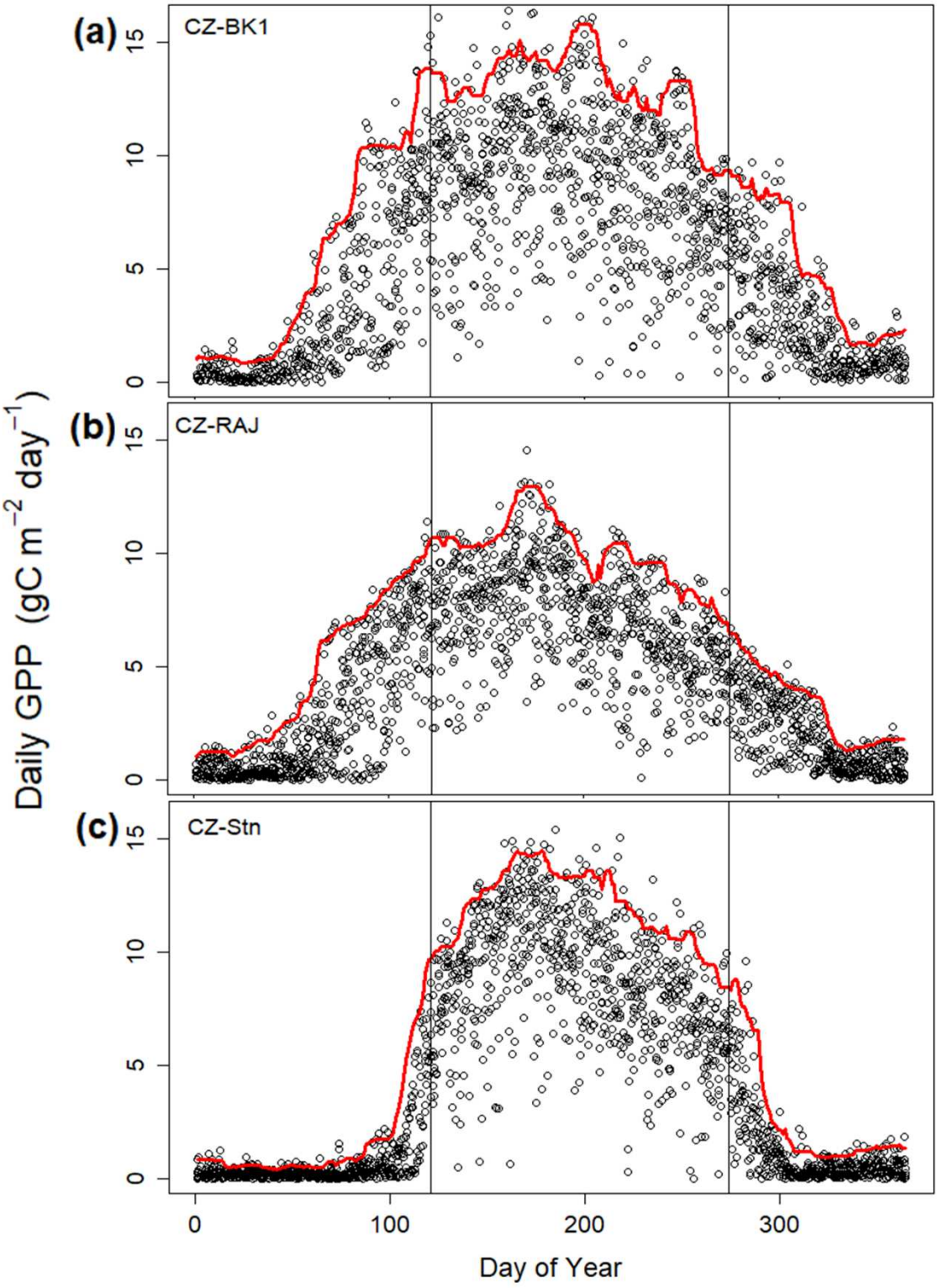

Fig. 5.4: Annual changes in the daily potential gross primary productivity (with the red line) using the daily sum values of gross primary productivity (GPP) for the spruce forest sites in (a) Bílý Kříž (CZ-BK1) and (b) Rájec (CZ-RAJ), and (c) the beech forest in Štítná (CZ-Stn) from 2012 - 2016.

The main growing season period during 2012-2016 is represented by the vertical lines.

The seasonal changes in the daily GPP_{norm} values during the main growing season period were compared across all the three forest sites (Figure 5.5). The DY period was characterized by a lower GPP_{norm} values showing depression of GPP in 2015 especially at the dry spruce forest site as compared to other years. Moreover, the GPP_{norm} values at the beech forest site were found to be comparatively higher at the beech forest site than at both spruce forest stands over the study period (Figure 5.5).

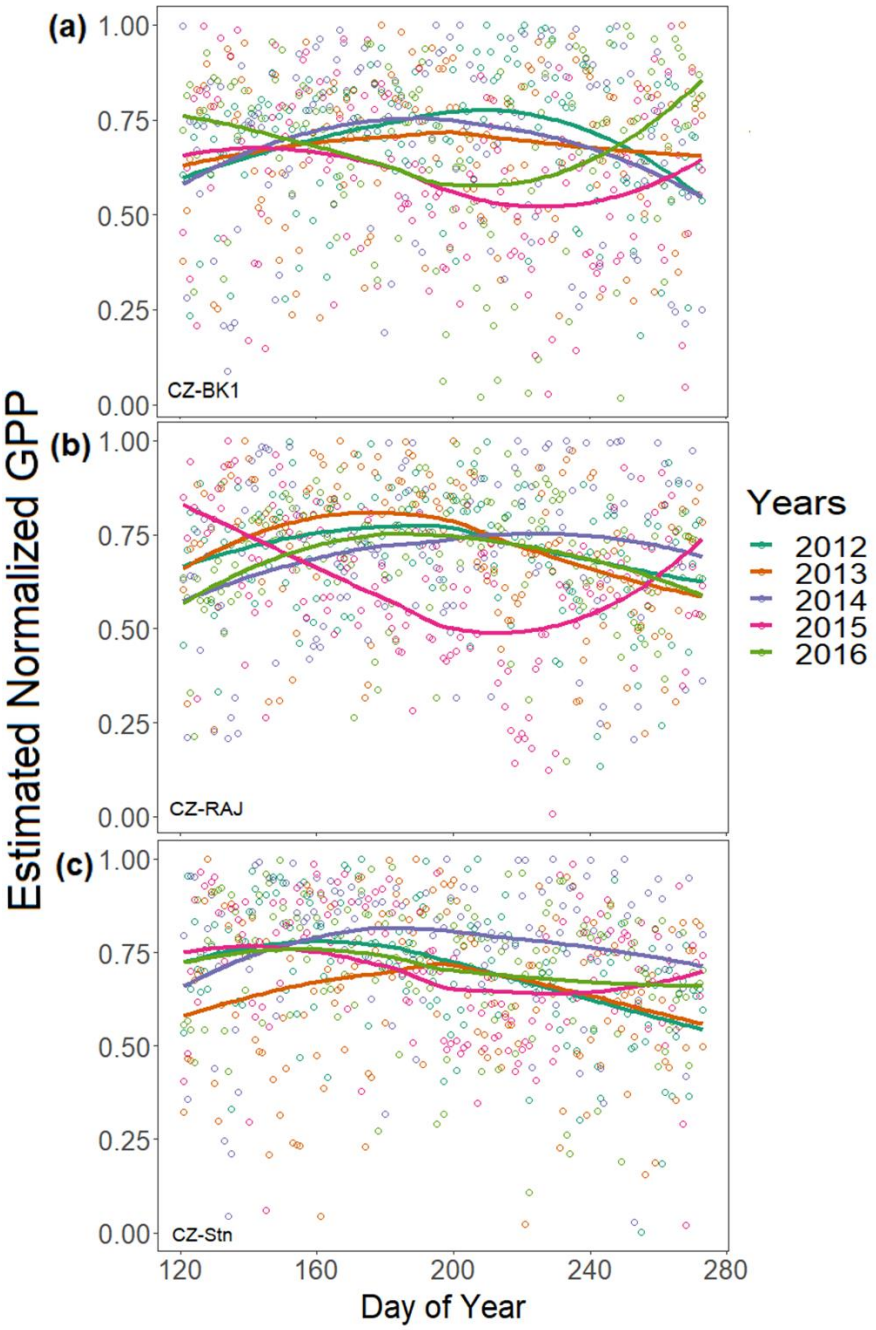

Fig. 5.5: Annual variations of estimated Normalized gross primary productivity (GPP_{norm}) within the spruce forest sites in Bílý Kříž (CZ-BK1) and Rájec (CZ-RAJ), and the beech forest in Štítná (CZ-Stn) during the main growing season of 2012 – 2016.

The smoothing spline curves was depicting the trends in seasonal courses of GPP_{norm} during the growing seasons of 2012 – 2016.

The Pearson correlation matrix (Fig. 5.6) to detect linearity in GPP_{norm} with the environmental variables shows a moderate positive linear relationship between GPP_{norm} and PAR across all the forest ecosystems. However, at both the dry spruce and beech forest sites, CNI showed a moderate positive linear relationship with $GPP_{norm,}$ unlike in the wet spruce forest with a non-linear relationship (Fig. 5.7). Also, at the wet spruce forest site, the correlation coefficients between GPP_{norm} and other environmental variables such as PAR, P, VPD and Tair were found to be statistically significant ($p < 0.05$). Statistically significant correlation coefficients between GPP_{norm} and PAR, CNI, SVWC, P and Ts, were obtained for the dry spruce forest ecosystem. Moreover, the correlation coefficients between GPP_{norm} and PAR, CNI, VPD, Tair and P were observed to be statistically significant ($p < 0.05$) at the beech forest site in Štítná.

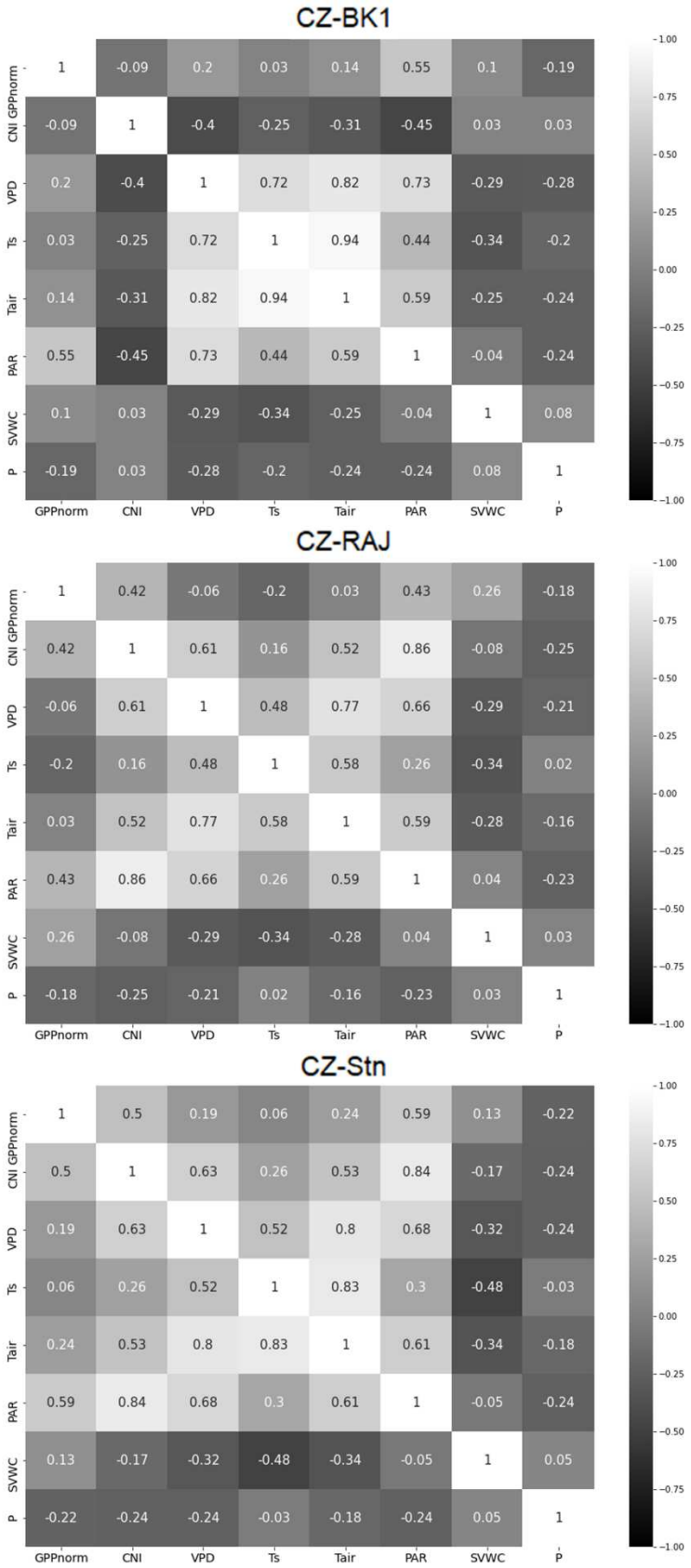
CZ-BK1
GPPnorm 1 -0.09 0.2 0.03 0.14 0.55 0.1 -0.19
CNI -0.09 1 -0.4 -0.25 -0.31 -0.45 0.03 0.03
VPD 0.2 -0.4 1 0.72 0.82 0.73 -0.29 -0.28
Ts 0.03 -0.25 0.72 1 0.94 0.44 -0.34 -0.2
Tair 0.14 -0.31 0.82 0.94 1 0.59 -0.25 -0.24
PAR 0.55 -0.45 0.73 0.44 0.59 1 -0.04 -0.24
SVWC 0.1 0.03 -0.29 -0.34 -0.25 -0.04 1 0.08
P -0.19 0.03 -0.28 -0.2 -0.24 -0.24 0.08 1
GPPnorm CNI VPD Ts Tair PAR SVWC P
1.00 0.75 0.50 0.25 0.00 −0.25 −0.50 −0.75 −1.00
CZ-RAJ
GPPnorm 1 0.42 -0.06 -0.2 0.03 0.43 0.26 -0.18
CNI 0.42 1 0.61 0.16 0.52 0.86 -0.08 -0.25
VPD -0.06 0.61 1 0.48 0.77 0.66 -0.29 -0.21
Ts -0.2 0.16 0.48 1 0.58 0.26 -0.34 0.02
Tair 0.03 0.52 0.77 0.58 1 0.59 -0.28 -0.16
PAR 0.43 0.86 0.66 0.26 0.59 1 0.04 -0.23
SVWC 0.26 -0.08 -0.29 -0.34 -0.28 0.04 1 0.03
P -0.18 -0.25 -0.21 0.02 -0.16 -0.23 0.03 1
GPPnorm CNI VPD Ts Tair PAR SVWC P
1.00 0.75 0.50 0.25 0.00 −0.25 −0.50 −0.75 −1.00
CZ-Stn
GPPnorm 1 0.5 0.19 0.06 0.24 0.59 0.13 -0.22
CNI 0.5 1 0.63 0.26 0.53 0.84 -0.17 -0.24
VPD 0.19 0.63 1 0.52 0.8 0.68 -0.32 -0.24
Ts 0.06 0.26 0.52 1 0.83 0.3 -0.48 -0.03
Tair 0.24 0.53 0.8 0.83 1 0.61 -0.34 -0.18
PAR 0.59 0.84 0.68 0.3 0.61 1 -0.05 -0.24
SVWC 0.13 -0.17 -0.32 -0.48 -0.34 -0.05 1 0.05
P -0.22 -0.24 -0.24 -0.03 -0.18 -0.24 0.05 1
GPPnorm CNI VPD Ts Tair PAR SVWC P
1.00 0.75 0.50 0.25 0.00 −0.25 −0.50 −0.75 −1.00

Fig. 5.6: Pearson correlation coefficient matrix showing correlation coefficient between the environmental variables (clearness index: CNI, photosynthetic available radiation: PAR, air temperature: Tair, soil temperature: Ts, the soil volumetric water content: SVWC, vapour pressure deficit: VPD, precipitation: P) and estimated Normalized gross primary productivity (GPP_{norm}) within the spruce forest sites in Bílý Kříž (CZ-BK1) and Rájec (CZ-RAJ), and for the beech forest stand in Štítná (CZ-Stn) during the main growing season of 2012-2016 (indicated in the upper panel).

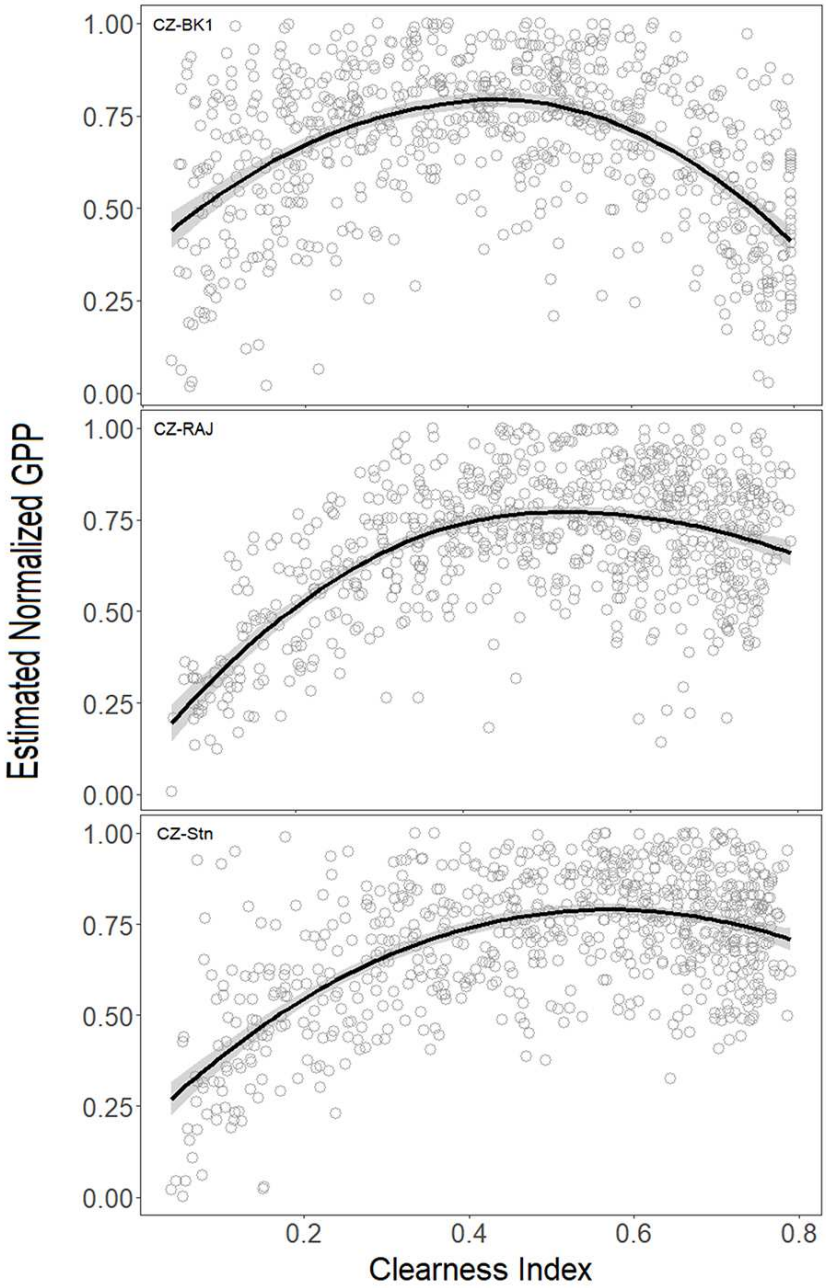

Figure 5.7: Correlation between the clearness index (CNI) and the estimated Normalized gross primary productivity (GPP_{norm}) within the spruce forest sites in Bílý Kříž (CZ-BK1) and Rájec (CZ-RAJ), and for the beech forest stand in Štítná (CZ-Stn) during the main growing season (May- September) of 2012-2016.

5.2.1 Normalized gross primary productivity (GPP_{norm}) prediction through stepwise multi-linear regression (SMLR)

In identifying the main environmental parameters that influence GPP_{norm} across both spruce forests and beech forest stands, an SMLR model was developed and evaluated (Fig. 5.8).

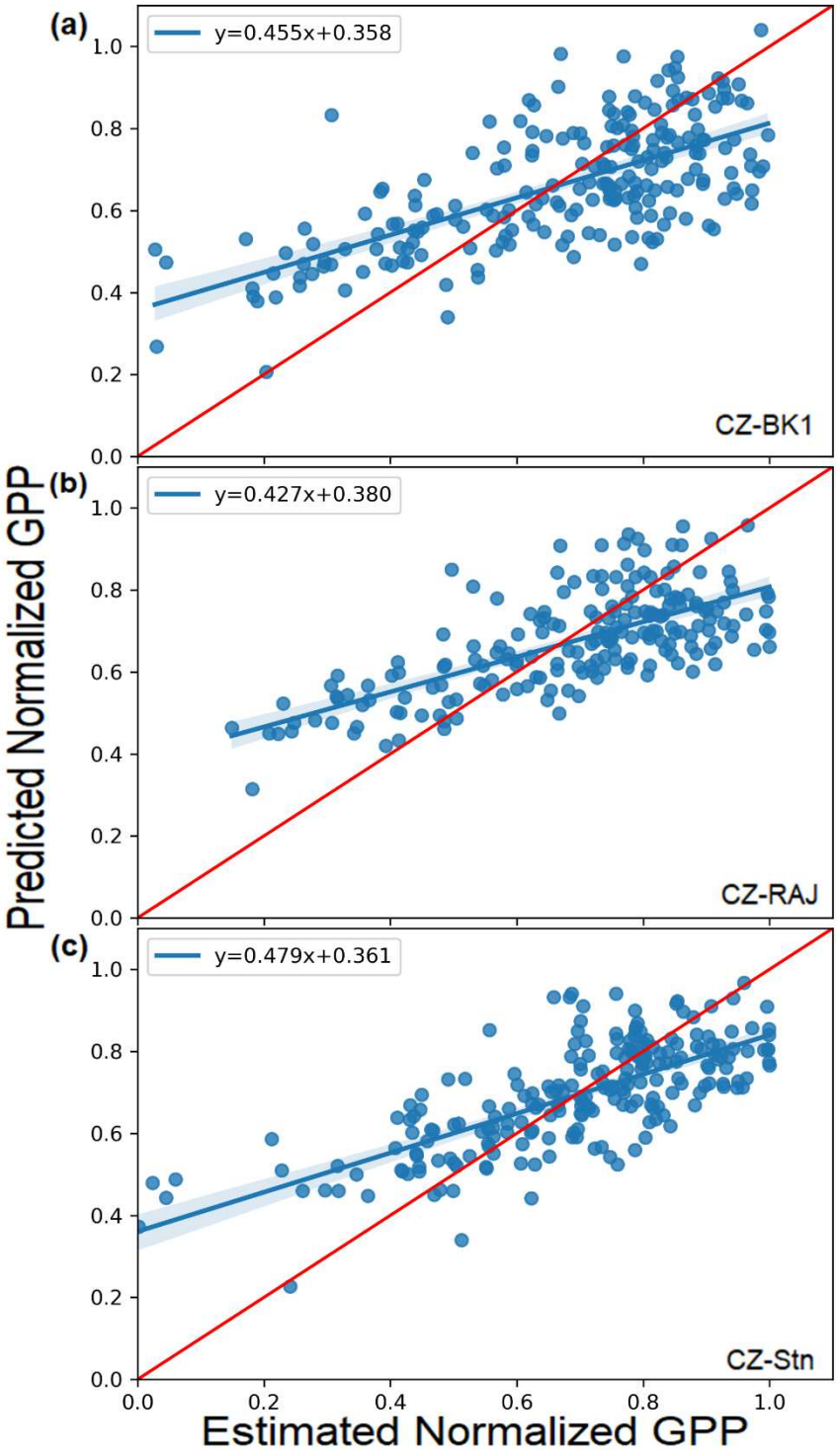

Fig. 5.8: Plot of predicted daily GPPnorm estimated from the stepwise multiple linear regression model (SMLR) vs. estimated daily normalized gross primary productivity (GPPnorm) within the spruce forest stands in (a) Bílý Kříž (CZ-BK1) and (b) Rájec (CZ-RAJ), and the (c) beech forest stand in Štítná (CZ-Stn).

The 1:1 relationship between the predicted GPP_{norm} and estimated GPP_{norm} values from the SMLR is shown by the red line. The 95% confidence interval is shown by the shaded blue line.

The results from the pearson correlation showed a good model fit (Figure 5.8 and Table 5.3) in GPP_{norm} prediction with strong linear relationship between the predicted and estimated GPP_{norm} values across all the forest ecosystems. However, the model overpredicted for lower GPP_{norm} values and also under predicted for high GPP_{norm} values across all the forest sites. Within the SMLR model, about 40 – 49% of the variance in GPP_{norm} prediction was influenced by PAR, CNI, SVWC, VPD, Tair, and Ts with a minimum prediction error (RMSE) of 0.14 at the dry spruce forest site.

From the results derived from the SMLR analyses, the coefficients of PAR, SVWC, VPD and Ts were statistically significant ($p < 0.01$) and found to have similar effects on GPP_{norm} at both spruce forest stands (Table 5.3 and Table 5.4). Additionally, at the wet spruce forest stand, CNI was found to have a secondary effect on GPP_{norm} values (Table 5.3). However, all the environmental variables (especially PAR, Ts and CNI) used in the SMLR model had significant effect on GPP_{norm} values at the beech forest stand in Štítná (Table 5.5).

Also, across both spruce forest stands, there were similar quadratic terms such as PAR^2, Ts^2, and CNI^2 that were statistically significant ($p < 0.01$) with negative coefficients. This indicated a downward slope in GPP_{norm} values with an increase in PAR, Ts and CNI values (Table 5.3 and Table 5.4). Moreover, VPD^2 and CNI^2 were statistically significant ($p < 0.01$) and inversely related to GPP_{norm} (Table 5.5). However, a negative coefficient of $SVWC^2$ across all the forest stands indicated an increase in GPP_{norm} with high SVWC values (Table 5.3 – Table 5.5).

The VPD:SVWC interaction term from the SMLR analyses was statistically significant ($p < 0.01$) and found to be similar across all the forest stands. This indicates the influence of both VPD and SVWC on GPP_{norm} values. Moreover, at the wet spruce forest stand in Bílý Kříž, the interactive effects between VPD and SVWC, PAR and Tair were statisitically significant ($p < 0.01$), whereas at the dry spruce forest stand in Rájec, GPP_{norm} was mostly affected by interactive terms between SVWC and other environmental variables such as PAR, CNI and VPD. In addition, interactive terms such as Ts:SVWC, Tair:SVWC, CNI:PAR, Tair:PAR, VPD:SVWC and VPD:Ts had significant effect on GPP_{norm} within the beech forest stand in Štítná.

Table 5.3: Coefficients of the significant environmental variables (clearness index: CNI; photosynthetic available radiation: PAR; air temperature: Tair; soil temperature: Ts; soil volumetric water content: SVWC; vapour pressure deficit: VPD) influencing normalized gross primary productivity (GPP_{norm}) from the stepwise multi-linear regression (SMLR) model at the wet spruce forest stand in Bílý Kříž (CZ-BK1).

	Estimate	Standard Error	t value	Pr (>| t |)
(Intercept)	-6.397 e-01	1.397 e-01	-4.581	5.47 e-06 ***
PAR	1.659e-01	1.541e-02	10.772	< 2e-16 ***
PAR^2	-8.813 e-03	1.025 e-03	8.601	< 2 e-16 ***
$SVWC^2$	-1.095e+01	1.938e+00	-5.649	2.34e-08 ***
PAR:Tair	-5.234e-03	9.454e-04	-5.536	4.36e-08 ***
SVWC	5.048e+00	9.514e-01	5.305	1.51e-07 ***
Ts:PAR	4.884e-03	1.062e-03	4.598	5.04e-06 ***
Ts^2	-2.002e-03	4.817e-04	-4.155	3.64e-05 ***
VPD:SVWC	9.490e-02	2.389e-02	3.972	7.84e-05 ***
CNI^2	-3.623e-01	1.025e-01	-3.533	0.000437 ***
CNI	4.589e-01	1.326e-01	3.461	0.000571***
VPD^2	-2.191e-03	7.005e-04	-3.128	0.001830 ***
VPD	-3.745e-02	1.525e-02	-2.456	0.014300 *
Ts	2.550e-02	1.077e-02	2.367	0.018214 *
VPD:PAR	3.094e-03	1.367e-03	2.264	0.023906 *

CNI:Tair	1.066e-02	5.007e-03	2.128	0.033690 *
CNI:PAR	-1.544e-02	7.571e-03	-2.039	0.041772 *
VPD:Tair	1.937e-03	9.802e-04	1.976	0.048507 *

Signif. codes: '***' $p \leq 0.001$ '**' $p \leq 0.01$ '*' $p \leq 0.05$

Table 5.4: Coefficients of the significant environmental variables (clearness index: CNI; photosynthetic available radiation: PAR; air temperature: Tair; soil temperature: Ts; soil volumetric water content: SVWC; vapour pressure deficit: VPD) influencing normalized gross primary productivity (GPPnorm) from the stepwise multi-linear regression (SMLR) model at the dry spruce forest stand in Rájec (CZ-RAJ).

	Estimate	Standard Error	t value	Pr (>| t |)
(Intercept)	1.2416627	0.2834895	4.380	1.39e-05 ***
PAR	0.1957506	0.0157165	12.455	< 2e-16 ***
PAR^2	-0.0055807	0.0006615	-8.436	< 2e-16 ***
Ts:SVWC	0.2931591	0.0448089	6.542	1.25e-10 ***
$Tair^2$	-0.0009479	0.0001752	-5.409	8.97e-08 ***
CNI^2	-0.9090371	0.1592056	-5.710	1.74e-08 ***
Ts^2	-0.0015452	0.0002921	-5.290	1.68e-07 ***
SVWC:CNI	4.0751744	0.8162736	4.992	7.71e-07 ***
Ts:Tair	0.0016139	0.0003835	4.208	2.94e-05 ***
PAR:SVWC	-0.3523768	0.0896162	-3.932	9.35e-05 ***
SVWC	-8.4537169	2.2630082	-3.736	0.000204 ***

VPD	-0.0364140	0.0102154	-3.565	0.000392 ***
Ts	-0.0404096	0.0149492	-2.703	0.007053 ***
VPD:SVWC	0.1377881	0.0518878	2.656	0.008118 ***
$SVWC^2$	10.9036492	5.0661812	2.152	0.031754 *

Signif. codes: '***' $p \leq 0.001$ '**' $p \leq 0.01$ '*' $p \leq 0.05$

Table 5.5: Coefficients of the significant environmental variables (clearness index: CNI; photosynthetic available radiation: PAR; air temperature: Tair; soil temperature: Ts; soil volumetric water content: SVWC; vapour pressure deficit: VPD) influencing normalized gross primary productivity (GPP_{norm}) from the stepwise multi-linear regression (SMLR) model at the beech forest site in Štítná (CZ-Stn).

	Estimate	Standard Error	t value	Pr (>| t |)
(Intercept)	1.6324051	0.2913214	5.603	3.00e-08 ***
PAR	0.1035450	0.0089856	11.523	< 2e-16 ***
Ts:SVWC	0.4954804	0.0627527	7.896	1.08e-14 ***
Ts	-0.1794898	0.0233970	-7.671	5.56e-14 ***
CNI	0.8213389	0.1378886	5.957	4.04e-09 ***
Tair	0.0988082	0.0178532	5.534	4.38e-08 ***
SVWC	-6.3883130	1.3261064	-4.817	1.78e-06 ***
Tair:SVWC	-0.2274474	0.0467787	-4.862	1.43e-06 ***
Tair:PAR	-0.0024049	0.0005103	-4.713	2.93e-06 ***
CNI:PAR	-0.0558883	0.0148897	-3.753	0.000189 ***

VPD^2	-0.0008560	0.0002309	-3.708	0.000225 ***
VPD:Ts	0.0021074	0.0006005	3.510	0.000477 ***
VPD	-0.0561466	0.0176605	-3.179	0.001540 ***
$SVWC^2$	4.9409576	1.5641808	3.159	0.001651 ***
VPD:SVWC	0.1048877	0.0339888	3.086	0.002107 ***
CNI^2	-0.5376705	0.2101539	-2.558	0.010718 *

Signif. codes: '***' $p \leq 0.001$ '**' $p \leq 0.01$ '*' $p \leq 0.05$

5.2.2 Normalized gross primary productivity (GPP_{norm}) prediction through random forest analyses (RF)

Comparison of the validation statistics from both the SMLR and RF models are shown in Table 5.6. The RF analyses showed higher R^2 (> 0.54) and pearson correlation values (> 0.70) with low RMSE (< 0.15) in GPP_{norm} prediction. This indicates the better performance of the RF model in predicting changes in GPP_{norm} with the environmental factors across the forest sites (Fig. 5.9).

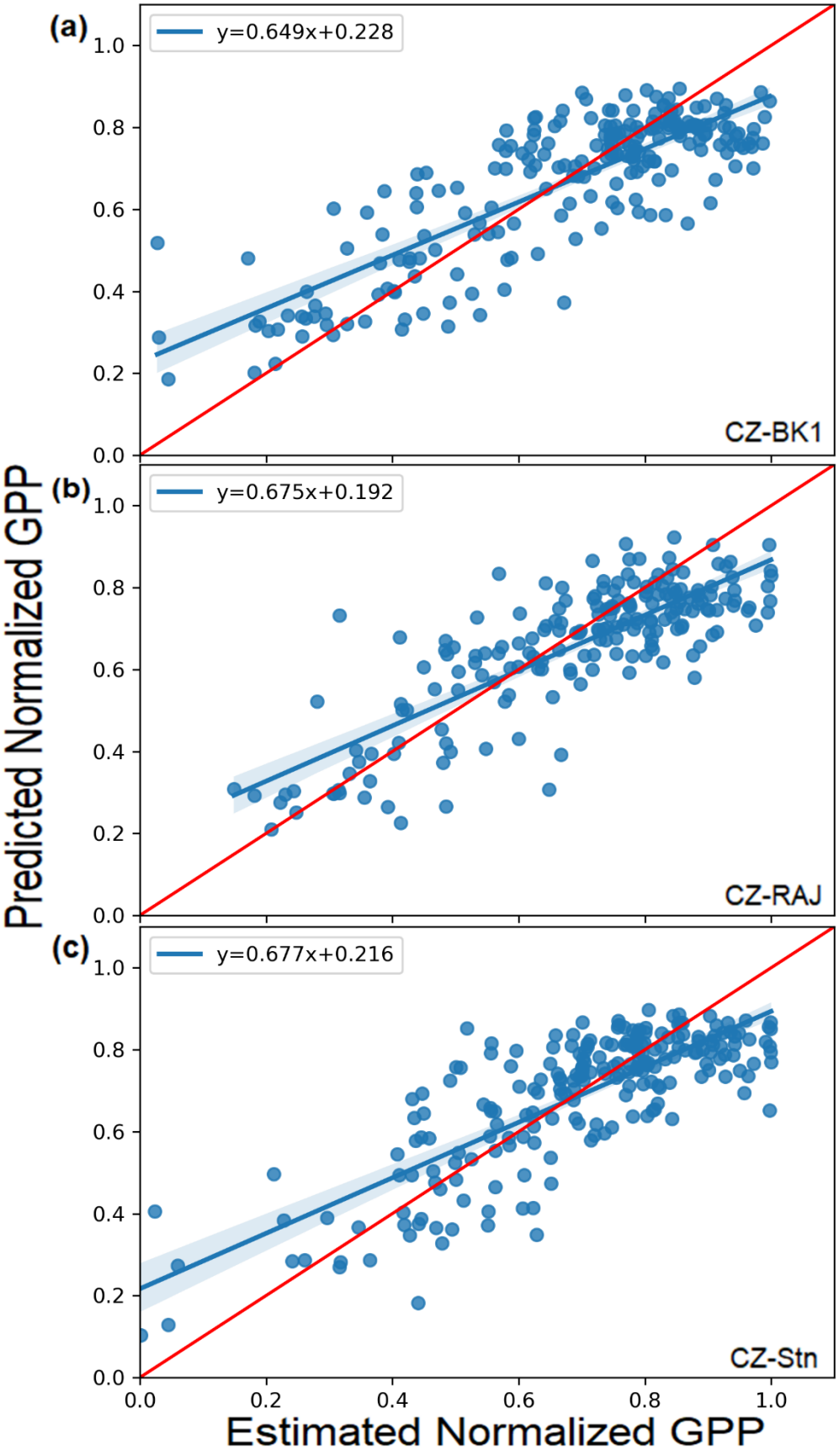

Fig. 5.9: Plot of predicted daily GPP_{norm} estimated from the the random forest (RF) analyses vs. estimated daily normalized gross primary productivity (GPP_{norm}) within the spruce forest stands

in (a) Bílý Kříž (CZ-BK1) and (b) Rájec (CZ-RAJ), and the (c) beech forest stand in Štítná (CZ-Stn). The 1:1 relationship between the predicted GPP_{norm} and estimated GPP_{norm} values from the RF are shown by the red line. The 95% confidence interval is shown by the shaded blue line.

Table 5.6: Comparison of the accuracy indicators (the Pearson correlation, root mean square error: RMSE, and R2 values) from both the stepwise multi-linear regression (SMLR) and random forest (RF) analyses in Normalized GPP (GPPnorm) prediction across the spruce forest stands in Bílý Kříž (CZ-BK1) and Rájec (CZ-RAJ), and the beech forest stand in Štítná (CZ-Stn) for the main growing season (May-September) of 2012 - 2016.

Variants	**CZ-BK1**		**CZ-RAJ**		**CZ-Stn**	
	SMLR	RF	SMLR	RF	SMLR	RF
Pearson correlation	0.67	0.82	0.69	0.82	0.72	0.79
R^2	0.43	0.65	0.44	0.62	0.51	0.60
RMSE	0.16	0.12	0.14	0.12	0.14	0.12

The importance of environmental variables in predicting GPP_{norm} derived using the mean decrease error of the RF analyses were derived and compared across all forest sites (Fig. 5.9). PAR was observed to be the most important environmental variable in GPP_{norm} prediction across all forest sites. VPD was also observed to be the second most important environmental variable affecting GPP_{norm} prediction at the spruce forest sites, unlike in the beech forest site where VPD was rather the third most important variable after SVWC. Similar output on environmental variables' importance was also observed across all the sites for both the SMLR and RF models. Moreover, the Ts, which is a function of the heat flux in the soil as well as the heat exchanges between the atmosphere and the soil, was observed to have higher importance at the dry spruce forest than at all the forest sites. Also, within the spruce forest sites, SVWC was found to have higher feature importance in the dry spruce forest than at the wet spruce forest site.

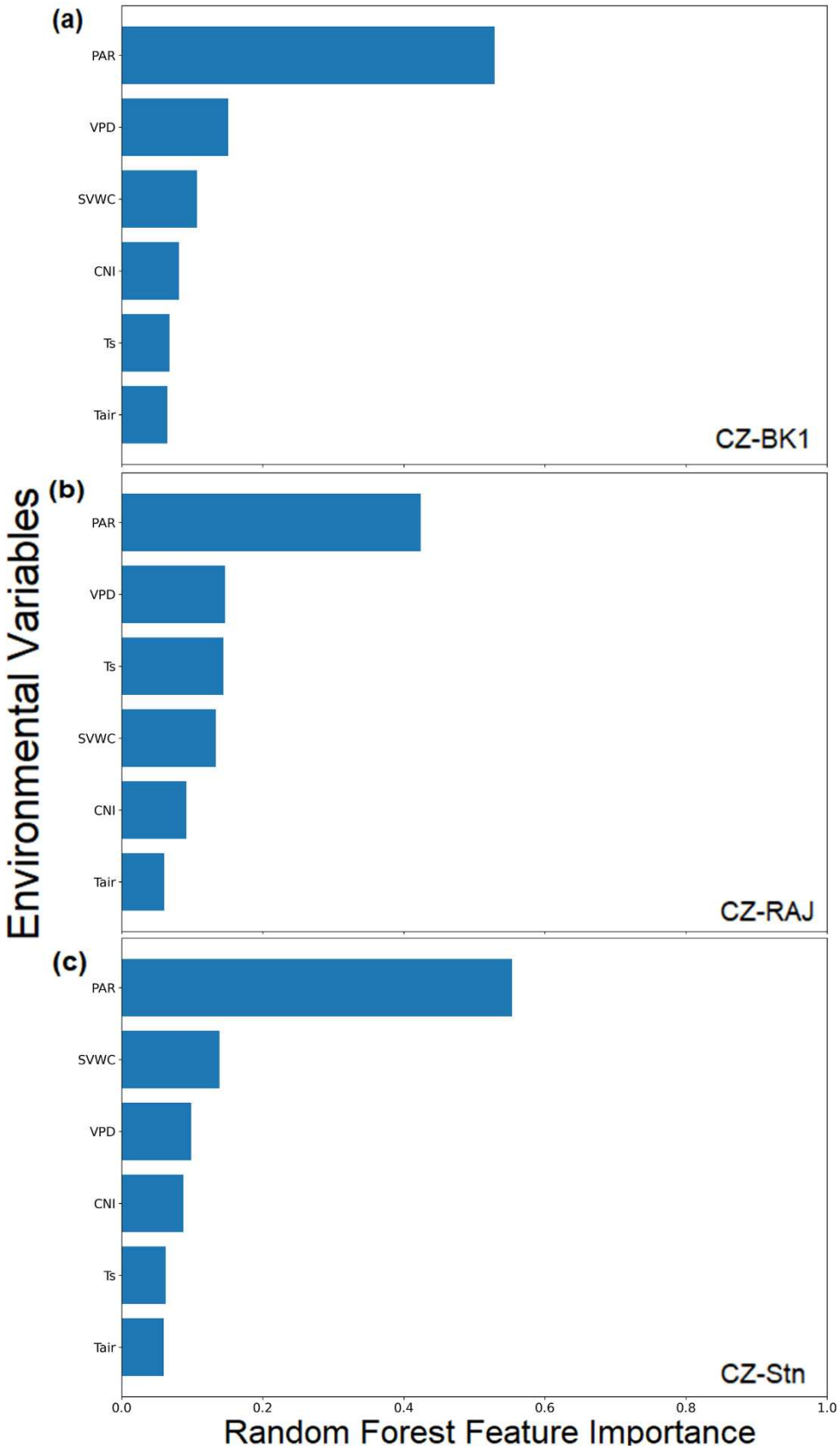

Fig. 5.9: Predictor variable importance measures from the random forest analyses for the spruce forest stands in (a) Bílý Kříž (CZ-BK1), and (b) Rájec (CZ-RAJ), and the (c) beech forest stand in Štítná (CZ-Stn).

The significant effect of environmental variables on GPP_{norm} prediction across all forest sites was graphically represented and compared in a decision tree (Fig. 5.10).

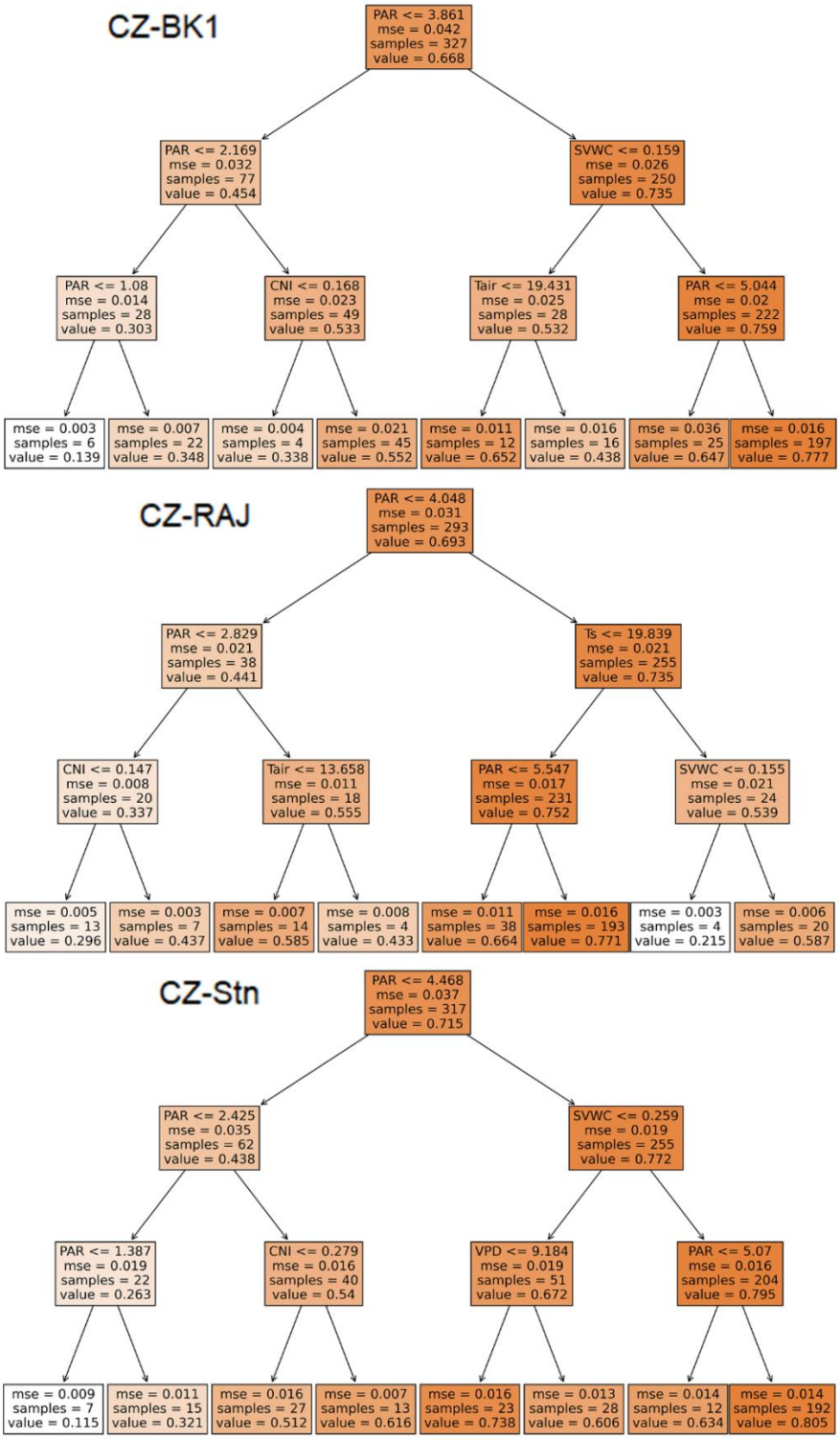

Fig. 5.10: Decision tree showing the influence of environmental variables (clearness index: CNI; photosynthetic available radiation: PAR; air temperature: Tair; soil temperature: Ts; soil volumetric water content: SVWC; vapour pressure deficit: VPD) on normalized GPP (GPP_{norm}) prediction at the spruce forest stands in Bílý Kříž (CZ-BK1) and Rájec (CZ-RAJ), and the beech forest stand in Štítná (CZ-Stn) from the random forest analyses. The mean square error (mse) shows the closeness of the predicted GPP_{norm} values to the estimated daily GPP_{norm} values. The light coloured areas indicate conditions leading to low GPP_{norm} values and the areas with deep colour show conditions leading to high GPP_{norm} values.

As seen from the decision tree, PAR is the most important environmental variable in grouping the GPP_{norm} values into high and low values across all the forest ecosystems. Within both spruce forest sites, higher GPP_{norm} values (right branches in Fig. 5.10) were separated by similar PAR thresholds of approximately 4 MJ m^{-2} day^{-1} while high GPP_{norm} values were realized at PAR values above 4 MJ m^{-2} day^{-1} at the beech forest site. However, the left branch in Fig. 5.10 represents exceptional cases with low PAR and GPP_{norm} values. These exceptional cases were mainly observed at the wet spruce forest with about 72 cases in comparison with about 38 cases in the dry spruce forest and with 62 cases in the beech forest. Moreover, there some periods at the dry spruce forest site when lower GPP_{norm} values were recorded at low SVWC values (< 0.16 m^3 m^{-3}; 4 cases) and CNI values (< 0.2; 13 cases). Additionally, other environmental variables aside from PAR were also important for the GPP_{norm} group separation. At the wet spruce forest site, SVWC values (< 0.16 m^3 m^{-3}; 250 cases) and Tair values (< 19 °C; 28 cases) were observed to have secondary effects on GPP_{norm} values. Also, lower GPP_{norm} values were attained at extremely low PAR (< 2.2 MJ m^{-2} day^{-1}) and CNI (< 0.2; 49 cases) values. In comparison with the RF predictor importance in Fig. 5.9, PAR, SVWC, and Tair variables were observed to be the main limiting factor of GPP_{norm} within the wet spruce forest ecosystem.

Moreover, at the dry spruce forest, the main limiting factors for GPP_{norm} values were found to be PAR, Ts (255 cases), and SVWC (24 cases). Also, lower GPP_{norm} values were realized on days with low PAR and CNI (≤ 0.2; 20 cases) values or for days characterized by extremely high Ts values (> 20 °C) with low SVWC (< 0.16 m^3 m^{-3}; 4 cases). However, higher GPP_{norm} values were realized on days characterized by Ts values approximately < 20 °C with PAR also approximately > 5.5 MJ m^{-2} day^{-1}.

At the beech forest site, PAR, SVWC and VPD values were found to have secondary effects on GPP_{norm} values. High GPP_{norm} values were realized on days characterized by high SVWC (> 0.3 m^3 m^{-3}) and PAR > 5.1 MJ m^{-2} day^{-1} (192 days). However, on days with low

SVWC (< 0.3 m^3 m^{-3}), VPD was the main limiting factor for GPP_{norm} values (51 cases). On such days with high VPD (> 9 hPa; 28 cases) GPP_{norm} values reduced.

5.3 Contrasting effects of drought on the carbon dynamics at two Norway spruce forests sites with different climatic conditions

As already observed from above, the response in GPP_{norm} for the spruce species was sensitive to environmental factors related to soil water availability. Thus, we further investigated the impact of a severe drought stress condition (like recorded in the summer of 2015) on two Norway spruce forest sites at different climates with contrasting water availability (cold and humid climate at Bílý Kříž vs. moderately warm and dry climate at Rájec). This comparative analysis of GPP is based on three years eddy covariance dataset, where 2015 represented the year with dry conditions while normal conditions characterized 2014 and 2016.

5.3.1 Light response curves (LRC) of GPP at spruce forest sites with different climates

The LRC parameters for the normal years (NY) of 2014 and 2016 are compared with those for the drought-affected year (DY) for both experimental spruce forest sites (Fig. 5.11; Table 5.4). The apparent quantum yield (α) at the wet spruce forest site in Bílý Kříž was found to be higher than in the dry spruce forest site at Rájec. During the NY, α in the wet spruce forest was 12% higher than in the dry spruce forest at PAR < 500 μmol m^{-2} s^{-1}. Moreover, during the DY, α at the dry spruce forest site further declined by 25% in comparison with that in the wet spruce forest site.

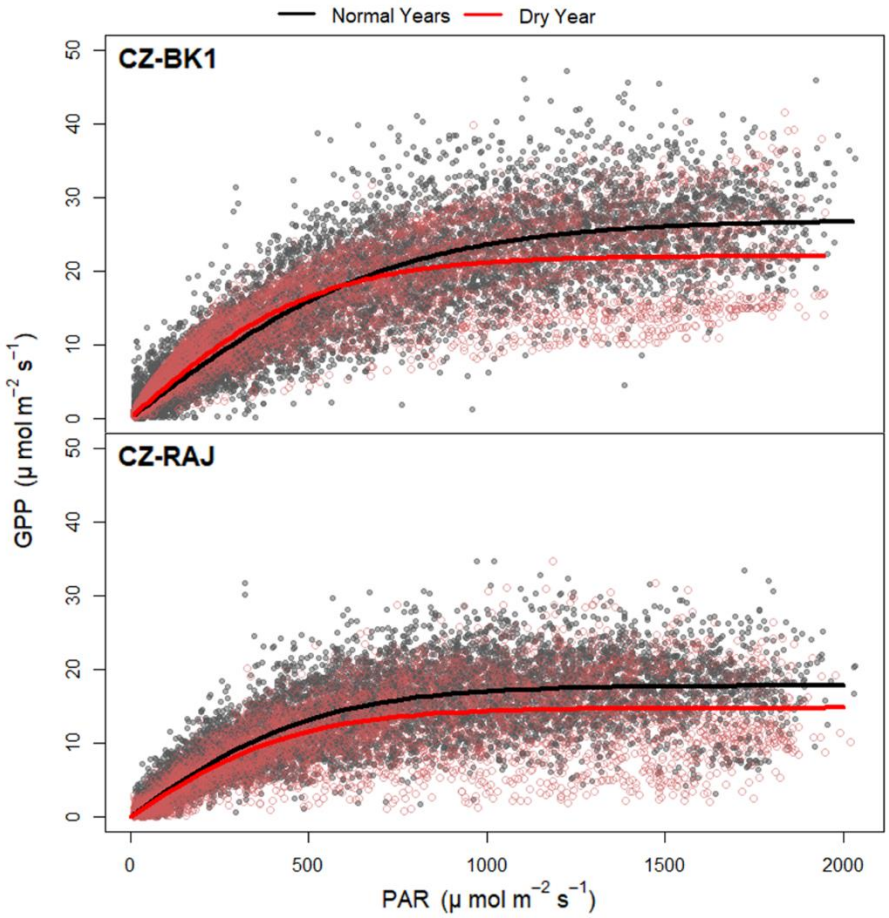

Fig. 5.11: The response of forest gross primary production (GPP) to photosynthetically active radiation during the years with normal conditions (2014 & 2016; shown with black line) and affected by drought stress (2015; shown with a red line) at the spruce forest stands in Bílý Kříž (CZ-BK1) and Rájec (CZ-RAJ). Half-hourly GPP values (in points) have been fitted using the logistic sigmoid light response curves (both black and red lines).

The value for the maximum gross primary production at light saturation (GPP_{max}) at the wet spruce forest in Bílý Kříž was generally higher than at the dry spruce forest in Rájec during the year from 2014 – 2016 (Fig. 5.11). Note that GPP_{max} in the wet spruce forest was 34% higher than in the dry spruce forest during the years with normal conditions (Table 5.7). However, there were a significant reduction in the GPP_{max} values recorded at both spruce forest stands during the DY period (18% decline in the wet spruce forest site and 17% decline in the dry spruce forest site) in comparison with those recorded for the NY. Also, it was further observed that the GPP_{max} value at the dry spruce forest site was 33% lower than that in the wet spruce forest stand during the DY period. Interestingly, the GPP_{max} value at the wet spruce forest site during the DY period still remained higher than the GPP_{max} value recorded at the dry spruce forest even during NY periods.

Table 5.7: The parameters of the Light response curve (LRC) for the normal (2014 and 2016) and dry (2015) year periods at the wet spruce forest stand in Bílý Kříž (CZ-BK1) and dry spruce forest stand in Rájec (CZ-RAJ) within the main growing season period (May – September). The apparent quantum yield shown by α, the maximum gross primary production at light saturation also shown as GPP_{max} and the coefficient of determination (R^2) have all been indicated in the table below.

Variants	**CZ-BK1**		**CZ-RAJ**	
	Years with Normal Conditions (2014 & 2016)	Dry Year (2015)	Years with Normal Conditions (2014 & 2016)	Dry Year (2015)
α [mol (CO_2) mol^{-1} (phot.)]	0.0383 ± 0.0003	0.0446 ± 0.0006	0.0338 ± 0.0003	0.0312 ± 0.0006
GPP_{max} [μmol m^{-2} s^{-1}]	26.91 ± 0.14	22.03 ± 0.13	17.77 ± 0.08	14.75 ± 0.12
R^2	0.88	0.78	0.78	0.73

5.3.2 Response of light response curve (LRC) residuals to VPD and SVWC at spruce forest sites with different climates

The applied LRC model showed the light response of the forest GPP. As such, its residuals were used to assess the additional effects of other environmental parameters such as VPD and SVWC (known to affect GPP; Fig. 5.12 and 5.13). Results showed that the residuals remained consistently more negative when VPD increased with declining SVWC values (depicting dry conditions). Thus, VPD was observed to significantly affect GPP than SVWC across both sites, as shown by the piecewise regression analysis (using the LRC residuals for 2014 – 2016). However, during the DY period, there were stronger effects of both VPD and SVWC on GPP at the dry spruce forest stand in Rájec. At the wet spruce forest stand in Bílý Kříž, a minimal effect of SVWC on GPP during the NY periods was mainly observed.

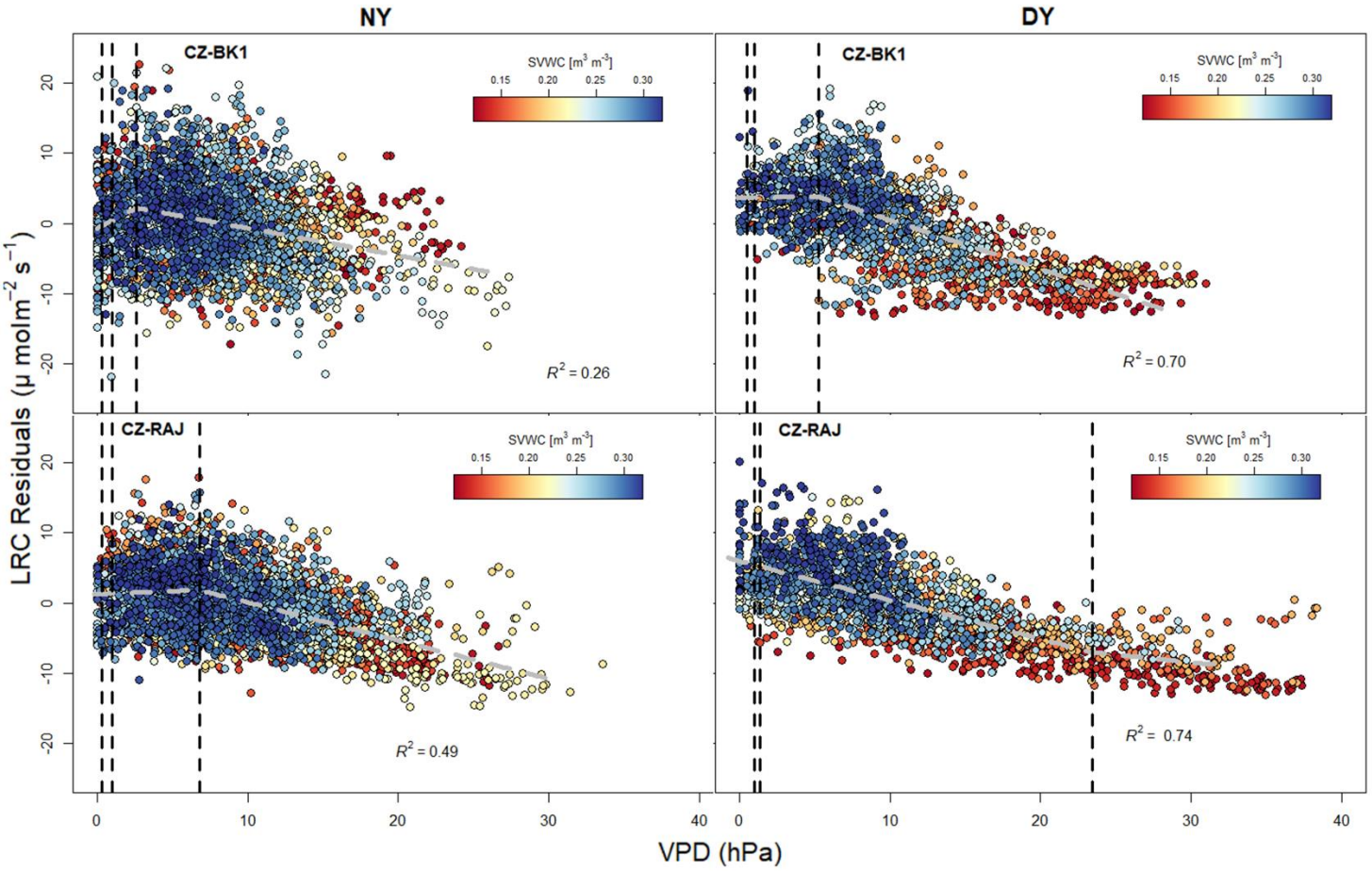

Fig. 5.12: Relationship between residuals of the light response curve (LRC) of gross primary production (GPP) and vapour pressure deficit (VPD) at the wet spruce forest stand in Bílý Kříž (CZ-BK1) and dry spruce forest stand in Rájec (CZ-RAJ) for the normal (NY) and dry years (DY). The red dots represent low soil volumetric water content (SVWC) conditions and the blue dots show high SVWC conditions. The black dashed lines represent the breakpoint values whereas the grey dashed lines show the piecewise regression model slope.

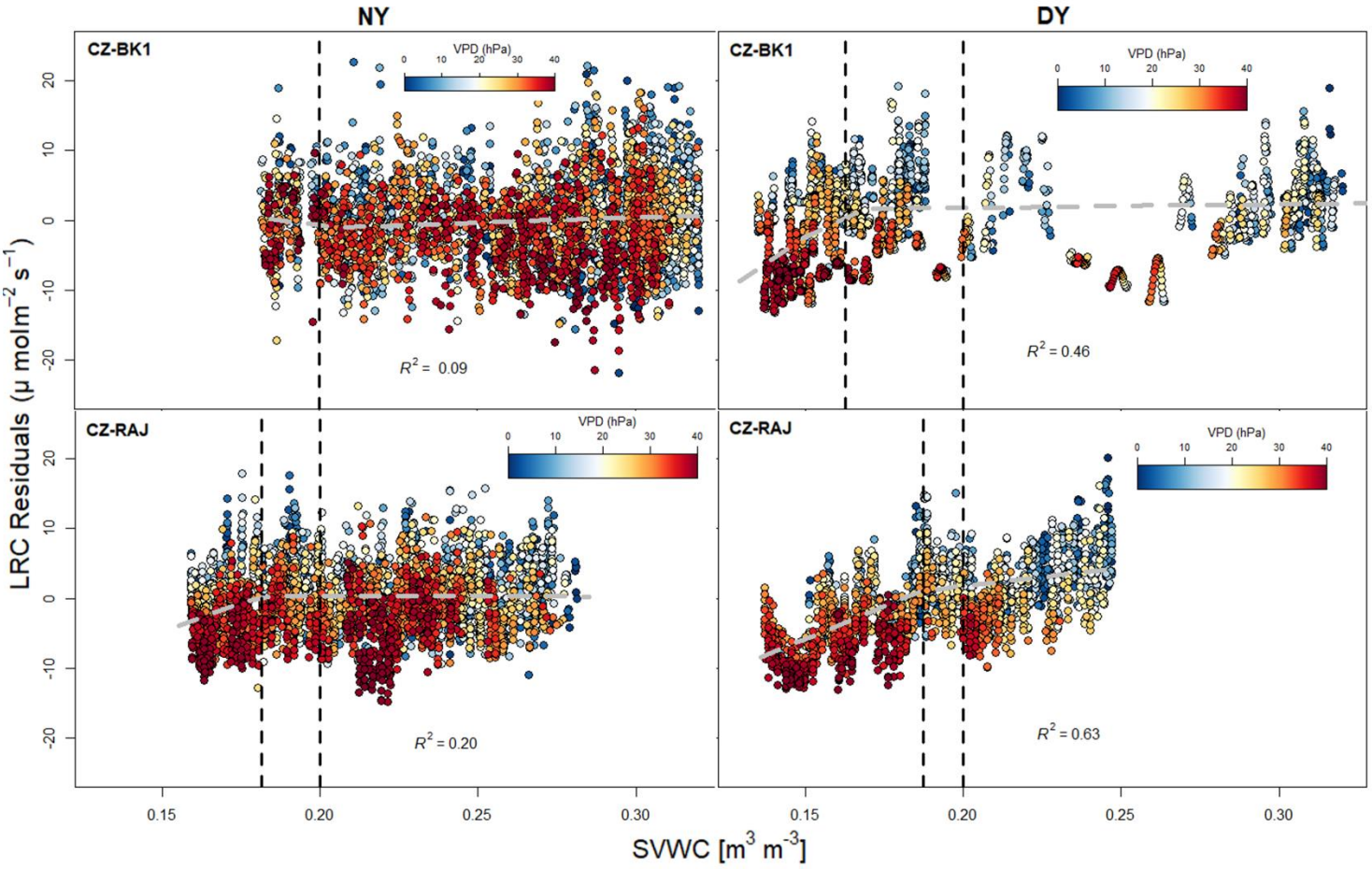

Fig. 5.13: Relationship between the residuals of the light response curve (LRC) of gross primary production (GPP) and the soil volumetric water content (SVWC) at the wet spruce forest stand in Bílý Kříž (CZ-BK1) and dry spruce forest stand in Rájec (CZ-RAJ) for the normal (NY) and dry years (DY). The red dots represent high VPD conditions and the blue dots show low VPD conditions. The black dashed lines represent the breakpoint values whereas the grey dashed lines show the piecewise regression model slope.

Overall, the relationship between the LRC residuals and changes in VPD and SVWC showed a biphasic response to drought except during the DY period at the dry spruce forest stand (Fig. 5.12). As observed in Table 5.8, all the breakpoints from the piecewise regression were statistically significant ($p < 0.001$). However, there were observed steeper slopes after the VPD breakpoint values from the initial slope for both DY and NY periods, especially at the dry spruce forest, and only for the DY period in the wet spruce forest stand. Therefore, GPP decreased faster after the breakpoint in the dry spruce forest than as observed in the wet spruce forest from 2014 – 2016. Moreover, GPP declined faster after the breakpoint across both sites for the DY period.

Table 5.8: Summary of the breakpoints and slopes of the piecewise regression showing the relationship between the residuals of the light response curve (LRC) to both vapour pressure deficit (VPD) and the soil volumetric water content (SVWC) over May – September.

Variants	**CZ-BK1**		**CZ-RAJ**	
	Years with Normal Conditions (2014 & 2016)	Dry Year (2015)	Years with Normal Conditions (2014 & 2016)	Dry Year (2015)
VPD [hPa]	2.6 ***	5.3 ***	6.8 ***	23.5 ***
Slope before breakpoint in VPD	1.12 ± 0.30	0.02 ± 0.12	0.08 ± 0.05	-0.55 ± 0.01
Slope after breakpoint in VPD	-0.39 ± 0.02	-0.70 ± 0.02	-0.54 ± 0.02	-0.22 ± 0.06
SVWC [m^3 m^{-3}]	0.20 ***	0.16 ***	0.18 ***	0.19 ***
Slope before breakpoint in SVWC	-85.49 ± 68.37	305.61 ± 23.43	164.61 ± 25.14	187.22 ± 8.78
Slope after breakpoint in SVWC	14.75 ± 2.60	5.03 ± 2.51	-1.27 ± 2.84	52.16 ± 6.24

Significant code for the breakpoint values: $p<0.01$ '***'

5.3.3 Impact of drought on the carbon fluxes at monthly timescale within the spruce forest sites with different climates

For a comprehensive comparison between the carbon fluxes of the NY and the DY in both spruce forest sites, the monthly averages of the daily sums of forest GPP and R_{eco} were investigated to assess the impact of drought on the net ecosystem production (NEP) for both spruce forest stands (Figs. 5.14, 5.15, and 5.16).

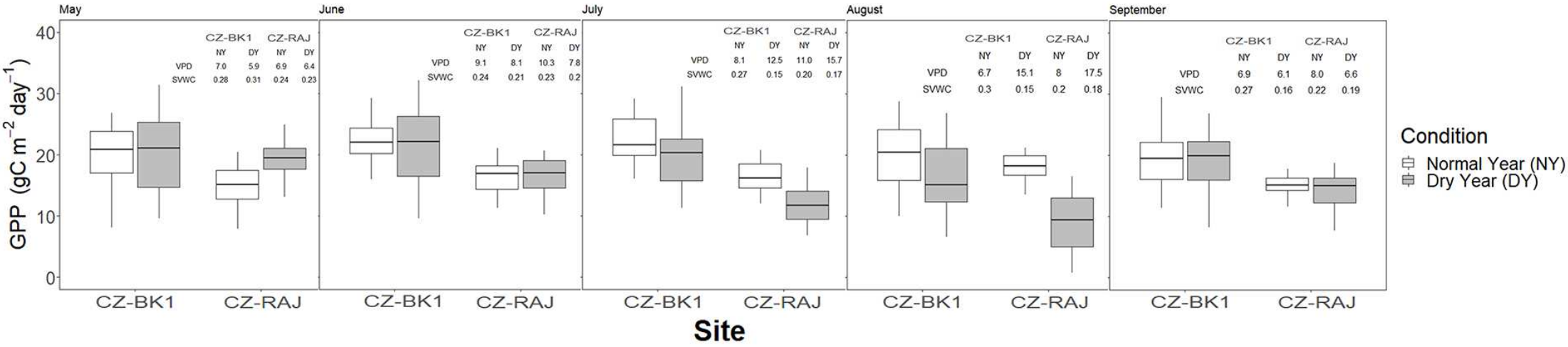

Fig. 5.14: Monthly mean daily sums of gross primary productivity (GPP) for May-September of the normal years (NY) and dry year (DY) at the wet spruce forest stand in Bílý Kříž (CZ-BK1) and dry spruce forest stand in Rájec (CZ-RAJ). The tables within the figure indicate the mean monthly vapour pressure deficit (VPD) and the mean monthly soil volumetric water content (SVWC) values from May-September for each forest station.

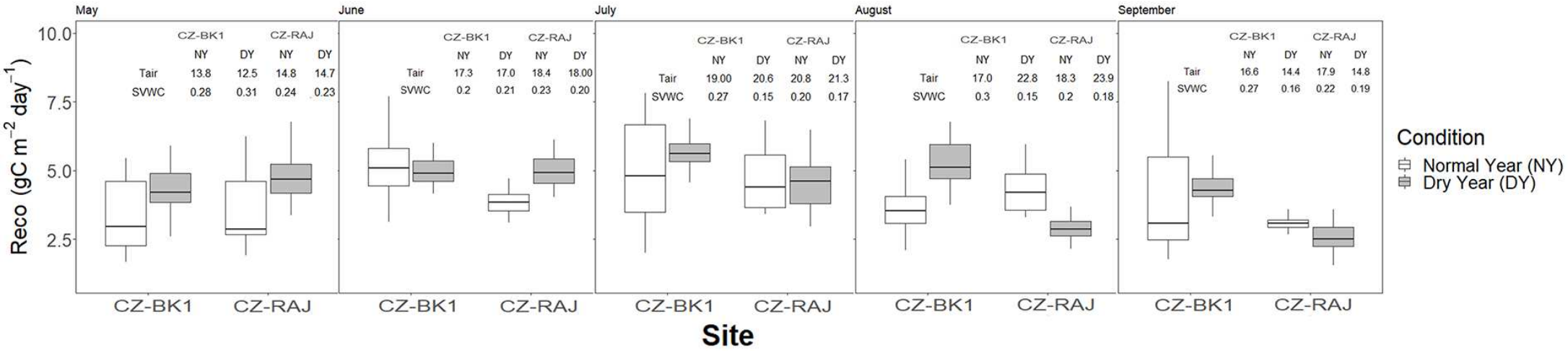

Fig. 5.15: Monthly mean daily sums of ecosystem respiration (R_{eco}) for May–September of the normal years (NY) and dry year (DY) at the wet spruce forest stand in Bílý Kříž (CZ-BK1) and dry spruce forest stand in Rájec (CZ-RAJ). The tables within the figure indicate the mean monthly air temperature (Tair) and the mean monthly soil volumetric water content (SVWC) values from May-September for each forest station.

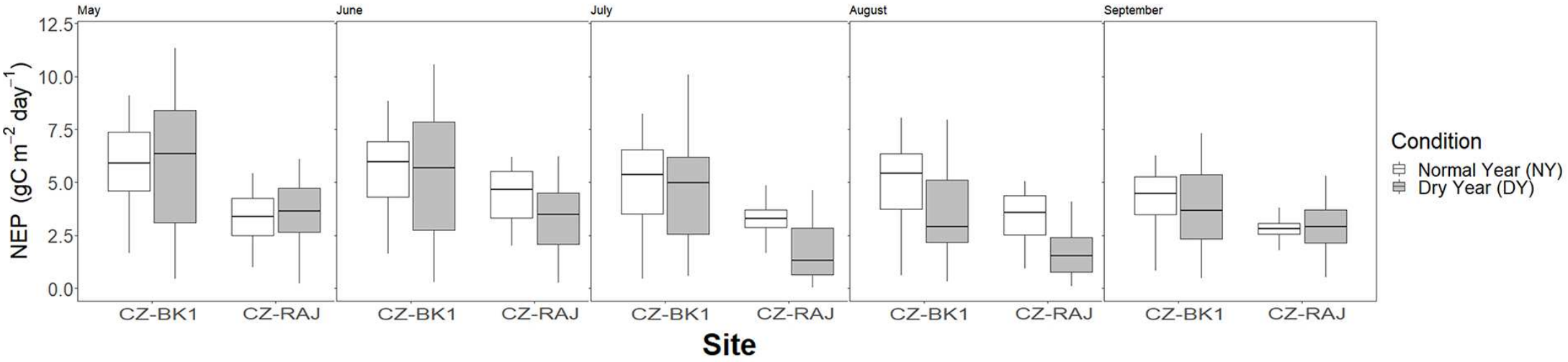

Fig. 5.16: Monthly mean daily sums of the net ecosystem production (NEP) for May – September of the normal years (NY) and dry year (DY) at the wet spruce forest stand in Bílý Kříž (CZ-BK1) and at the dry spruce forest stand in Rájec (CZ-RAJ).

The total GPP during the main growing season period of the DY was observed to decline by 14% in the dry spruce forest as compared to a 6% decline in the wet spruce forest site. There were also observed statistically significant differences ($p < 0.001$) in the mean monthly GPP values recorded for July and August of the DY as compared to that of the NY at both forest sites, especially in the dry spruce forest site (Fig. 5.14). Interestingly, the significant reduction of the mean monthly GPP values at both spruce forest sites during July and August coincided with high mean daily VPD values (exceeding 12 hPa) and low mean daily SVWC values (< 0.16 m^3 m^{-3}) as compared to the same period for the adjacent years during the NY periods.

Moreover, there was an observed increase in the mean monthly R_{eco} values during July - September of the DY period, except in August within the wet spruce forest (Fig. 5.15). These months (July – August) within the DY period were characterized by high mean air temperatures (above 20 °C) with low mean daily SVWC values (< 0.19 m^3 m^{-3}) in comparison with the two other adjacent years. Also, during the DY period within the dry spruce forest site, monthly mean R_{eco} values significantly decreased as compared to the years with normal conditions.

Additionally, at the dry spruce forest in Rájec, there was a significant decline in the mean monthly NEP values by 38% during the dry year period than a 12% decrease in the mean monthly NEP values at the wet spruce forest stand in Bílý Kříž (Fig. 5.16). Also, during July and August, there were statistically significant differences ($p < 0.001$) in the mean monthly NEP across both spruce forest stands. Therefore, causing a significant decline in the mean monthly NEP values during the DY period as compared to the two other adjacent years, especially within the dry spruce forest site.

Generally, the large decline in GPP, R_{eco} and NEP during the dry year period (especially from July - August) at the dry spruce forest site showed that the impact of the drought was more severe in the spruce forest site with a moderately dry climate than at the wet spruce forest site. However, during the months of July - August of the DY period, R_{eco} at the wet spruce forest site was observed to have significantly increased as compared to that in the adjacent years with normal conditions.

6 DISCUSSION

The results confirm the humid and cool climate within the spruce forest station at Bílý Kříž with high mean SVWC and low mean Tair values (Fig. 5.1) during most part of the growing season as compared to the moderately dry climate in Rájec (Květoň & Žák, 2007). Though there were warmer conditions (high Tair values) within the beech forest site in Štítná, the higher SVWC values recorded during the entire period under study indicated a higher rate of soil evaporation that cooled the soil within this site. Additionally, the wet spruce forest was generally characterized with a high yearly precipitation pattern compared to that in the dry spruce and beech forest sites (with higher atmospheric evaporative demand than the mean annual precipitation). Moreover, the effect of the severe drought stress condition during the summer of 2015 was mainly experienced at the dry spruce forest site with high Tair and VPD values than at the wet spruce forest ecosystem (Orth et al., 2016; Van Lanen et al., 2016; Ionita et al., 2017; Trnka et al., 2020). Low precipitation patterns and low SVWC values were mainly recorded in 2015 across both spruce forest sites as compared to the immediate adjacent years of 2014 and 2016. The impact of this summer drought condition experienced in 2015 was further used to determine the difference in responses of forest GPP among similar forest ecosystems (such as spruce species) grown under different climates with contrasting water availability.

6.1 Environmental effects on potential gross primary productivity (GPP_{pot}) in spruce and beech forests using a set of regression methods

To identify the main environmental variables that influenced changes in the ratio between the actual and optimal gross primary productivity (GPP_{norm}) across the three forest ecosystems (beech and two spruce forest sites grown under contrasting climatic conditions), two sets of regression models (SMLR and RF) were applied and compared. The presented results showed that the RF regression model outperformed the SMLR and proved to be highly effective in predicting the changes in GPP_{norm} across all sites (Table 5.6). It's worth noting that statistics from these regression analyses may not be enough to show the mechanistic cause of

the observed patterns but rather provide useful information on the key environmental variables and the impact of their significant interactions on GPP_{norm} within the specific forest site.

Generally, diffuse radiation (PAR) across both forest types was the most significant or important variable influencing GPP_{norm} using both the SMLR and RF regression methods. The PAR values (~ 4.0 MJ m^{-2} day^{-1}) were found to increase the light use efficiency and forest GPP across all the forest ecosystems. This shows the impact of the total intensity of PAR and its diffuse fraction on forest ecosystem photosynthesis across the forest types during the growing season (Urban et al., 2012). However, the intensity, duration and quality of PAR penetrating the forest canopy and reaching the forest floor may differ for spruce and beech forests due to their different crown structures (Lichtenthaler et al., 2007; Leuchner et al., 2012). In the beech and dry spruce forest sites, the GPP_{norm} was observed to increase with CNI until it saturates at some point (Fig. 5.6 and A1), indicating that high GPP_{norm} values were realized within these forest ecosystems under partly cloudy conditions. This is as a result of anisotropic diffuse radiation entering the forest canopy at its west-southwest slope orientation under such partly cloudy conditions (Čater and Diaci, 2017). On the other hand, at the wet spruce forest site, the effective penetration of anisotropic diffuse radiation at all layers of the forest canopy, especially in shaded leaves, was only reached under cloudy conditions, which led to the high realization of high GPP_{norm} values (Fig. A1 and Fig. A2; Urban et al., 2012). Lower GPP_{norm} were realized at extremely lower PAR values (< 2.5 MJ m^{-2} day^{-1}).

Moreover, analyses from SMLR and RF showed some similarities in the importance of the environmental variables that influenced GPP_{norm} at all forest sites. For instance, aside from PAR, VPD and SVWC were observed to have secondary effects on GPP_{norm}. SVWC was found to be the main limiting factor after PAR for grouping GPP_{norm} values within the wet spruce forest (Fig. 5.10; Cias et al., 2005; Chapin et al., 2011; Ågren and Andersson, 2012). However, the groupings of GPP_{norm} values at the dry spruce forest were decided by Ts, SVWC Tair, and CNI values (Fig. 5.10). In addition, the sum for the Ts and SVWC variables at the dry spruce forest stand were higher than that of both the wet spruce and beech forest sites (approximately 0.2; Fig. 5.9) further indicating their importance in grouping GPP_{norm} values. The significant interactions between Ts and other variables such as SVWC, VPD, CNI, Tair (as also confirmed in analyses from the SMLR) in predicting GPP_{norm} values show interactions of multiple environmental factors limited forest productivity at the dry spruce forest. Thus, the complexity in identifying other environmental parameters that drive GPP_{norm} values other than PAR. These confirm earlier studies by Lopes de Gerenyu et al. (2005) and Jassal et al. (2008) on the

sensitivity of forest GPP to soil moisture, which modulates the effects of solar radiation and Ts on carbon uptake within ecosystems characterized by a moderately drier climate. The intensity of radiation received by the soil affects Ts, the availability of soil moisture to plants and other biological processes in plants (Nishimura and Laroque, 2011; Zang et al., 2012; Boden et al., 2014; Novick et al., 2016; Sulman et al., 2016; Krupková et al., 2019). Thus, at higher temperatures and low SVWC as was observed in the dry spruce forest during the study period (Fig. 5.10), reduced water uptake reduces the rate of photosynthesis. This was the case for 24 cases in the dry spruce forest when strong ephadic drought led to the realization of lower GPP_{norm} values (~ 0.22). There were 16 cases of ephadic drought in the wet spruce forest, but the impact was not as severe as in the dry spruce forest (GPP_{norm} value of 0.44 at the wet spruce forest site). High GPP_{norm} values were realized at the dry spruce forest site on days with high PAR (> 5.5 MJ m^{-2} day^{-1}) and low Ts values (< 20 °C) for 193 cases. However, within the wet spruce forest site, high GPP_{norm} values were realized at approximately the same PAR values but for 197 cases when SVWC > 0.16 m^3 m^{-3}. This indicates the significant impact of water vailability on GPPnorm within the wet spruce forest ecosystem. Generally, the sensitivity of GPP_{norm} to environmental factors related to water availability such as SVWC, temperature (Ts and Tair) and VPD within these spruce forests depict the isohydric strategy in the spruce species in reducing stomatal conductance at early stages of soil drought (Kodrik and Kodrik, 2002; Gu et al., 2006; Hlásny et al., 2017; McGloin et al., 2019).

At the beech forest site, PAR and SVWC were identified as the main limiting factor for photosynthesis (Fig. 6 and 7). However, VPD only had a secondary effect and limited GPP_{norm} only after SVWC was observed to be low (< 0.3 m^3 m^{-3}; 51 cases). However, the impact of high VPD on GPP_{norm} within the beech forest site was minimal compared to the other forest ecosystems, with a GPP_{norm} value of approximately 0.61. At the spruce forest sites, under higher temperatures and lower SVWC, there was a significant decline in the GPP_{norm} values (0.22 at the dry spruce forest and 0.44 at the wet spruce forest site). Thus, in contrast to the spruce species, an anisohydric strategy exhibited by the beech species, with less stomatal control to soil drought, enables carbon uptake even under prolonged exposure to mild or moderate drought stress conditions (Leuschner, 2009; Nikolova et al., 2009; Pretzsch et al., 2020).

6.2 Contrasting effects of drought on the carbon dynamics at two Norway spruce forests sites with different climatic conditions

Due to the isohydric behaviour of the spruce species, the study assessed the contrasting effects of the 2015 severe summer drought on both the wet and dry spruce forest ecosystems. Results from the study corroborate earlier published results by Orth et al. (2016); Van Lanen et al. (2016), and Ionita et al. (2017) of the occurrence of severe drought stress conditions during the summer of 2015 across Europe (Table 5.2) as compared to the adjacent years (2014 and 2016). July and August of the DY period were characterized by high mean monthly Tair values (> 20 °C), with high mean monthly VPD values (> 10 hPa), and low mean monthly SVWC values (< 0.19 m^3 m^{-3}) across both spruce forest ecosystems. This shows the significant impact of the drought in 2015 during July - August.

Findings from this study show the significant decline in the rate of forest ecosystem photosynthesis (with the immediate closure of the stomata) by high VPD, Tair, and soil water deficit during July - August of 2015. Thus, both forest GPP and NEP significantly reduced stands during the DY period of 2015, especially in the dry spruce forest in Rájec than at the wet spruce forest in Bílý Kříž (Fig. 5.14 and Fig. 5.16). The strong decline in forest GPP and NEP with low SVWC conditions at the dry spruce forest ecosystem was due to the high atmospheric evaporative demand experienced at this forest ecosystem as compared to that in the wet spruce forest (Krupková et al., 2018). However, within the humid climatic conditions of the wet spruce forest site, an increase in Tair even for the months of July - August in 2015 only aided by the rise in the kinetics of enzymes participating in microbial decomposition and root respiration under warm conditions, thereby causing an increase in the overall forest ecosystem respiration (Reichstein et al., 2007; Jassal et al., 2008; Mahecha et al., 2010; Wu et al., 2011; Frank et al., 2015; van Gorsel et al., 2016; von Buttlar et al., 2017).

Additionally, plotting the residuals from the LRC model against VPD and SVWC using a piecewise regression analysis highlights the effects of both VPD and SVWC on forest ecosystem GPP, since both photosynthesis and transpiration are mediated stomatal conductance which are affected by these environmental variables. A steeper decline in the forest ecosystem GPP (Fig. 5.12 and Table 5.8) was observed with increasing VPD values across both forest stands even under non-drought years (when SVWC was non-limiting). This further supports recent findings, that show that high VPD values aggravate drought effects in forests due to the

quick changes over very short timescales within a day, even without dry soil conditions (Ruehr et al., 2014; Novick et al., 2016; Sulman et al., 2016). These results also explain the strong suppression of GPP by high VPD even during the years with normal conditions (2014 and 2016), as the SPEI (for determining dryness) indicates some observed changes in temperature and soil moisture on longer time scales of weeks or months (Sheffield et al., 2012; Potopová et al., 2016). Therefore, there is the need to incorporate the influence of such quick changes in VPD on the photosynthetic rate with limitations in SVWC into future LRC models to better analyse the impact of drought on GPP especially at different forest ecosystems that are exposed to regular strong edaphic droughts (Lasslop et al., 2010; Migliavacca et al., 2010; Laaha et al., 2017; Pretzsch et al., 2018).

7 CONCLUSIONS

Forest productivity is strongly dependent on species type and site-specific environmental conditions. Thus, in this study, the main environmental variables that influences the ratio between the actual and optimal gross primary productivity (GPP) across central European beech (at Štítná) and spruce (at Bílý Kříž and Rájec) species were identified by developing and comparing results from two set of regression models - the traditional Stepwise multiple linear regression model (SMLR) and Random forest (RF) regression model. The RF model outperformed the SMLR and proved to be highly effective in predicting the important environmental factors that influence GPP_{norm} at all sites. The anisotropic diffuse radiation entering the forest canopy and reaching the ground under cloudy conditions at the wet spruce forest stand and partly conditions within the dry spruce and beech forest was observed to be the main limiting environmental factors of the ecosystem photosynthesis. However, there were secondary effects from some other environmental variables such as the vapour pressure deficit, soil moisture, and temperature (air and soil) on the ecosystem photosynthesis, depending on the local conditions and forest type. The occurrence of edaphic drought cases was mostly recorded at the spruce forest than at the beech forest site and this had significant impact on GPP_{norm}, especially in the moderately drier climate at Rájec. This explains the isohydric behaviour of the spruce species in sustaining the plant's functionality while reducing forest GPP. However, in contrast to the spruce species, beech exhibited an anisohydric strategy that enabled carbon uptake even under prolonged exposure to mild or moderate drought stress conditions with less stomatal control to soil drought.

The results of this study further revealed the strong influence of VPD on carbon uptake within forest ecosystems characterized by precipitation typically equal or smaller than the atmospheric evaporative demand. Therefore, increasing the vulnerability of the Norway spruce forest to the severity of drought, especially at sites with moderately dry climate such as in the dry spruce forest site at Rájec. Moreover, the drought effects on forest ecosystem photosynthesis was further worsened by the decline in soil moisture. The effect of high VPD and low SVWC values on GPP was especially noticeable during the severe drought stress conditions within the drought year of 2015.

Consequently, the study suggests that elevated temperatures due to climate change, will further exacerbate the drought impacts on forest (Norway spruce) ecosystems at sites with precipitation equal or smaller than the atmospheric evaporative demand. The significant decline

in the forest GPP and NEP as was observed in the dry year of 2015 questions not only the sustainable productivity but also the existence of Norway spruce *per se* in such areas, considering the prolonged period of drought in future climatic conditions. These findings also call for more studies on forest productivity across other different forest types and contrasting climatic conditions, as productivity is strongly dependent on species type and site-specific environmental conditions.

REFERENCES

Ago, E. E., Serça, D., Agbossou, E. K., Galle, S., & Aubinet, M. (2015). Carbon dioxide fluxes from a degraded woodland in West Africa and their responses to main environmental factors. *Carbon balance and management*, *10*(1), 22.

Ågren, G. I., & Andersson, F. O. (2011). *Terrestrial ecosystem ecology: principles and applications*. Cambridge University Press.

Ahas, R., Aasa, A., Menzel, A., Fedotova, V. G., & Scheifinger, H. (2002). Changes in European spring phenology. *International Journal of Climatology: A Journal of the Royal Meteorological Society*, *22*(14), 1727-1738.

Allen, R.G., Pereira, L.S., Raes, D. and Smith, M., 1998. Crop evapotranspiration - Guidelines for computing crop water requirements - FAO Irrigation and drainage paper 56, Rome, Italy, 290 pp.

Allen, C. D., Macalady, A. K., Chenchouni, H., Bachelet, D., McDowell, N., Vennetier, M., & Gonzalez, P. (2010). A global overview of drought and heat-induced tree mortality reveals emerging climate change risks for forests. *Forest ecology and management*, *259*(4), 660-684.

Ainsworth, E. A., & Rogers, A. (2007). The response of photosynthesis and stomatal conductance to rising [CO2]: mechanisms and environmental interactions. *Plant, cell & environment*, *30*(3), 258-270.

Aitken, S. N., Yeaman, S., Holliday, J. A., Wang, T., & Curtis-McLane, S. (2008). Adaptation, migration or extirpation: climate change outcomes for tree populations. *Evolutionary applications*, *1*(1), 95-111.

Alekseychik, P., Mammarella, I., Launiainen, S., Rannik, Ü., & Vesala, T. (2013). Evolution of the nocturnal decoupled layer in a pine forest canopy. *Agricultural and forest meteorology*, *174*, 15-27.

Andrew J. Oliphant, 2012. Geography Compass Volume 6, Issue 12, pages 689–705, Terrestrial Ecosystem-Atmosphere Exchange of CO_2, Water and Energy from FLUXNET; Review and Meta-Analysis of a Global *in-situ* Observatory.

Angert, A., Biraud, S., Bonfils, C., Buermann, W., & Fung, I. (2004). CO2 seasonality indicates origins of post-Pinatubo sink. *Geophysical Research Letters*, *31*(11).

Aspinwall, M. J., Vårhammar, A., Blackman, C. J., Tjoelker, M. G., Ahrens, C., Byrne, M., ... & Rymer, P. D. (2017). Adaptation and acclimation both influence photosynthetic and respiratory temperature responses in Corymbia calophylla. *Tree Physiology*, *37*(8), 1095-1112.

Aubinet, M., Vesala, T., & Papale, D. (Eds.). (2012). *Eddy covariance: a practical guide to measurement and data analysis*. Springer Science & Business Media.

Augspurger, C. K. (2008). Early spring leaf out enhances growth and survival of saplings in a temperate deciduous forest. *Oecologia*, *156*(2), 281-286.

Balandier, P., Marquier, A., Gaudio, N., Wehrlen, L., Casella, E., Coll, L., ... & Harmer, R. (2009, May). Methods for describing light capture by understorey weeds in temperate forests: consequences for tree regeneration. In *Final COST E47 conference Forest vegetation management towards environmental sustainability* (pp. p-73). University of Copenhagen, Forest and Landscape Denmark.

Baldocchi, D. D., Hincks, B. B., & Meyers, T. P. (1988). Measuring biosphere-atmosphere exchanges of biologically related gases with micrometeorological methods. *Ecology*, *69*(5), 1331-1340.

Baldocchi, D., Falge, E., Gu, L., Olson, R., Hollinger, D., Running, S., ... & Fuentes, J. (2001). FLUXNET: A new tool to study the temporal and spatial variability of ecosystem–scale carbon dioxide, water vapor, and energy flux densities. *Bulletin of the American Meteorological Society*, *82*(11), 2415-2434.

Baldocchi, D. D. (2003). Assessing the eddy covariance technique for evaluating carbon dioxide exchange rates of ecosystems: past, present and future. *Global change biology*, *9*(4), 479-492.

Baldocchi, D. (2008). 'Breathing'of the terrestrial biosphere: lessons learned from a global network of carbon dioxide flux measurement systems. *Australian Journal of Botany*, *56*(1), 1-26.

Baldocchi, D. (2014). Measuring fluxes of trace gases and energy between ecosystems and the atmosphere–the state and future of the eddy covariance method. *Global change biology*, *20*(12), 3600-3609.

Barr, A. G., Black, T. A., Hogg, E. H., Kljun, N., Morgenstern, K., & Nesic, Z. (2004). Inter-annual variability in the leaf area index of a boreal aspen-hazelnut forest in relation to net ecosystem production. *Agricultural and forest meteorology*, *126*(3), 237-255.

Barr, A. G., Black, T. A., Hogg, E. H., Griffis, T. J., Morgenstern, K., Kljun, N., ... & Nesic, Z. (2007). Climatic controls on the carbon and water balances of a boreal aspen forest, 1994–2003. *Global Change Biology*, *13*(3), 561-576.

Barr, A. G., Richardson, A. D., Hollinger, D. Y., Papale, D., Arain, M. A., Black, T. A., ... & Schaeffer, K. (2013). Use of change-point detection for friction–velocity threshold evaluation in eddy-covariance studies. *Agricultural and forest meteorology*, *171*, 31-45.

Beaubien, E. G., & Freeland, H. J. (2000). Spring phenology trends in Alberta, Canada: links to ocean temperature. *International Journal of Biometeorology*, *44*(2), 53-59.

Beer, C., Reichstein, M., Tomelleri, E., Ciais, P., Jung, M., Carvalhais, N., ... & Bondeau, A. (2010). Terrestrial gross carbon dioxide uptake: global distribution and covariation with climate. *Science*, 1184984.

Beguería, S., Vicente-Serrano, S.M., Reig, F. and Latorre, B., (2014). Standardized precipitation evapotranspiration index (SPEI) revisited: parameter fitting, evapotranspiration models, tools, datasets and drought monitoring. International Journal of Climatology, 34(10): 3001-3023.

Beguería, S. Vicente-Serrano, S.M. 2017. SPEI: Calculation of the Standardised Precipitation-Evapotranspiration Index. R package version 1.7. https://CRAN.R-project.org/package=SPEI

Beikircher, B., & Mayr, S. (2009). Intraspecific differences in drought tolerance and acclimation in hydraulics of Ligustrum vulgare and Viburnum lantana. *Tree Physiology*, *29*(6), 765-775.

Belcher, S. E. (2005). Mixing and transport in urban areas. *Philosophical Transactions of the Royal Society A: Mathematical, Physical and Engineering Sciences*, *363*(1837), 2947-2968.

Belcher, S. E., Harman, I. N., & Finnigan, J. J. (2012). The wind in the willows: flows in forest canopies in complex terrain. *Annual Review of Fluid Mechanics*, *44*, 479-504.

Bergeron, O., Margolis, H. A., Coursolle, C., & Giasson, M. A. (2008). How does forest harvest influence carbon dioxide fluxes of black spruce ecosystems in eastern North America?. *Agricultural and Forest Meteorology*, *148*(4), 537-548.

Binkley, D., Campoe, O. C., Gspaltl, M., & Forrester, D. I. (2013). Light absorption and use efficiency in forests: why patterns differ for trees and stands. *Forest ecology and management*, *288*, 5-13.

Black, T. A., Chen, W. J., Barr, A. G., Arain, M. A., Chen, Z., Nesic, Z., ... & Yang, P. C. (2000). Increased carbon sequestration by a boreal deciduous forest in years with a warm spring. *Geophysical Research Letters*, *27*(9), 1271-1274.

Boardman, N. T. (1977). Comparative photosynthesis of sun and shade plants. *Annual review of plant physiology*, *28*(1), 355-377.

Boden, S., Kahle, H. P., von Wilpert, K., & Spiecker, H. (2014). Resilience of Norway spruce (Picea abies (L.) Karst) growth to changing climatic conditions in Southwest Germany. *Forest Ecology and Management*, *315*, 12-21.

Bonan, G. B. (2008). Forests and climate change: forcings, feedbacks, and the climate benefits of forests. *Science*, *320*(5882), 1444-1449.

Bonan, G. (2015). *Ecological climatology: concepts and applications*. Cambridge University Press.

Bond-Lamberty, B., Gower, S. T., Ahl, D. E., & Thornton, P. E. (2005). Reimplementation of the Biome-BGC model to simulate successional change. *Tree Physiology*, *25*(4), 413-424.

Bosveld, F. C., Holtslag, A. A. M., & Van Den Hurk, B. J. J. M. (1999). Nighttime convection in the interior of a dense Douglas fir forest. *Boundary-Layer Meteorology*, *93*(2), 171-195.

Brantley, S. T., & Young, D. R. (2009). Contribution of sunflecks is minimal in expanding shrub thickets compared to temperate forest. *Ecology*, *90*(4), 1021-1029.

Breshears, D. D. (2006). The grassland–forest continuum: trends in ecosystem properties for woody plant mosaics? *Frontiers in Ecology and the Environment*, *4*(2), 96-104.

Bréda, N., Huc, R., Granier, A., & Dreyer, E. (2006). Temperate forest trees and stands under severe drought: a review of ecophysiological responses, adaptation processes and long-term consequences. *Annals of Forest Science*, *63*(6), 625-644.

Breiman, L. (2013). Breiman and Cutler's random forests for classification and regression. Package 'randomForest'. *Institute for Statistics and Mathematics, Vienna University of Economics and Business*.

Brienen, R. J., Phillips, O. L., Feldpausch, T. R., Gloor, E., Baker, T. R., Lloyd, J., ... & Zagt, R. J. (2015). Long-term decline of the Amazon carbon sink. *Nature*, *519*(7543), 344-348.

Brodribb, T. J., Feild, T. S., & Sack, L. (2010). Viewing leaf structure and evolution from a hydraulic perspective. *Functional Plant Biology*, *37*(6), 488-498.

Brooks, S. P., & Gelman, A. (1998). General methods for monitoring convergence of iterative simulations. *Journal of computational and graphical statistics*, *7*(4), 434-455.

Brunet, Y., & Irvine, M. R. (2000). The control of coherent eddies in vegetation canopies: streamwise structure spacing, canopy shear scale and atmospheric stability. *Boundary-Layer Meteorology*, *94*(1), 139-163.

Buras, A., Rammig, A., & Zang, C. S. (2020). Quantifying impacts of the 2018 drought on European ecosystems in comparison to 2003. *Biogeosciences*, *17*(6), 1655-1672.

Busing, R. T., & Fujimori, T. (2005). Biomass, production and woody detritus in an old coast redwood (Sequoia sempervirens) forest. *Plant Ecology*, *177*(2), 177-188.

Canadell, J. G., Le Quéré, C., Raupach, M. R., Field, C. B., Buitenhuis, E. T., Ciais, P., ... & Marland, G. (2007). Contributions to accelerating atmospheric CO2 growth from economic activity, carbon intensity, and efficiency of natural sinks. *Proceedings of the national academy of sciences*, *104*(47), 18866-18870.

Čater, M., & Diaci, J. (2017). Divergent response of European beech, silver fir and Norway spruce advance regeneration to increased light levels following natural disturbance. *Forest Ecology and Management*, *399*, 206-212.

Cao, M., Prince, S. D., Small, J., & Goetz, S. J. (2004). Remotely sensed interannual variations and trends in terrestrial net primary productivity 1981–2000. *Ecosystems*, *7*(3), 233-242.

Cava, D., Giostra, U., Siqueira, M., & Katul, G. (2004). Organised motion and radiative perturbations in the nocturnal canopy sublayer above an even-aged pine forest. *Boundary-Layer Meteorology*, *112*(1), 129-157.

Chapin III, F. S., Matson, P. A., & Vitousek, P. (2011). *Principles of terrestrial ecosystem ecology*. Springer Science & Business Media.

Chen, I. C., Hill, J. K., Ohlemüller, R., Roy, D. B., & Thomas, C. D. (2011). Rapid range shifts of species associated with high levels of climate warming. *Science*, *333*(6045), 1024-1026.

Christensen, J. H., Hewitson, B., Busuioc, A., Chen, A., & Gao, X. (2007). Coauthors, 2007: Regional climate projections. *Climate Change 2007: The Physical Science Basis*, 847-940.

Chuine, I., & Beaubien, E. G. (2001). Phenology is a major determinant of tree species range. *Ecology Letters*, *4*(5), 500-510.

Churkina, G., Schimel, D., Braswell, B. H., & Xiao, X. (2005). Spatial analysis of growing season length control over net ecosystem exchange. *Global Change Biology*, *11*(10), 1777-1787.

Cleland, E. E., Chuine, I., Menzel, A., Mooney, H. A., & Schwartz, M. D. (2007). Shifting plant phenology in response to global change. *Trends in ecology & evolution*, *22*(7), 357-365.

Ciais, P., Reichstein, M., Viovy, N., Granier, A., Ogée, J., Allard, V., ... & Chevallier, F. (2005). Europe-wide reduction in primary productivity caused by the heat and drought in 2003. *Nature*, *437*(7058), 529.

Cook, B. D., Bolstad, P. V., Martin, J. G., Heinsch, F. A., Davis, K. J., Wang, W., ... & Teclaw, R. M. (2008). Using light-use and production efficiency models to predict photosynthesis and net carbon exchange during forest canopy disturbance. *Ecosystems*, *11*(1), 26-44.

Cox, P. M., Pearson, D., Booth, B. B., Friedlingstein, P., Huntingford, C., Jones, C. D., & Luke, C. M. (2013). Sensitivity of tropical carbon to climate change constrained by carbon dioxide variability. *Nature*, *494*(7437), 341.

Dai, A. (2013). Increasing drought under global warming in observations and models. *Nature Climate Change*, *3*(1), 52-58.

Davies, R. B. (2002). Hypothesis testing when a nuisance parameter is present only under the alternative: linear model case. *Biometrika*, 484-489.

Debat, V., & David, P. (2001). Mapping phenotypes: canalization, plasticity and developmental stability. *Trends in ecology & evolution*, *16*(10), 555-561.

De Boeck, H. J., & Verbeeck, H. (2011). Drought-associated changes in climate and their relevance for ecosystem experiments and models. *Biogeosciences*, *8*(5), 1121-1130.

Devine, W. D., & Harrington, C. A. (2008). Influence of four tree shelter types on microclimate and seedling performance of Oregon white oak and western redcedar.

Dreiss, L. M., & Volin, J. C. (2013). Influence of leaf phenology and site nitrogen on invasive species establishment in temperate deciduous forest understories. *Forest Ecology and Management*, *296*, 1-8.

Dupont, S., & Patton, E. G. (2012). Momentum and scalar transport within a vegetation canopy following atmospheric stability and seasonal canopy changes: the CHATS experiment. *Atmospheric Chemistry and Physics*, *12*(13), 5913-5935.

Duursma, R. A., & Mäkelä, A. (2007). Summary models for light interception and light-use efficiency of non-homogeneous canopies. *Tree physiology*, *27*(6), 859-870.

Ensminger, I., Schmidt, L., & Lloyd, J. (2008). Soil temperature and intermittent frost modulate the rate of recovery of photosynthesis in Scots pine under simulated spring conditions. *New Phytologist*, *177*(2), 428-442.

Evans, F. C. (1956). Ecosystem as the basic unit in ecology. *Science* **123,** 1127–1128.

Ewers, B. E., Gower, S. T., Bond-Lamberty, B., & Wang, C. K. (2005). Effects of stand age and tree species on canopy transpiration and average stomatal conductance of boreal forests. *Plant, Cell & Environment*, *28*(5), 660-678.

Falge, E., Baldocchi, D., Tenhunen, J., Aubinet, M., Bakwin, P., Berbigier, P., ... & Wofsy, S. (2002). Seasonality of ecosystem respiration and gross primary production as derived from FLUXNET measurements. *Agricultural and Forest Meteorology*, *113*(1-4), 53-74.

Finnigan, J. J. (2004). A re-evaluation of long-term flux measurement techniques part II: coordinate systems. *Boundary-Layer Meteorology*, *113*(1), 1-41.

Fischer, M., Zenone, T., Trnka, M., Orság, M., Montagnani, L., Ward, E. J., ... & Ceulemans, R. (2018). Water requirements of short rotation poplar coppice: Experimental and modelling analyses across Europe. *Agricultural and Forest Meteorology*, *250*, 343-360.

Fleisher, D. H., Timlin, D. J., Yang, Y., & Reddy, V. R. (2010). Simulation of potato gas exchange rates using SPUDSIM. *Agricultural and forest meteorology*, *150*(3), 432-442.

Foken, T., & Wichura, B. (1996). Tools for quality assessment of surface-based flux measurements. *Agricultural and forest meteorology*, *78*(1-2), 83-105.

Foken, T. (2008). The energy balance closure problem: an overview. *Ecological Applications*, *18*(6), 1351-1367.

Foken, T., Leuning, R., Oncley, S. R., Mauder, M., & Aubinet, M. (2012). Corrections and data quality control. In *Eddy covariance* (pp. 85-131). Springer, Dordrecht.

Frank, D., Reichstein, M., Bahn, M., Thonicke, K., Frank, D., Mahecha, M. D., ... & Beer, C. (2015). Effects of climate extremes on the terrestrial carbon cycle: concepts, processes and potential future impacts. *Global Change Biology*, *21*(8), 2861-2880.

Friedlingstein, P., Jones, M., O'sullivan, M., Andrew, R., Hauck, J., Peters, G., ... & DBakker, O. (2019). Global carbon budget 2019. *Earth System Science Data*, *11*(4), 1783-1838.

Fu, Y. H., Geng, X., Hao, F., Vitasse, Y., Zohner, C. M., Zhang, X., ... & Janssens, I. A. (2019). Shortened temperature-relevant period of spring leaf-out in temperate-zone trees. *Global change biology*, *25*(12), 4282-4290.

Fu, Z., Ciais, P., Bastos, A., Stoy, P. C., Yang, H., Green, J. K., ... & Koebsch, F. (2020). Sensitivity of gross primary productivity to climatic drivers during the summer drought

of 2018 in Europe. *Philosophical Transactions of the Royal Society B*, *375*(1810), 20190747.

Garratt, J. R. (1994). The atmospheric boundary layer. *Earth-Science Reviews*, *37*(1-2), 89-134.

Gaumont-Guay, D., Black, T. A., Barr, A. G., Jassal, R. S., & Nesic, Z. (2008). Biophysical controls on rhizospheric and heterotrophic components of soil respiration in a boreal black spruce stand. *Tree Physiology*, *28*(2), 161-171.

Gelman, A., & Rubin, D. B. (1992). Inference from iterative simulation using multiple sequences. *Statistical science*, *7*(4), 457-472.

George, J. P., Schueler, S., Karanitsch-Ackerl, S., Mayer, K., Klumpp, R. T., & Grabner, M. (2015). Inter-and intra-specific variation in drought sensitivity in Abies spec. and its relation to wood density and growth traits. *Agricultural and forest meteorology*, *214*, 430-443.

Gill, D. S., Amthor, J. S., & Bormann, F. H. (1998). Leaf phenology, photosynthesis, and the persistence of saplings and shrubs in a mature northern hardwood forest. *Tree Physiology*, *18*(5), 281-289.

Goulden, M. L., Munger, J. W., Fan, S. M., Daube, B. C., & Wofsy, S. C. (1996). Measurements of carbon sequestration by long-term eddy covariance: Methods and a critical evaluation of accuracy. *Global change biology*, *2*(3), 169-182.

Grace, J. (2004). Understanding and managing the global carbon cycle. *Journal of Ecology*, *92*(2), 189-202.

Granier, A., Reichstein, M., Bréda, N., Janssens, I. A., Falge, E., Ciais, P., ... & Buchmann, N. (2007). Evidence for soil water control on carbon and water dynamics in European forests during the extremely dry year: 2003. *Agricultural and forest meteorology*, *143*(1-2), 123-145.

Grelle, A., Lindroth, A., & Mölder, M. (1999). Seasonal variation of boreal forest surface conductance and evaporation. *Agricultural and forest meteorology*, *98*, 563-578.

Griffis, T. J., Black, T. A., Gaumont-Guay, D., Drewitt, G. B., Nesic, Z., Barr, A. G., ... & Kljun, N. (2004). Seasonal variation and partitioning of ecosystem respiration in a southern boreal aspen forest. *Agricultural and Forest meteorology*, *125*(3), 207-223.

Groisman, P. Y., Karl, T. R., & Knight, R. W. (1994). Observed impact of snow cover on the heat balance and the rise of continental spring temperatures. *Science*, *263*(5144), 198-200.

Grossiord, C., Buckley, T. N., Cernusak, L. A., Novick, K. A., Poulter, B., Siegwolf, R. T., ... & McDowell, N. G. (2020). Plant responses to rising vapor pressure deficit. *New Phytologist*, *226*(6), 1550-1566.

Gu, L., Baldocchi, D., Verma, S. B., Black, T. A., Vesala, T., Falge, E. M., & Dowty, P. R. (2002a). Advantages of diffuse radiation for terrestrial ecosystem productivity. *Journal of Geophysical Research: Atmospheres*, *107*(D6).

Gu, L.; Meyers, T.; Pallardy, S.G.; Hanson, P.J.; Yang, B.; Heuer, M.; Hosman, K.P.; Riggs, J.S.; Sluss, D.; Wullschleger, S.D. Climatic drivers of forest productivity in Central Europe. Agric. For. Meteorol. (2002b), 234, 258–273.

Gu, L., Baldocchi, D. D., Wofsy, S. C., Munger, J. W., Michalsky, J. J., Urbanski, S. P., & Boden, T. A. (2003). Response of a deciduous forest to the Mount Pinatubo eruption: enhanced photosynthesis. *Science*, *299*(5615), 2035-2038.

Gu, L., Meyers, T., Pallardy, S. G., Hanson, P. J., Yang, B., Heuer, M., ... & Wullschleger, S. D. (2006). Direct and indirect effects of atmospheric conditions and soil moisture on surface energy partitioning revealed by a prolonged drought at a temperate forest site. *Journal of Geophysical Research: Atmospheres*, *111*(D16).

Gu, L., Post, W. M., Baldocchi, D. D., Black, T. A., Suyker, A. E., Verma, S. B., ... & Wofsy, S. C. (2009). Characterizing the seasonal dynamics of plant community photosynthesis across a range of vegetation types. In *Phenology of ecosystem processes* (pp. 35-58). Springer, New York, NY.

Haggagy, M. E. N. A. (2003). A sodar-based investigation of the atmospheric boundary layer: Berichte des Meteorologischen Institutes der Universität Freiburg.

Hardwick, S. R., Toumi, R., Pfeifer, M., Turner, E. C., Nilus, R., & Ewers, R. M. (2015). The relationship between leaf area index and microclimate in tropical forest and oil palm plantation: Forest disturbance drives changes in microclimate. *Agricultural and Forest Meteorology*, *201*, 187-195.

Haustein, K., Allen, M. R., Forster, P. M., Otto, F. E. L., Mitchell, D. M., Matthews, H. D., & Frame, D. J. (2017). A real-time global warming index. *Scientific reports*, *7*(1), 1-6.

Hansen, J., Ruedy, R., Sato, M., Lo, K., 2006. GISS Surface Temperature Analysis. Global Temperature Trends: 2005 Summation. NASA Goddard Institute for Space Studies and Columbia University Earth Institute, New York, NY 10025, USA.

Hartig, F., Minunno, F., Paul, S. 2019. BayesianTools: General-Purpose MCMC and SMC Samplers and Tools for Bayesian Statistics. R package version 0.1.6. https://CRAN.R-project.org/package=BayesianTools

Herbst, M., Rosier, P. T., Morecroft, M. D., & Gowing, D. J. (2008). Comparative measurements of transpiration and canopy conductance in two mixed deciduous woodlands differing in structure and species composition. *Tree physiology*, *28*(6), 959-970.

Hlásny, T., Trombik, J., Bošeľa, M., Merganič, J., Marušák, R., Šebeň, V., ... & Trnka, M. (2017). Climatic drivers of forest productivity in Central Europe. *Agricultural and Forest Meteorology*, *234*, 258-273.

Hoch, W. A., Singsaas, E. L., & McCown, B. H. (2003). Resorption protection. Anthocyanins facilitate nutrient recovery in autumn by shielding leaves from potentially damaging light levels. *Plant physiology*, *133*(3), 1296-1305.

Hogg, E. H., Brandt, J. P., & Kochtubajda, B. (2002). Growth and dieback of aspen forests in northwestern Alberta, Canada, in relation to climate and insects. *Canadian Journal of Forest Research*, *32*(5), 823-832.

Hollinger, D. Y., Aber, J., Dail, B., Davidson, E. A., Goltz, S. M., Hughes, H., ... & Scott, N. A. (2004). Spatial and temporal variability in forest–atmosphere CO2 exchange. *Global Change Biology*, *10*(10), 1689-1706.

Horton, D. E., Johnson, N. C., Singh, D., Swain, D. L., Rajaratnam, B., & Diffenbaugh, N. S. (2015). Contribution of changes in atmospheric circulation patterns to extreme temperature trends. *Nature*, *522*(7557), 465-469.

Houghton, J. T., Ding, Y. D. J. G., Griggs, D. J., Noguer, M., van der Linden, P. J., Dai, X., ... & Johnson, C. A. (2001). *Climate change 2001: the scientific basis*. The Press Syndicate of the University of Cambridge.

Horst, T. W., & Lenschow, D. H. (2009). Attenuation of scalar fluxes measured with spatially-displaced sensors. *Boundary-layer meteorology*, *130*(2), 275-300.

Hu, Z., Li, S., Yu, G., Sun, X., Zhang, L., Han, S., & Li, Y. (2013). Modeling evapotranspiration by combing a two-source model, a leaf stomatal model, and a light-use efficiency model. *Journal of Hydrology*, *501*, 186-192.

Hui, D., Deng, Q., Tian, H., & Luo, Y. (2017). Climate change and carbon sequestration in forest ecosystems. *Handbook of Climate Change Mitigation and Adaptation*, 555-594.

Huntington, T. G. (2006). Evidence for intensification of the global water cycle: review and synthesis. *Journal of Hydrology*, *319*(1), 83-95.

Hutchison, B. A., & Matt, D. R. (1977). The distribution of solar radiation within a deciduous forest. *Ecological Monographs*, *47*(2), 185-207.

Ibrom, A., Dellwik, E., Larsen, S. E., & Pilegaard, K. I. M. (2007). On the use of the Webb–Pearman–Leuning theory for closed-path eddy correlation measurements. *Tellus B: Chemical and Physical Meteorology*, *59*(5), 937-946.

Ionita, M., Tallaksen, L., Kingston, D., Stagge, J., Laaha, G., Van Lanen, H., ... & Haslinger, K. (2017). The European 2015 drought from a climatological perspective. *Hydrology and Earth System Sciences*, *21*, 1397-1419.

IPCC (2013). Climate Change 2013: The Physical Science Basis. Contribution of Working Group I to the Fifth Assessment Report of the Intergovernmental Panel on Climate Change. Cambridge University Press, Cambridge.

Jacob, D., Kotova, L., Teichmann, C., Sobolowski, S. P., Vautard, R., Donnelly, C., ... & Sakalli, A. (2018). Climate impacts in Europe under + 1.5 C global warming. *Earth's Future*, *6*(2), 264-285.

Jackson, R. B., Canadell, J., Ehleringer, J. R., Mooney, H. A., Sala, O. E., & Schulze, E. D. (1996). A global analysis of root distributions for terrestrial biomes. *Oecologia*, *108*(3), 389-411.

Jackson, S. T., Webb, R. S., Anderson, K. H., Overpeck, J. T., Webb III, T., Williams, J. W., & Hansen, B. C. (2000). Vegetation and environment in eastern North America during the last glacial maximum. *Quaternary Science Reviews*, *19*(6), 489-508.

Jackson, R. B., Lechowicz, M. J., Li, X., & Mooney, H. A. (2001). Phenology, growth, and allocation in global terrestrial productivity. *Terrestrial global productivity*, 61-82.

Jassal, R. S., Black, T. A., Novak, M. D., GAUMONT-GUAY, D. A. V. I. D., & Nesic, Z. (2008). Effect of soil water stress on soil respiration and its temperature sensitivity in an 18-year-old temperate Douglas-fir stand. *Global Change Biology*, *14*(6), 1305-1318.

Jezkova, T., & Wiens, J. J. (2016). Rates of change in climatic niches in plant and animal populations are much slower than projected climate change. *Proceedings of the Royal Society B: Biological Sciences*, *283*(1843), 20162104.

Jiao-jun, Z., Xiu-fen, L. I., Yutaka, G., & Takeshi, M. (2004). Wind profiles in and over trees. *Journal of Forestry Research*, *15*(4), 305-312.

Jocher, G., De Simon, G., Hörnlund, T., Linder, S., Lundmark, T., Marshall, J., ... & Peichl, M. (2017). Apparent winter CO2 uptake by a boreal forest due to decoupling. *Agricultural and Forest Meteorology*, *232*, 23-34.

Jocher, G., Marshall, J., Nilsson, M. B., Linder, S., De Simon, G., Hörnlund, T., ... & Peichl, M. (2018). Impact of canopy decoupling and subcanopy advection on the annual carbon

balance of a boreal scots pine forest as derived from eddy covariance. *Journal of Geophysical Research: Biogeosciences*, *123*(2), 303-325.

Jocher, G., Fischer, M., Šigut, L., Pavelka, M., Sedlák, P., & Katul, G. (2020). Assessing decoupling of above and below canopy air masses at a Norway spruce stand in complex terrain. *Agricultural and Forest Meteorology*, *294*, 108149.

Jung, M., Reichstein, M., Ciais, P., Seneviratne, S. I., Sheffield, J., Goulden, M. L., ... & Dolman, A. J. (2010). Recent decline in the global land evapotranspiration trend due to limited moisture supply. *Nature*, *467*(7318), 951-954.

Katul, G. G., Cava, D., Siqueira, M., & Poggi, D. (2013). Scalar turbulence within the canopy sublayer. *Coherent flow structures at Earth's Surface*, 73-95.

Keller, D. P., Lenton, A., Littleton, E. W., Oschlies, A., Scott, V., & Vaughan, N. E. (2018). The effects of carbon dioxide removal on the carbon cycle. *Current climate change reports*, *4*(3), 250-265.

Kenderes, K., Mihók, B., & Standovár, T. (2008). Thirty years of gap dynamics in a Central European beech forest reserve. *Forestry*, *81*(1), 111-123.

Kljun, N., Calanca, P., Rotach, M. W., & Schmid, H. P. (2004). A simple parameterisation for flux footprint predictions. *Boundary-Layer Meteorology*, *112*(3), 503-523.

Kmet, J., Ditmarová, L., Kurjak, D., & Priwitzer, T. (2011). Physiological response of Norway spruce foliage in the drought vegetation period 2009. *Beskydy*, *4*(2), 109-118.

Kodrik, J., & Kodrik, M. (2002). Root biomass of beech as a factor influencing the wind tree stability. *J. For. Sci*, *48*, 549-564.

Kormann, R., & Meixner, F. X. (2001). An analytical footprint model for non-neutral stratification. *Boundary-Layer Meteorology*, *99*(2), 207-224.

Kowalska, N., Szatniewska, J., Stojanović, M., Šigut, L., & Pavelka, M. (2019, January). Analysis of floodplain forest sensitivity to drought. In *Geophysical Research Abstracts* (Vol. 21).

Krämer, S., & Green, D. M. (2000). Acid and alkaline phosphatase dynamics and their relationship to soil microclimate in a semiarid woodland. *Soil biology and biochemistry*, *32*(2), 179-188.

Krejza, J., Cienciala, E., Světlík, J., Bellan, M., Noyer, E., Horáček, P., ... & Marek, M. V. (2020). Evidence of climate-induced stress of Norway spruce along elevation gradient preceding the current dieback in Central Europe. *Trees*, 1-17.

Krupková, L., Havránková, K., Krejza, J., Sedlák, P., & Marek, M. V. (2019). Impact of water scarcity on spruce and beech forests. *Journal of Forestry Research*, *30*(3), 899-909.

Kudo, G., Ida, T. Y., & Tani, T. (2008). Linkages between phenology, pollination, photosynthesis, and reproduction in deciduous forest understory plants. *Ecology*, *89*(2), 321-331.

Květoň, V., & Žák, M. (2007). New climate atlas of Czechia. *Studia Geophysica et Geodaetica*, *51*(2), 345-349.

Laaha, G., Gauster, T., Tallaksen, L., Vidal, J. P., Stahl, K., Prudhomme, C., ... & Adler, M. J. (2017). The European 2015 drought from a hydrological perspective.

Lal, R., Smith, P., Jungkunst, H. F., Mitsch, W. J., Lehmann, J., Nair, P. R., ... & Skorupa, A. L. (2018). The carbon sequestration potential of terrestrial ecosystems. *Journal of Soil and Water Conservation*, *73*(6), 145A-152A.

Lasslop, G., Reichstein, M., Papale, D., Richardson, A. D., Arneth, A., Barr, A., ... & Wohlfahrt, G. (2010). Separation of net ecosystem exchange into assimilation and respiration using a light response curve approach: critical issues and global evaluation. *Global Change Biology*, *16*(1), 187-208.

Law, B. E., Thornton, P. E., Irvine, J., Anthoni, P. M., & Van Tuyl, S. (2001). Carbon storage and fluxes in ponderosa pine forests at different developmental stages. *Global Change Biology*, *7*(7), 755-777.

Le Quéré, C., Andres, R. J., Boden, T., Conway, T., Houghton, R. A., House, J. I., ... & Andrew, R. M. (2013). The global carbon budget 1959–2011, Earth Syst. Sci. Data, 5, 165–185.

Le Quéré, C., Andrew, R. M., Friedlingstein, P., Sitch, S., Hauck, J., Pongratz, J., ... & Zheng, B. (2018). Global carbon budget 2018. *Earth System Science Data*, *10*(4), 2141-2194.

Lee, X., Neumann, H. H., Hartog, G. D. E. N., Mickle, R. E., Fuentes, J. D., Black, T. A., ... & Blanken, P. D. (1997). Observation of gravity waves in a boreal forest. *Boundary-layer meteorology*, *84*(3), 383-398.

Lee, X., & Finnigan, J. (2004). Coordinate systems and flux bias error. In *Handbook of Micrometeorology* (pp. 33-66). Springer, Dordrecht.

Lee, X. (2017). Fundamentals of Boundary-Layer Meteorology.

Lee X. (2018) Flow in Plant Canopies. In: Fundamentals of Boundary-Layer Meteorology. Springer Atmospheric Sciences. Springer, Cham, https://doi.org/10.1007/978-3-319-60853-2_5

Leuchner, M., Hertel, C., Rötzer, T., Seifert, T., Weigt, R., Werner, H., & Menzel, A. (2012). Solar radiation as a driver for growth and competition in forest stands. In *Growth and Defence in Plants* (pp. 175-191). Springer, Berlin, Heidelberg.

Leuschner, C. (2009). Die Trockenheitsempfindlichkeit der Rotbuche vor dem Hintergrund des prognostizierten Klimawandels.

Lenoir, J., Gégout, J. C., Guisan, A., Vittoz, P., Wohlgemuth, T., Zimmermann, N. E., ... & Svenning, J. C. (2010). Going against the flow: potential mechanisms for unexpected downslope range shifts in a warming climate. *Ecography*, *33*(2), 295-303.

Levi, Y., Dayan, U., Levy, I., & Broday, D. M. (2020). On the association between characteristics of the atmospheric boundary layer and air pollution concentrations. *Atmospheric Research*, *231*, 104675.

Liaw, A., & Wiener, M. (2002). Classification and regression by randomForest. *R news*, *2*(3), 18-22.

Liaw, A., & Wiener, M. (2015). Breiman and Cutler's Random Forests for Classification and Regression Version (4.6–12).

Lichtenthaler, H. K., Ač, A., Marek, M. V., Kalina, J., & Urban, O. (2007). Differences in pigment composition, photosynthetic rates and chlorophyll fluorescence images of sun and shade leaves of four tree species. *Plant Physiology and Biochemistry*, *45*(8), 577-588.

Lieth, H. (Ed.). (2013). *Phenology and seasonality modeling* (Vol. 8). Springer Science & Business Media.

Linderholm, H. W. (2006). Growing season changes in the last century. *Agricultural and forest meteorology*, *137*(1-2), 1-14.

Lopes de Gerenyu, V. O., Rozanova, L. N., & Kudeyarov, V. N. (2005). Effect of soil temperature and moisture on CO_2 evolution rate of cultivated Phaeozem: analyses of a long-term field experiment. *Plant, Soil and Environment-UZPI (Czech Republic)*.

Lovett, G. M., Cole, J. J., & Pace, M. L. (2006). Is net ecosystem production equal to ecosystem carbon accumulation?. *Ecosystems*, *9*(1), 152-155.

Lu, P., Yu, Q., Liu, J., & Lee, X. (2006). Advance of tree-flowering dates in response to urban climate change. *Agricultural and Forest Meteorology*, *138*(1-4), 120-131.

Lundmark, T., Hällgren, J. E., & Degermark, C. (1988). Effects of summer frost oh the gas exchange of field-grown Pinus sylvestris L. seedlings. *Scandinavian Journal of Forest Research*, *3*(1-4), 441-448.

Ma, J., Yan, X., Dong, W., & Chou, J. (2015). Gross primary production of global forest ecosystems has been overestimated. *Scientific reports*, *5*, 10820.

Ma, X., Huete, A., Cleverly, J., Eamus, D., Chevallier, F., Joiner, J., ... & Xie, Z. (2016). Drought rapidly diminishes the large net CO_2 uptake in 2011 over semi-arid Australia. *Scientific reports*, *6*, 37747.

Mäenpää, M., Riikonen, J., Kontunen-Soppela, S., Rousi, M., & Oksanen, E. (2011). Vertical profiles reveal impact of ozone and temperature on carbon assimilation of Betula pendula and Populus tremula. *Tree Physiology*, *31*(8), 808-818.

Mahecha, M. D., Reichstein, M., Carvalhais, N., Lasslop, G., Lange, H., Seneviratne, S. I., Vargas, R., Ammann, C., Arain, M. A., Cescatti, A., Janssens, I. A., Migliavacca, M., Montagnani, L., and Richardson, A. D. (2010): Global convergence in the temperature sensitivity of respiration at ecosystem level, Science, 329, 838–840.

Malhi, Y., Franklin, J., Seddon, N., Solan, M., Turner, M. G., Field, C. B., & Knowlton, N. (2020). Climate change and ecosystems: Threats, opportunities and solutions.

Marchin, R. M., Broadhead, A. A., Bostic, L. E., Dunn, R. R., & Hoffmann, W. A. (2016). Stomatal acclimation to vapour pressure deficit doubles transpiration of small tree seedlings with warming. *Plant, cell & environment*, *39*(10), 2221-2234.

Marek, M. V., Janouš, D., Taufarová, K., Havránková, K., Pavelka, M., Kaplan, V., & Marková, I. (2011). Carbon exchange between ecosystems and atmosphere in the Czech Republic is affected by climate factors. *Environmental pollution*, *159*(5), 1035-1039.

Massman, W. J., & Lee, X. (2002). Eddy covariance flux corrections and uncertainties in long-term studies of carbon and energy exchanges. *Agricultural and Forest Meteorology*, *113*(1-4), 121-144.

Mauder, M., & Foken, T. (2004). Documentation and instruction manual of the eddy covariance software package TK2, Univ. *Bayreuth, Abt. Mikrometeorol., ISSN*, *161489166*, 26-42.

Mauder, M., Desjardins, R. L., Pattey, E., Gao, Z., & Van Haarlem, R. (2008). Measurement of the sensible eddy heat flux based on spatial averaging of continuous ground-based observations. *Boundary-layer meteorology*, *128*(1), 151-172.

Mauder, M., Cuntz, M., Drüe, C., Graf, A., Rebmann, C., Schmid, H. P., ... & Steinbrecher, R. (2013). A strategy for quality and uncertainty assessment of long-term eddy-covariance measurements. *Agricultural and Forest Meteorology*, *169*, 122-135.

McCarthy, H. R., Pataki, D. E., & Jenerette, G. D. (2011). Plant water-use efficiency as a metric of urban ecosystem services. *Ecological Applications*, *21*(8), 3115-3127.

McDonald, G. T., & Lane, M. B. (2004). Converging global indicators for sustainable forest management. *Forest policy and economics*, *6*(1), 63-70.

McGloin, R., Šigut, L., Havránková, K., Dušek, J., Pavelka, M., & Sedlák, P. (2018). Energy balance closure at a variety of ecosystems in Central Europe with contrasting topographies. *Agricultural and Forest Meteorology*, *248*, 418-431.

McGloin, R., Šigut, L., Fischer, M., Foltýnová, L., Chawla, S., Trnka, M., ... & Marek, M. V. (2019). Available energy partitioning during drought at two Norway spruce forests and a European Beech forest in Central Europe. *Journal of Geophysical Research: Atmospheres*, *124*(7), 3726-3742.

Mensah, C., Šigut, L., Fischer, M., Foltýnová, L., Jocher, G., Acosta, M., ... & Marek, M. V. (2021a). Assessing the Contrasting Effects of the Exceptional 2015 Drought on the Carbon Dynamics in Two Norway Spruce Forest Ecosystems. *Atmosphere*, *12*(8), 988.

Mensah, C., Šigut, L., Fischer, M., Foltýnová, L., Jocher, G., Urban, O., ... & Marek, M. V. (2021b). Environmental Effects on Normalized Gross Primary Productivity in Beech and Norway Spruce Forests. *Atmosphere*, *12*(9), 1128.

Menzel, A., & Fabian, P. (1999). Growing season extended in Europe. *Nature*, *397*(6721), 659-659.

Migliavacca, M., Reichstein, M., Richardson, A. D., Colombo, R., Sutton, M. A., Lasslop, G., ... & Mahecha, M. D. (2011). Semi empirical modeling of abiotic and biotic factors controlling ecosystem respiration across eddy covariance sites. *Global Change Biology*, *17*(1), 390-409.

Miles, J. W. (1964). Baroclinic instability of the zonal wind. *Reviews of Geophysics*, *2*(1), 155-176.

Mishra, A. K., & Singh, V. P. (2010). A review of drought concepts. *Journal of hydrology*, *391*(1-2), 202-216.

Mitchell, J. F. (1989). The "greenhouse" effect and climate change. *Reviews of Geophysics*, *27*(1), 115-139.

Moffat, A. M. (2010). A new methodology to interpret high resolution measurements of net carbon fluxes between terrestrial ecosystems and the atmosphere.

Moncrieff, J. B., Malhi, Y., & Leuning, R. (1996). The propagation of errors in long-term measurements of land-atmosphere fluxes of carbon and water. *Global change biology*, *2*(3), 231-240.

Moncrieff, J. B., Jarvis, P. G., & Valentini, R. (2000). Canopy fluxes. In *Methods in ecosystem science* (pp. 161-180). Springer, New York, NY.

Monsi, M., & Saeki, T. (2005). On the factor light in plant communities and its importance for matter production. *Annals of Botany*, *95*(3), 549.

Monin, A. S., & Obukhov, A. M. (1954). Basic laws of turbulent mixing in the surface layer of the atmosphere. *Contrib. Geophys. Inst. Acad. Sci. USSR*, *151*(163), e187.

Monson, R. K., & Baldocchi, D. (2014). Fluxes of biogenic volatile compounds between plants and the atmosphere. *Terrestrial Biosphere-Atmosphere fluxes*, 395-414.

Monteith, J., & Unsworth, M. (2013). *Principles of environmental physics: plants, animals, and the atmosphere*. Academic Press.

Muggeo, V. M. (2003). Estimating regression models with unknown break-points. *Statistics in medicine*, *22*(19), 3055-3071.

Muraoka, H., Tang, Y., Terashima, I., Koizumi, H., & Washitani, I. (2000). Contributions of diffusional limitation, photoinhibition and photorespiration to midday depression of photosynthesis in Arisaema heterophyllum in natural high light. *Plant, Cell & Environment*, *23*(3), 235-250.

Murthy, I. K., Varghese, V., & Prasad, K. D. (2019). Competing Demands on Land: Implications for Carbon Sink Enhancement and Potential of Forest Sector in Karnataka to Contribute to the INDC Forest Goal of India.

Nadezhdina, N., Urban, J., Čermák, J., Nadezhdin, V., & Kantor, P. (2014). Comparative study of long-term water uptake of Norway spruce and Douglas-fir in Moravian upland. *Journal of Hydrology and Hydromechanics*, *62*(1), 1-6.

Nemani, R. R., Keeling, C. D., Hashimoto, H., Jolly, W. M., Piper, S. C., Tucker, C. J., ... & Running, S. W. (2003). Climate-driven increases in global terrestrial net primary production from 1982 to 1999. *science*, *300*(5625), 1560-1563.

Nikolova, P. S., Raspe, S., Andersen, C. P., Mainiero, R., Blaschke, H., Matyssek, R., & Häberle, K. H. (2009). Effects of the extreme drought in 2003 on soil respiration in a mixed forest. *European Journal of Forest Research*, *128*(2), 87-98.

Nishimura, P. H., & Laroque, C. P. (2011). Observed continentality in radial growth–climate relationships in a twelve site network in western Labrador, Canada. *Dendrochronologia*, *29*(1), 17-23.

Niu, S., Xing, X., Zhang, Z. H. E., Xia, J., Zhou, X., Song, B., ... & Wan, S. (2011). Water-use efficiency in response to climate change: from leaf to ecosystem in a temperate steppe. *Global Change Biology*, *17*(2), 1073-1082.

Noormets, A., Chen, J., & Crow, T. R. (2007). Age-dependent changes in ecosystem carbon fluxes in managed forests in northern Wisconsin, USA. *Ecosystems*, *10*(2), 187-203.

Noormets, A., Desai, A. R., Cook, B. D., Euskirchen, E. S., Ricciuto, D. M., Davis, K. J., ... & Su, H. B. (2008). Moisture sensitivity of ecosystem respiration: comparison of 14 forest ecosystems in the Upper Great Lakes Region, USA. *agricultural and forest meteorology*, *148*(2), 216-230.

Novick, K. A., Ficklin, D. L., Stoy, P. C., Williams, C. A., Bohrer, G., Oishi, A. C., ... & Scott, R. L. (2016). The increasing importance of atmospheric demand for ecosystem water and carbon fluxes. *Nature climate change*, *6*(11), 1023-1027.

Oren, R., Sperry, J. S., Katul, G. G., Pataki, D. E., Ewers, B. E., Phillips, N., & Schäfer, K. V. R. (1999). Survey and synthesis of intra-and interspecific variation in stomatal sensitivity to vapour pressure deficit. *Plant, Cell & Environment*, *22*(12), 1515-1526.

Orth, R., & Seneviratne, S. I. (2015). Introduction of a simple-model-based land surface dataset for Europe. *Environmental Research Letters*, *10*(4), 044012.

Orth, R., Zscheischler, J., & Seneviratne, S. I. (2016). Record dry summer in 2015 challenges precipitation projections in Central Europe. *Scientific reports*, *6*, 28334.

Papale, D., Reichstein, M., Aubinet, M., Canfora, E., Bernhofer, C., Kutsch, W., ... & Yakir, D. (2006). Towards a standardized processing of Net Ecosystem Exchange measured with eddy covariance technique: algorithms and uncertainty estimation. *Biogeosciences*, *3*(4), 571-583.

Parmesan, C., & Yohe, G. (2003). A globally coherent fingerprint of climate change impacts across natural systems. *Nature*, *421*(6918), 37-42.

Pan, Y., Birdsey, R. A., Fang, J., Houghton, R., Kauppi, P. E., Kurz, W. A., ... & Ciais, P. (2011). A large and persistent carbon sink in the world's forests. *Science*, 1201609.

Pastorello, G., Trotta, C., Canfora, E., Chu, H., Christianson, D., Cheah, Y. W., ... & Law, B. (2020). The FLUXNET2015 dataset and the ONEFlux processing pipeline for eddy covariance data. *Scientific data*, *7*(1), 1-27.

Paw U, K. T., Baldocchi, D., Meyers, T. P., and Wilson, K. B.: 2000, 'Correction of Eddy-Covariance Measurements Incorporating both Advective Effects and Density Fluxes', *Boundary-Layer Meteorol*. **97**, 487–511.

Pfleiderer, P., & Coumou, D. (2018). Quantification of temperature persistence over the Northern Hemisphere land-area. *Climate Dynamics*, *51*(1), 627-637.

Piao, S., Ciais, P., Friedlingstein, P., Peylin, P., Reichstein, M., Luyssaert, S., ... & Vesala, T. (2008). Net carbon dioxide losses of northern ecosystems in response to autumn warming. *Nature*, *451*(7174), 49-52.

Piao, S., Ciais, P., Huang, Y., Shen, Z., Peng, S., Li, J., ... & Friedlingstein, P. (2010). The impacts of climate change on water resources and agriculture in China. *Nature*, *467*(7311), 43-51.

Prentice, I. C., Farquhar, G. D., Fasham, M. J. R., Goulden, M. L., Heimann, M., Jaramillo, V. J., ... & Yool, A. (2001). The carbon cycle and atmospheric CO_2. In *Climate Change 2000: The Science of Climate Change. Contributions of Working Group I to the Third Assessment Report of the Intergovernmental Panel on Climate Change* (pp. 183-237). Cambridge University Press.

Pretzsch, H., Schütze, G., & Biber, P. (2018). Drought can favour the growth of small in relation to tall trees in mature stands of Norway spruce and European beech. *Forest Ecosystems*, *5*(1), 20.

Pretzsch, H., Grams, T., Häberle, K. H., Pritsch, K., Bauerle, T., & Rötzer, T. (2020). Growth and mortality of Norway spruce and European beech in monospecific and mixed-species stands under natural episodic and experimentally extended drought. Results of the KROOF throughfall exclusion experiment. *Trees*, *34*(4), 957-970.

Potopová, V., Boroneanţ, C., Možný, M., & Soukup, J. (2016). Driving role of snow cover on soil moisture and drought development during the growing season in the Czech Republic. *International Journal of Climatology*, *36*(11), 3741-3758.

Potužníková, K., Sedlák, P., & Koucká Knížová, P. (2015). Detection of low-frequency organized structures in night-time air flow within a spruce canopy on the upwind and downwind sides of a mountain ridge. *Atmospheric Science Letters*, *16*(4), 432-437.

Pugh, T. A., Lindeskog, M., Smith, B., Poulter, B., Arneth, A., Haverd, V., & Calle, L. (2019). Role of forest regrowth in global carbon sink dynamics. *Proceedings of the National Academy of Sciences*, *116*(10), 4382-4387.

Qie, L., Lewis, S. L., Sullivan, M. J., Lopez-Gonzalez, G., Pickavance, G. C., Sunderland, T., ... & Banin, L. F. (2017). Long-term carbon sink in Borneo's forests halted by drought and vulnerable to edge effects. *Nature communications*, *8*(1), 1966.

Queck, R., & Bernhofer, C. (2010). Constructing wind profiles in forests from limited measurements of wind and vegetation structure. *Agricultural and forest meteorology*, *150*(5), 724-735.

R Core Team (2018). R: A language and environment for statistical computing. R Foundation for Statistical Computing, Vienna, Austria. URL https://www.R-project.org/.

Raynor, G. S. (1971). Wind and temperature structure in a coniferous forest and a contiguous field. *Forest Science*, *17*(3), 351-363.

Reichstein, M., Rey, A., Freibauer, A., Tenhunen, J., Valentini, R., Banza, J., ... & Yakir, D. (2003). Modeling temporal and large-scale spatial variability of soil respiration from soil water availability, temperature and vegetation productivity indices. *Global biogeochemical cycles*, *17*(4).

Reichstein, M., Falge, E., Baldocchi, D., Papale, D., Aubinet, M., Berbigier, P., ... & Grünwald, T. (2005). On the separation of net ecosystem exchange into assimilation and ecosystem respiration: review and improved algorithm. *Global Change Biology*, *11*(9), 1424-1439.

Reichstein, M., Ciais, P., Papale, D., Valentini, R., Running, S., Viovy, N., ... & Aubinet, M. (2007). Reduction of ecosystem productivity and respiration during the European summer 2003 climate anomaly: a joint flux tower, remote sensing and modelling analysis. *Global Change Biology*, *13*(3), 634-651.

Reichstein, M., Bahn, M., Ciais, P., Frank, D., Mahecha, M. D., Seneviratne, S. I., ... & Papale, D. (2013). Climate extremes and the carbon cycle. *Nature*, *500*(7462), 287.

Richardson, L. F. (1920). The supply of energy from and to atmospheric eddies. *Proceedings of the Royal Society of London. Series A, Containing Papers of a Mathematical and Physical Character*, *97*(686), 354-373.

Richardson, A. D., Bailey, A. S., Denny, E. G., Martin, C. W., & O'KEEFE, J. O. H. N. (2006). Phenology of a northern hardwood forest canopy. *Global Change Biology*, *12*(7), 1174-1188.

Richardson, A. D., Hollinger, D. Y., Aber, J. D., Ollinger, S. V., & Braswell, B. H. (2007). Environmental variation is directly responsible for short-but not long-term variation in forest-atmosphere carbon exchange. *Global Change Biology*, *13*(4), 788-803.

Richardson, A. D., & O'Keefe, J. (2009). Phenological differences between understory and overstory. In *Phenology of ecosystem processes* (pp. 87-117). Springer, New York, NY.

Rossi, G., Cancelliere, A., & Pereira, L. S. (Eds.). (2003). *Tools for drought mitigation in Mediterranean Regions* (Vol. 44). Springer Science & Business Media.

Roderick, M. L., Farquhar, G. D., Berry, S. L., & Noble, I. R. (2001). On the direct effect of clouds and atmospheric particles on the productivity and structure of vegetation. *Oecologia*, *129*(1), 21-30.

Rötzer, T., Häberle, K. H., Kallenbach, C., Matyssek, R., Schütze, G., & Pretzsch, H. (2017). Tree species and size drive water consumption of beech/spruce forests-a simulation study highlighting growth under water limitation. *Plant and Soil*, *418*(1), 337-356.

Ruehr, N. K., Law, B. E., Quandt, D., & Williams, M. (2014). Effects of heat and drought on carbon and water dynamics in a regenerating semi-arid pine forest: a combined experimental and modeling approach. *Biogeosciences*, *11*(15).

Rustad, L. E. (2008). The response of terrestrial ecosystems to global climate change: towards an integrated approach. *Science of the total environment*, *404*(2-3), 222-235.

Sachs, L. (2013). *Angewandte statistik: anwendung statistischer methoden*. Springer-Verlag.

Sage, R. F., & Kubien, D. S. (2007). The temperature response of C3 and C4 photosynthesis. *Plant, cell & environment*, *30*(9), 1086-1106.

Sánchez, G., Serrano, A., & Cancillo, M. L. (2012). Effect of cloudiness on solar global, solar diffuse and terrestrial downward radiation at Badajoz (Southwestern Spain). *Optica pura y aplicada*, *45*(1), 33-38.

Schimel, D., Stephens, B. B., & Fisher, J. B. (2015). Effect of increasing CO_2 on the terrestrial carbon cycle. *Proceedings of the National Academy of Sciences*, *112*(2), 436-441.

Schimel, D. S., House, J. I., Hibbard, K. A., Bousquet, P., Ciais, P., Peylin, P., ... & Canadell, J. (2001). Recent patterns and mechanisms of carbon exchange by terrestrial ecosystems. *Nature*, *414*(6860), 169-172.

Schilperoort, B., Coenders-Gerrits, M., Jiménez Rodríguez, C., van der Tol, C., Van De Wiel, B., & Savenije, H. (2020). Decoupling of a Douglas fir canopy: a look into the subcanopy with continuous vertical temperature profiles. *Biogeosciences*, *17*(24), 6423-6439.

Schwartz, M. D. (Ed.). (2003). *Phenology: an integrative environmental science* (p. 564). Dordrecht: Kluwer Academic Publishers.

Schwartz, M. D., Ahas, R., & Aasa, A. (2006). Onset of spring starting earlier across the Northern Hemisphere. *Global change biology*, *12*(2), 343-351.

Seibert, P., Beyrich, F., Gryning, S. E., Joffre, S., Rasmussen, A., & Tercier, P. (2000). Review and intercomparison of operational methods for the determination of the mixing height. *Atmospheric environment*, *34*(7), 1001-1027.

Sheffield, J., Wood, E. F., & Roderick, M. L. (2012). Little change in global drought over the past 60 years. *Nature*, *491*(7424), 435-438.

Shen, M., Tang, Y., Chen, J., Yang, X., Wang, C., Cui, X., ... & Cong, N. (2014). Earlier-season vegetation has greater temperature sensitivity of spring phenology in Northern Hemisphere. *PloS one*, *9*(2), e88178.

Sherry, R. A., Zhou, X., Gu, S., Arnone, J. A., Schimel, D. S., Verburg, P. S., ... & Luo, Y. (2007). Divergence of reproductive phenology under climate warming. *Proceedings of the National Academy of Sciences*, *104*(1), 198-202.

Shukla, P. R., Skea, J., Calvo Buendia, E., Masson-Delmotte, V., Pörtner, H. O., Roberts, D. C., ... & Malley, J. (2019). IPCC, 2019: Climate Change and Land: an IPCC special report on climate change, desertification, land degradation, sustainable land management, food security, and greenhouse gas fluxes in terrestrial ecosystems.

Siebicke, L., Hunner, M., & Foken, T. (2012). Aspects of CO2 advection measurements. *Theoretical and applied climatology*, *109*(1-2), 109-131.

Sippel, S., Forkel, M., Rammig, A., Thonicke, K., Flach, M., Heimann, M., ... & Mahecha, M. D. (2017). Contrasting and interacting changes in simulated spring and summer carbon cycle extremes in European ecosystems. *Environmental Research Letters*, *12*(7), 075006.

Sparks, T. H., Jeffree, E. P., & Jeffree, C. E. (2000). An examination of the relationship between flowering times and temperature at the national scale using long-term phenological records from the UK. *International Journal of Biometeorology*, *44*(2), 82-87.

Sprugel, D. G. (1989). The relationship of evergreenness, crown architecture, and leaf size. *The american naturalist*, *133*(4), 465-479.

Stocker, T. F., Qin, D., Plattner, G. K., Tignor, M. M., Allen, S. K., Boschung, J., ... & Midgley, P. M. (2014). Climate Change 2013: The physical science basis. contribution of working group I to the fifth assessment report of IPCC the intergovernmental panel on climate change.

Stull, R. B. (1988). *An introduction to boundary layer meteorology* (Vol. 13). Springer Science & Business Media.

Sultan, S. E. (2000). Phenotypic plasticity for plant development, function and life history. *Trends in plant science*, *5*(12), 537-542.

Sulman, B. N., Roman, D. T., Yi, K., Wang, L., Phillips, R. P., & Novick, K. A. (2016). High atmospheric demand for water can limit forest carbon uptake and transpiration as severely as dry soil. *Geophysical Research Letters*, *43*(18), 9686-9695.

Sun, Y., Piao, S., Huang, M., Ciais, P., Zeng, Z., Cheng, L., ... & Zeng, H. (2016). Global patterns and climate drivers of water-use efficiency in terrestrial ecosystems deduced from satellite-based datasets and carbon cycle models. *Global Ecology and Biogeography*, *25*(3), 311-323.

Suvanto, S., Nöjd, P., Henttonen, H. M., Beuker, E., & Mäkinen, H. (2016). Geographical patterns in the radial growth response of Norway spruce provenances to climatic variation. *Agricultural and Forest Meteorology*, *222*, 10-20.

Sypka, P., & Starzak, R. (2013). Simplified, empirical model of wind speed profile under canopy of Istebna spruce stand in mountain valley. *Agricultural and forest meteorology*, *171*, 220-233.

Tang, J., Baldocchi, D. D., & Xu, L. (2005). Tree photosynthesis modulates soil respiration on a diurnal time scale. *Global Change Biology*, *11*(8), 1298-1304.

Tape, K. E. N., Sturm, M., & Racine, C. (2006). The evidence for shrub expansion in Northern Alaska and the Pan-Arctic. *Global change biology*, *12*(4), 686-702.

Taiz, L., & Zeiger, E. (2010). Plant physiology. ed. *Sunderland, MA: Sinauer associates*.

Team, C. W., Pachauri, R. K., & Meyer, L. A. (2014). IPCC, 2014: Climate Change 2014: Synthesis Report. Contribution of Working Groups I. *II and III to the Fifth Assessment Report of the intergovernmental panel on Climate Change. IPCC, Geneva, Switzerland*, *151*.

Teuling, A. J., Seneviratne, S. I., Stöckli, R., Reichstein, M., Moors, E., Ciais, P., ... & Wohlfahrt, G. (2010). Contrasting response of European forest and grassland energy exchange to heatwaves. *Nature geoscience*, *3*(10), 722-727.

Thimijan, R. W., & Heins, R. D. (1983). Photometric, radiometric, and quantum light units of measure: a review of procedures for interconversion. *HortScience*, *18*(6), 818-822.

Thomas, C., Mayer, J. C., Meixner, F. X., & Foken, T. (2006). Analysis of low-frequency turbulence above tall vegetation using a Doppler sodar. *Boundary-Layer Meteorology*, *119*(3), 563-587.

Thomas, C. K., Martin, J. G., Law, B. E., & Davis, K. (2013). Toward biologically meaningful net carbon exchange estimates for tall, dense canopies: Multi-level eddy covariance observations and canopy coupling regimes in a mature Douglas-fir forest in Oregon. *Agricultural and forest meteorology*, *173*, 14-27.

Tian, M., Yu, G., He, N., & Hou, J. (2016). Leaf morphological and anatomical traits from tropical to temperate coniferous forests: Mechanisms and influencing factors. *Scientific Reports*, *6*(1), 1-10.

Trnka, M., Hlavinka, P., Možný, M., Semerádová, D., Štěpánek, P., Balek, J., ... & Farda, A. (2020). Czech Drought Monitor System for Monitoring and Forecasting Agricultural Drought and Drought Impacts. *International Journal of Climatology*.

Turnipseed, A. A., Anderson, D. E., Blanken, P. D., Baugh, W. M., & Monson, R. K. (2003). Airflows and turbulent flux measurements in mountainous terrain: Part 1. Canopy and local effects. *Agricultural and Forest Meteorology*, *119*(1-2), 1-21.

United Nations Framework Convention on Climate Change *(1992) United Nations Framework Convention on Climate Change, United Nations, Rio de Janeiro, 1992 (United Nations Framework Convention on Climate Change, Bonn, Germany) Available at: www.unfccc.int/resource/ccsites/senegal/conven.html.*

Urban, O., Janouš, D., Pokorný, R., Marková, I., Pavelka, M., Fojtík, Z., ... & Marek, M. V. (2001). Glass domes with adjustable windows: A novel technique for exposing juvenile forest stands to elevated CO2 concentration. *Photosynthetica*, *39*(3), 395-401.

Urban, O., JANOUŠ, D., Acosta, M., CZERNÝ, R., Markova, I., NavrATil, M., ... & ŠPUNDA, V. (2007). Ecophysiological controls over the net ecosystem exchange of mountain spruce stand. Comparison of the response in direct vs. diffuse solar radiation. *Global Change Biology*, *13*(1), 157-168.

Urban, O., Klem, K., Ač, A., Havránková, K., Holišová, P., Navrátil, M., ... & Tomášková, I. (2012). Impact of clear and cloudy sky conditions on the vertical distribution of photosynthetic CO_2 uptake within a spruce canopy. *Functional Ecology*, *26*(1), 46-55.

Urban, O., Klem, K., Holišová, P., Šigut, L., Šprtová, M., Teslová-Navrátilová, P., ... & Grace, J. (2014). Impact of elevated CO_2 concentration on dynamics of leaf photosynthesis in Fagus sylvatica is modulated by sky conditions. *Environmental pollution*, *185*, 271-280.

van Gorsel, E., Finnigan, J. J., Harman, I. N., & Leuning, R. (2008). 9A. 4 CHARACTERISTICS OF CANOPY TURBULENCE DURING THE TRANSITION FROM CONVECTIVE TO STABLE STRATIFICATION.

Van Gorsel, E., Wolf, S., Cleverly, J., Isaac, P., Haverd, V., Ewenz, C., ... & Griebel, A. (2016). Carbon uptake and water use in woodlands and forests in southern Australia during an extreme heat wave event in the" angry Summer" of 2012/2013. *Biogeosciences*, *13*(21), 5947-5964.

Van Lanen, H. A., Laaha, G., Kingston, D. G., Gauster, T., Ionita, M., Vidal, J. P., ... & Delus, C. (2016). Hydrology needed to manage droughts: the 2015 European case. *Hydrological Processes*, *30*(17), 3097-3104.

Vesala, T., Kljun, N., Rannik, Ü., Rinne, J., Sogachev, A., Markkanen, T., ... & Leclerc, M. Y. (2008). Flux and concentration footprint modelling: State of the art. *Environmental Pollution*, *152*(3), 653-666.

Vicente-Serrano, S.M., Beguería, S. and López-Moreno, J.I., 2010. A Multiscalar Drought Index Sensitive to Global Warming: The Standardized Precipitation Evapotranspiration Index. Journal of Climate, 23(7): 1696-1718.

von Buttlar, J., Zscheischler, J., Rammig, A., Sippel, S., Reichstein, M., Knohl, A., ... & Cescatti, A. (2017). Impacts of droughts and extreme temperature events on gross primary production and ecosystem respiration: a systematic assessment across ecosystems and climate zones. *Biogeosciences Discussions*.

Vitasse, Y., Delzon, S., Dufrêne, E., Pontailler, J. Y., Louvet, J. M., Kremer, A., & Michalet, R. (2009). Leaf phenology sensitivity to temperature in European trees: Do within-species populations exhibit similar responses? *Agricultural and forest meteorology*, *149*(5), 735-744.

Vitasse, Y., & Basler, D. (2013). What role for photoperiod in the bud burst phenology of European beech. *European Journal of Forest Research*, *132*(1), 1-8.

Vitasse, Y., Ursenbacher, S., Klein, G., Bohnenstengel, T., Chittaro, Y., Delestrade, A., ... & Lenoir, J. (2021). Phenological and elevational shifts of plants, animals and fungi under climate change in the E uropean A lps. *Biological Reviews*.

Vose, J. M., Peterson, D. L., & Patel-Weynand, T. (2012). Effects of climatic variability and change on forest ecosystems: a comprehensive science synthesis for the US forest sector. *General Technical Report-Pacific Northwest Research Station, USDA Forest Service*, (PNW-GTR-870).

Waring, R. H., & Running, S. W. (2010). *Forest ecosystems: analysis at multiple scales*. Elsevier.

Wang, L., Chen, W., & Zhou, W. (2014). Assessment of future drought in Southwest China based on CMIP5 multimodel projections. *Advances in Atmospheric Sciences*, *31*(5), 1035-1050.

Way, D. A., DOMEC, J. C., & Jackson, R. B. (2013). Elevated growth temperatures alter hydraulic characteristics in trembling aspen (Populus tremuloides) seedlings: implications for tree drought tolerance. *Plant, cell & environment*, *36*(1), 103-115.

Way, D. A., & Montgomery, R. A. (2015). Photoperiod constraints on tree phenology, performance and migration in a warming world. *Plant, cell & environment*, *38*(9), 1725-1736.

White, M. A., & Nemani, R. R. (2003). Canopy duration has little influence on annual carbon storage in the deciduous broad leaf forest. *Global change biology*, *9*(7), 967-972.

Wilczak, J. M., Oncley, S. P., & Stage, S. A. (2001). Sonic anemometer tilt correction algorithms. *Boundary-Layer Meteorology*, *99*(1), 127-150.

Wilson, K., Goldstein, A., Falge, E., Aubinet, M., Baldocchi, D., Berbigier, P., ... & Verma, S. (2002). Energy balance closure at FLUXNET sites. *Agricultural and Forest Meteorology*, *113*(1-4), 223-243.

Wolf, S., Eugster, W., Ammann, C., Häni, M., Zielis, S., Hiller, R., ... & Buchmann, N. (2013). Contrasting response of grassland versus forest carbon and water fluxes to spring drought in Switzerland. *Environmental Research Letters*, *8*(3), 035007.

Wu, S. H., Jansson, P. E., & Kolari, P. (2011). Modeling seasonal course of carbon fluxes and evapotranspiration in response to low temperature and moisture in a boreal Scots pine ecosystem. *Ecological modelling*, *222*(17), 3103-3119.

Wutzler, T., Lucas-Moffat, A., Migliavacca, M., Knauer, J., Sickel, K., Šigut, L., ... & Reichstein, M. (2018). Basic and extensible post-processing of eddy covariance flux data with REddyProc. *Biogeosciences*, *15*(16), 5015-5030.

www. slideplayer.com/slide/2407916/ (accessed on 7th March 2021)

www. geo.libretexts.org/ (accessed on 7th March 2021)

Xiao, X., Zhang, Q., Braswell, B., Urbanski, S., Boles, S., Wofsy, S., ... & Ojima, D. (2004). Modeling gross primary production of temperate deciduous broadleaf forest using satellite images and climate data. *Remote Sensing of Environment*, *91*(2), 256-270.

Xie, Z., Wang, L., Jia, B., & Yuan, X. (2016). Measuring and modeling the impact of a severe drought on terrestrial ecosystem CO_2 and water fluxes in a subtropical forest. *Journal of Geophysical Research: Biogeosciences*, *121*(10), 2576-2587.

Xu, L., Samanta, A., Costa, M. H., Ganguly, S., Nemani, R. R., & Myneni, R. B. (2011). Widespread decline in greenness of Amazonian vegetation due to the 2010 drought. *Geophysical Research Letters*, *38*(7).

Yi, C., Monson, R. K., Zhai, Z., Anderson, D. E., Lamb, B., Allwine, G., ... & Burns, S. P. (2005). Modeling and measuring the nocturnal drainage flow in a high-elevation, subalpine forest with complex terrain. *Journal of Geophysical Research: Atmospheres*, *110*(D22).

Yu, M., Li, Q., Hayes, M. J., Svoboda, M. D., & Heim, R. R. (2014). Are droughts becoming more frequent or severe in China based on the standardized precipitation evapotranspiration index: 1951–2010?. *International Journal of Climatology*, *34*(3), 545-558.

Zang, C., Pretzsch, H., & Rothe, A. (2012). Size-dependent responses to summer drought in Scots pine, Norway spruce and common oak. *Trees*, *26*(2), 557-569.

Zeng, N., Qian, H., Roedenbeck, C., & Heimann, M. (2005). Impact of 1998–2002 midlatitude drought and warming on terrestrial ecosystem and the global carbon cycle. *Geophysical Research Letters*, *32*(22).

Zeng, Z., Piao, S., Lin, X., Yin, G., Peng, S., Ciais, P., & Myneni, R. B. (2012). Global evapotranspiration over the past three decades: estimation based on the water balance equation combined with empirical models. *Environmental Research Letters*, *7*(1), 014026.

Zhao, M., & Running, S. W. (2010). Drought-induced reduction in global terrestrial net primary production from 2000 through 2009. *science*, *329*(5994), 940-943.

Zhu, J., Matsuzaki, T., & Sakioka, K. (2000). Wind speeds within a single crown of Japanese black pine (Pinus thunbergii Parl.). *Forest Ecology and Management*, *135*(1-3), 19-31.

Zhu, W., Van Hout, R., Luznik, L., Kang, H. S., Katz, J., & Meneveau, C. (2006). A comparison of PIV measurements of canopy turbulence performed in the field and in a wind tunnel model. *Experiments in fluids*, *41*(2), 309-318.

Zhu, Q., Jiang, H., Peng, C., Liu, J., Wei, X., Fang, X., ... & Yu, S. (2011). Evaluating the effects of future climate change and elevated CO2 on the water use efficiency in terrestrial ecosystems of China. *Ecological Modelling*, *222*(14), 2414-2429.

Zscheischler, J., & Seneviratne, S. I. (2017). Dependence of drivers affects risks associated with compound events. *Science advances*, *3*(6), e1700263.

APPENDIX

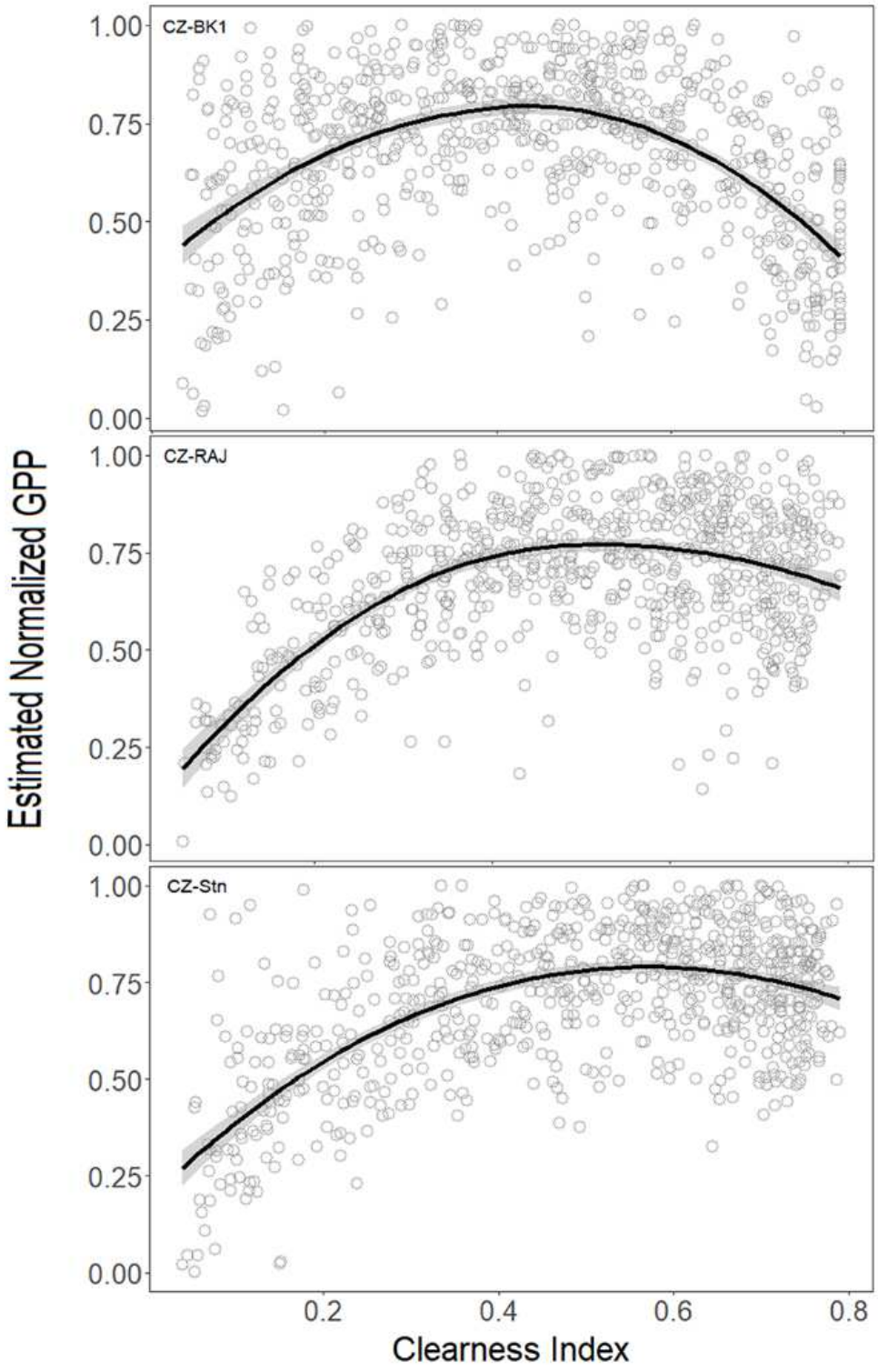

Fig. A1: Correlation between the estimated Normalized gross primary productivity (GPP_{norm}) within the wet and dry spruce forests and beech forest ecosystems from May-September of 2012-2016.

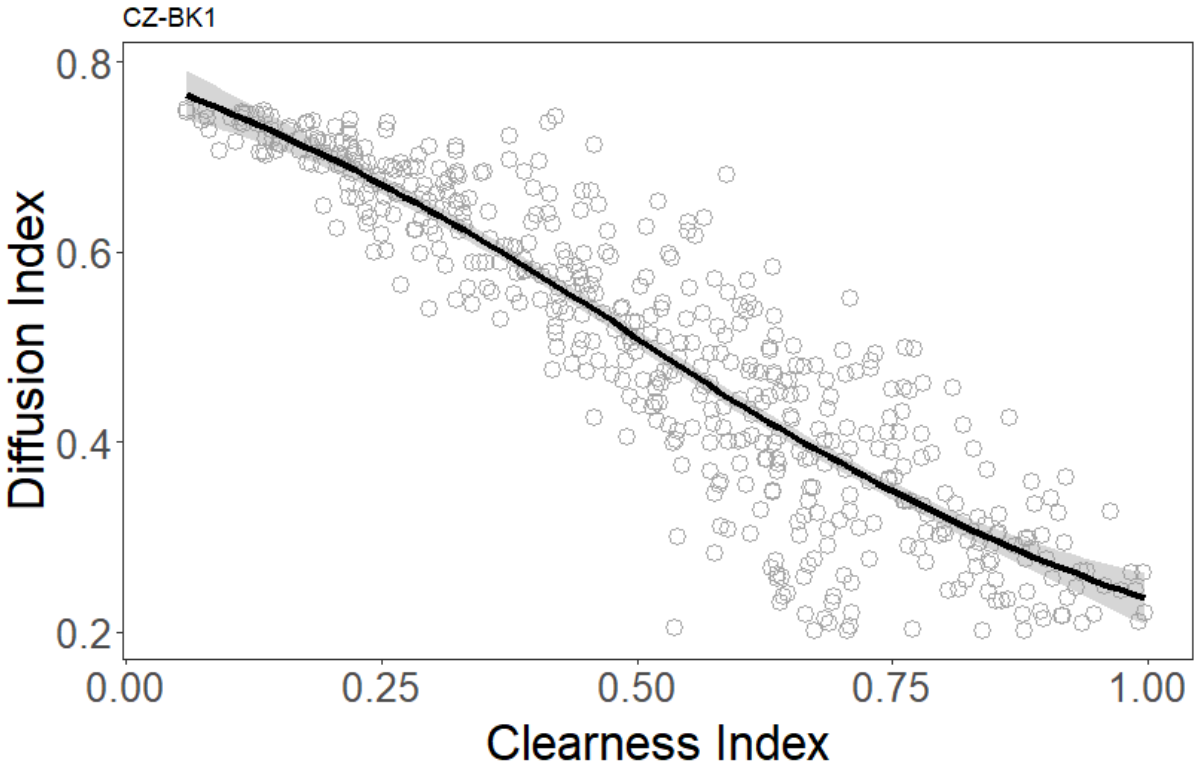

Fig. A2: Correlation of daily Diffusion Index (DI) with daily Clearness Index (CNI) for the wet spruce forest (CZ-BK1) from May-September of 2012-2016, showing diffuse radiation on partly cloudy days (highest point).